Copper binding of the glycolytic enzyme glyceraldehyde 3-phosphate dehydrogenase in *Staphylococcus aureus*

Jack Stevenson

Doctor of Philosophy

Institute for Cell and Molecular Biosciences

September 2015

Abstract

Staphylococcus aureus is a Gram positive bacterium which is predominantly commensal, but which can also be a human and animal pathogen, able to cause serious infections. It is becoming an increasing problem due to it becoming resistant to modern antibiotics. In common with most bacteria, *S. aureus* requires small quantities of the essential metal copper, but they also experience toxicity when exposed to high concentrations of copper, a metal that has been used for its antimicrobial properties for centuries. However, the mechanism of such toxicity remains elusive.

Here, the effect of copper toxicity on *S. aureus* has been investigated in order to understand how excess copper ions affect its physiology. The growth of *S. aureus* was found to be inhibited in media containing elevated copper, and the extent of this inhibition was shown to be dependent on the type of growth medium used. Analysis of soluble extracts from *S. aureus* cells exposed to elevated copper led to the identification of a cytoplasmic enzyme, GapA, which binds copper. GapA is a member of the well-characterised family of the glyceraldehyde-3-phosphate dehydrogenase (GAPDH) enzymes, and is not a metalloprotein. Copper inhibition of the activity of the *S. aureus* GapA enzyme was demonstrated, both in *S. aureus* cell extracts and with recombinant enzyme *in vitro*, using a specific enzyme activity assay.

Analysis of the purified recombinant GapA enzyme *in vitro* demonstrated a copper binding stoichiometry of one Cu(I) ion to each GapA monomer using analytical size-exclusion chromatography and spectrophotometry, and evidence is presented that suggests high affinity Cu(I) binding of biochemical relevance. Some preliminary evidence is provided that the Cu(I) binding site on the GapA protein includes the thiol group of cysteine 151 located within the active site, consistent with predictions based on published crystal structures, and explaining the observed copper-dependent inhibition of enzyme activity.

This is the first evidence of copper binding to a non-metalloprotein within the cytoplasm of *S. aureus* and adds to mounting evidence that aberrant binding of copper to cytosolic proteins contributes to bacterial copper toxicity.

Acknowledgements

Most of all I would like to acknowledge the input of my supervisor, Dr Kevin Waldron, for his much appreciated help with this work. Throughout my PhD he has been constantly available for guidance, advice and discussion whenever I have needed him. I have thoroughly enjoyed spending time working in his lab and will always fondly remember my time spent with him and his group. I would also like to thank the post-doctoral members of the Waldron group, Dr Emma Tarrant and Dr Gus Pelicioli-Riboldi for their invaluable help and friendship. A special mention must be made of Anna Barwinska-Sendra who joined the Waldron group a year after myself and who quickly became an invaluable support of mine, Anna has contributed hugely to the Waldron lab in terms of its organisation and efficiency and without this often invisible contribution I'm not sure how I would have managed. I would also like to thank members of the Salgado group, who share a lab with the Waldron group at this time, for their help and friendship. I would also like to thank members of the Lewis group for their particular help with protein purification and getting the right dose of laughter on a tough day; Professor Chris Dennison and his group, for all things regarding copper; and other 'miscellaneous' members of the institute, past and present; Stuart York, Deborah Attwood, Dr Will Stanley, Dr Martin Sim, Suzanne Escolme, Dr Luisa Wakeling, Professor Dianne Ford, Professor Grant Burgess and Dr Susanne Pohl. Thanks must also go to Professor Colin Harwood who has helped me with several much appreciated guiding discussions with regards to the direction of my work.

I would also like to thank the Morrissey group at the University of Leicester for kindly letting us utilise their strains and for letting me spend some time in their lab, as well as Dr Saito of the Woods Hole Oceanographic Institute in Massachusetts for performing mass spectrometry analysis on samples that aided in the conclusion of this work.

Outside of the institute I would like to thank my flatmates over the last few years for helping me to live a happy and fun-filled life and keeping me sane; Semeli Platsaki, Ashleigh Wilson, Amy Priestley, Rhiannon Parrett, Emma Thomas and last but not least, David Graham. Also my friends Gina Ledgard, Fiona Richardson and Alex Phillips who always make me smile; and all of my other friends whose names I cannot list here. Finally I would like to acknowledge my family for their help in all things; specifically my sister Lily who is a light in my life, and my parents, Lesley and Paul, from whom I get all the support, love and guidance anyone could ever ask for.

Contents

Table of Figures

Abbreviations

Abbreviation	Full name
A	absorbance
APS	ammonium persulphate
ATP	adenosine triphosphate
BCA	bicinchoninic acid
BCS	bathocuproine disulphonate
bp	base pair
BSA	bovine calf serum
c	concentration
CA	community-associated
CCR	carbon catabolite repression
CPC	cysteine-proline-cysteine
cv	column volumes
DNA	deoxyribonucleic acid
DTNB	5,5'-dithiobis-(2-nitrobenzoic acid)
DTT	dithiolthreitol
EDTA	ethylenediaminetetraacetic acid
Fe-S	Iron-Sulphur
FPLC	fast protein liquid chromatography
g	grams
g	gravitational force
G3P	glyceraldehyde 3-phosphate
GAPDH	glyceraldehyde 3-phosphate dehydrogenase
GTP	guanidine triphosphate
HA	healthcare-associated
HEPES	4-(2-hydroxyethyl)-1-piperazineethanesulfonic acid
HMA	heavy metal associated
IAA	iminodiacetic acid-agarose
ICP-MS	inductively coupled plasma mass-spectrometry
IPTG	isopropyl β-D-1-thiogalactopyranoside
kb	kilobase
kDa	kilo-Dalton
l	path length
LB	lysogeny broth
M	molar
mAu	milli absorbance units
mg	milligrams
ml	millilitres
MLST	multi-locus sequence typing
mM	millimolar
mRNA	messenger ribonucleic acid

MRSA	methicillin resistant *Staphylococcus aureus*
MSCRAMM	microbial surface components recognizing adhesive matrix molecules
MSSA	methicillin resistant *Staphylococcus aureus*
NAD^+/NADH	nicotinamide adenine dinucleotide/reduced NAD^+
$NADP^+$/NADPH	nicotinamide adenine dinucleotide phosphate/reduced $NADP^+$
NCTC	National Collection of Type Cultures
nm	nanometres
NTA	nitrilotriacetic acid
°C	degrees Celsius
OD	optical density
ORF	open reading frame
PCR	polymerase chain reaction
PDB	Protein Data Bank
PFGE	pulse-field gel electrophoresis
pI	iso-electric point
ppb	parts per billion
ppm	parts per million
PPP	pentose phosphate pathway
PSM	phenol-soluble modulins
PTS	phosphoenolpyruvate sugar phosphotransferase system
PVL	Panton-Valentine leukocidin
RNA	ribonucleic acid
ROS	reactive oxygen species
rpm	revolutions per minute
SDS	sodium dodecyl sulphate
SDS-PAGE	sodium dodecyl sulphate-polyacrylamide gel electrophoresis
SEC	size exclusion chromatography
TAE	Tris base, acetic acid, EDTA
TCA	tri-carboxylic acid
TCEP	tris(2-carboxyethyl)phosphine
TEMED	tetramethylethylenediamine
TEV	tobacco etch virus
TM	tris minimal medium
Tris	tris(hydroxymethyl)aminomethane
TSB	tryptic soy broth
TSM	Tris succinate medium
UV	ultra-violet
VRSA	vancomycin resistant *Staphylococcus aureus*
w/v	weight to volume
WT	wild-type
µg	micrograms
µl	microlitres
µM	micromolar
Ɛ	extinction coefficient

Chapter 1. Introduction

1.1 Preface

Staphylococcus aureus (*S. aureus*) is a species of Gram-positive bacteria morphologically classed as cocci, which grows in small clusters resembling a bunch of grapes (*staphylē* being the Greek for grape and *kókkos* for granule). Typically colonies appear golden in colour due to its production of the staphyloxanthin pigment (*aureus* being from the Latin for golden)[1]. It exists commensally with humans and other mammalian species, being found on the skin of millions of people without causing disease[2]. However, in carriers with compromised immune systems or due to increased virulence of current strains, *S. aureus* may cause a wide range of pathological conditions, the symptoms of which depend heavily on the locality of the infection and the genetics of the pathogen and host. Infections can result in a wide range of symptoms, from mild skin lesions through to life-threatening systemic diseases in severe cases.

The advent and eventual widespread use of antibiotics from the middle of the 20th century saw a dramatic fall in morbidity due to *S. aureus*, a trend that continued until the end of the century. However, penicillin resistance was reported as early as 1948[3], with initial reports of methicillin resistance first emerging in the United Kingdom just a year after methicillin was brought into general use in 1960[4]. These were quickly followed by further reports from around the developed world. By 2014, there had been incidences of *S. aureus* resistance to all classes of clinically available, non-experimental antibiotics[5-7].

This trend of broadening and increasing antibiotic resistance presents modern medicine with the concerning prospect of returning to the pre-antibiotic world, in which patients with virulent *S. aureus* infections suffered mortality rates of around 80%[8]. Without an adequate increase in our ability to treat emerging antibiotic resistant strains, morbidity and mortality from *S. aureus* infection is likely to increase.

Modern antibiotics are often thought of as the only defence against infectious pathogens. However, other agents and practices that have a significant effect on the incidence and spread of such diseases should also be considered as they may present effective concurrent or alternative remedies.

Recently, the transition metal copper has been deployed for use in the manufacture of clinical devices and dressings such as catheters and plasters. Some hospitals have also trialled the use of copper-coated door handles, copper-coated surgical trolleys and other copper-coated utensils that are easily contaminated[9,10]. These practices have proven effective at preventing surface contamination and therefore spread of *S. aureus* and other species of bacteria.

Copper is an effective wide-spectrum antimicrobial agent, but the antibacterial mechanism of copper is poorly understood despite its increasing clinical usage. The literature is awash with statements alluding to the production of reactive oxygen species, mis-metallation, and erroneous binding by copper. These mechanisms may all have a role to play in copper toxicity, but thorough interrogation of existing evidence remains paramount and further research into the mechanisms of copper toxicity is required.

Despite this bactericidal nature, copper is also a bio-metal; that is, it is utilised by organisms, including *S. aureus*, for the essential function of numerous enzymes, for many of which it is indispensable.

Faced with mounting antibiotic resistance to *S. aureus*, it is imperative that all forms of antibacterial agents be exploited for their properties. In order to do this most effectively with copper, an understanding of its bactericidal properties and its mechanism of action warrants further investigation, which will enable us to develop more cost-effective copper-dependent treatments and to assess the risk of copper resistance developing in bacteria. A broad aim of this body of work is to develop a deeper understanding of copper toxicity in *S. aureus*.

1.2 Staphylococcus aureus

1.2.1 Morphology and Pathogenesis

The Gram-positive bacterium *S. aureus* is a non-motile, pathogenic, cocci bacterial species that can cause opportunistic disease in numerous mammalian species including cows, horses, pigs and humans, where it can have a significant impact on health. The closely related non-pathogenic bacterium *Staphylococcus epidermidis* is commensal in most populations (although it can also cause disease in rare cases[11]). Equally, *S. aureus* has also been found to be commensal on the skin in variable populations; a recent European study found the rate of commensality to be between 15 and 25% in 9 countries studied[2]. It is unclear how commensal strains develop pathogenicity.

Virulence determinants of *S. aureus* include catalase, alpha-toxin, gamma-toxin, Panton-Valentine leukocidin (PVL) and phenol soluble modulins (PSMs), as well as those belonging to the MSCRAMM (microbial surface components recognizing adhesive matrix molecules) family[12,13]. These either are or are not present in various clonal strains, and their presence or absence dictates strain virulence. Notably, PVL genes are actually endogenous to a bacteriophage of *S. aureus*, and contribute to particularly aggressive staphylococcal necrotic lesion pathology most commonly seen in USA300 and related strains of *S. aureus*[14,15]. Antibiotic resistance of *S. aureus* is well documented and many strains are now susceptible to just a few 'antibiotics of last resort'[7].

This pathogen is a major cause of nosocomial infections, contributing to lengthier stays in hospitals and sometimes causing secondary systemic disease in patients that can be fatal[16]. This detracts not only from patient welfare but also has high long-term healthcare costs. In the UK and other parts of the developed world, recent increases in hygiene precautions have gone some way in preventing nosocomial spread[17,18], but *S. aureus* infections remain a significant problem.

More recently, outbreaks of community acquired *S. aureus* have been identified as being caused by strains with separate genotypes, with different virulence factors to those traditionally found in hospitals[19]. Yet these have been found to be increasing their presence in hospital settings too[20,21], demonstrating the rapidity at which different strains can be transferred between settings.

Due to the aforementioned capability of *S. aureus* to infect farm animals, outbreaks are also a problem for the agricultural sector[22]. Both nosocomial and community *S. aureus* infections in man, alongside livestock epidemics, place a heavy healthcare and financial burden upon their respective sectors, making new strategies for effective treatment and prevention of this pathogen a high priority for research.

1.2.2 Nomenclature and Strains

The nomenclature regarding strain variants of *S. aureus* is complex. Historically, healthcare associated (HA), community associated (CA) and livestock associated (LA) samples collected around the world have been recorded separately, often according to different classification systems, meaning that there is no way of knowing the relationships of all documented stains without very significant effort. Laboratory strain collections usually derive from a clinical isolate, extending this problem to these groups of strains. In this work, use has been made of several strains that are all derivatives of the parent strain *S. aureus* NCTC8325 (see Table 2.1).

NCTC8325 was isolated in 1960 from a sepsis patient and was chosen as a model *S. aureus* strain due to its sensitivity to all antibiotics used at that time[23]. As part of the Richard Novick strain collection it was designated RN1. Subsequently, this strain was found to harbour a number of prophages as well as mutations in the *rsbU* and *tcaR* genes. Step-wise removal of said prophages produced the strain 8325-4 (also known as RN0450), and further targeted correction of the mutated *rsbU* gene gave rise to SH1000[24]. These modifications of RN1/NCTC8325 and its derivatives allow SH1000 to be used as an adequate model organism when compared to a number of other common model strains in existence[23]. The restoration of a functional *rsbU* is particularly noteworthy due to its complex and seemingly global regulatory function.

The *rsbU* gene encodes a phosphatase that is part of the *sigB* operon that regulates production of a secondary sigma factor, σB[25]. Sigma factors are important regulatory proteins that form a holoenzyme with the ribonucleic acid (RNA) polymerase core unit, allowing transcription to take place. *S. aureus* σB is important during stationary phase and under particular stress conditions for appropriate expression of numerous genes[25]. It has also been suggested to play a role in regulating the global regulatory operons *agr*

and *sar*[26] as well as in antibiotic resistance[27]. Its absence results in a number of phenotypic changes during infection models and in laboratory work, making its presence essential for proper comparison to wild-type strains. Hence, care must be taken to check that the *rsbU* status of strains is known.

'NCTC' of NCTC8325 is an acronym for National Collection of Type Cultures, the institution where this strain was first recorded in the UK, and 'RN' of RN1 are the initials of Richard Novick a Professor of microbiology who specialised in the study of *S. aureus;* these strains are therefore named somewhat arbitrarily. An international standardised method of naming and categorising the many strains of *S. aureus* has not been agreed. However, methods of categorising them into some sort of genetic order have been established and from these a convention for naming strains seems to be emerging – something which would very much aid in the study of this organism. Four methods are currently in use for the molecular typing of *S. aureus*; pulsed-field gel-electrophoresis (PFGE), *spa* typing, multi-locus sequence typing (MLST) and, for methicillin resistant *Staphylococcus aureus* (MRSA) strains, SCC*mec* typing.

1.2.3 Clinical relevance, Epidemiology and Commensality

The study of *S. aureus* would not warrant as much attention as it receives if it were not for the pathogenic nature of the organism. *S. aureus* is the aetiological agent of a wide range of diseases varying greatly in severity and manifestation, as demonstrated in Figure 1.1. Despite its description around a century ago and even with constant improvements in healthcare and novel therapeutics, *S. aureus* remains a significant nosocomial problem and is evolving into a virulent community-acquired infection.

Much of what we know about *S. aureus* epidemiology is focused on its occurrence in the developed world, with little known about its presence or genetics in Africa, South America, and Asia (excluding Japan)[28]. However, from data gathered it is thought that approximately one-fifth to one-third of people carry *S. aureus* commensally[28], mostly nasally, although the carriage rate and strain variants carried can differ greatly from region to region[2], highlighting the genetic diversity of *S. aureus*. The mechanisms that dictate whether a strain will be commensal or pathogenic are complex, being governed by both the genetics of the bacteria and host. One recent study observed that USA300,

the pathogenic MRSA strain currently prevalent in the United States, was more virulent than a well-characterised commensal strain, A502; but resulted in a lower level of interferon I (IFN I) signalling than its commensal counterpart. However, if the commensal strain managed to bypass the mucosal barrier it resulted in higher mortality in a mouse model than USA300[29]. Further research is required, but such studies demonstrate a high likelihood that a large range of factors influences the virulence, commensality and invasiveness of strains.

In Europe, North America, Australia and Japan, where *S. aureus* has presented a major challenge and expense to healthcare organisations, *S. aureus* exists as a collection of various strains of methicillin sensitive and methicillin resistant *S. aureus* (MSSA and MRSA respectively)[30].

The precise origins of the first MRSA strains are unknown, but it was first reported in 1961 in the United Kingdom, and then quickly reported subsequently in the United States, Japan and Australia[5]. Further mutations, plasmid acquisition and horizontal gene transfer between strains has led to modern MRSA strains being widespread and resistant to many antibiotics. Most strains remain sensitive to the glycopeptide class of antibiotics, including vancomycin, although some with reduced sensitivity to these are emerging[5,31].

Commensal clinical infections of individuals with deficient immune systems may in cases lead to more serious symptoms and diseases (examples of which are shown in Figure 1.1). Notably, copper has been found to have a role to play within the innate immune system that forms part of the host defences against S. aureus. The innate immune system is the non-adaptive part of the immune system found throughout most clades of life, including in humans.

Numerous studies have shown that copper deficiency in humans leads to neutropenia and to the impaired capability of neutrophils to kill bacteria, this has been shown to be reversed upon dietary supplementation with copper[32]. What is less clear is the mechanism by which copper exerts its antimicrobial activity within the phagosome or how it contributes to increased defence against *S. aureus* infections in the first place.

As discussed later in section 1.4.1, copper is thought to cause damage to biological systems via two main routes; catalysis of the formation of reactive oxygen species that cause further downstream damage and damage to proteins via direct binding of copper. Copper accumulates within phagosomes inside of neutrophils and then exerts its toxic effects upon the bacterial cell upon phagocytosis[33]. Moreover ATP7A, a host copper transporting protein found at the host pathogen interface, as well as bacterial copper efflux pumps have been found to play a significant role in bactericidal activity in macrophages. The absence of the former results in reduced bacterial clearance and lack of the latter results in an increase in clearance, suggesting that the presence of copper is a strong contributing factor in the immune response, the absence of which can lead to increased survival of bacteria within a host [34].

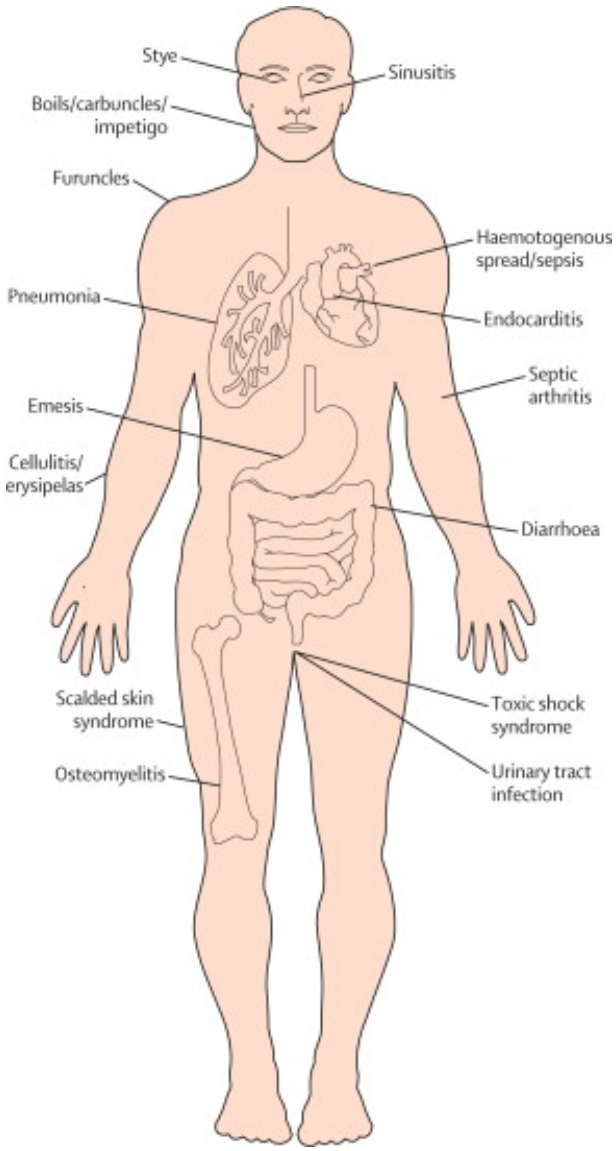

Figure 1.1. Conditions caused by *S. aureus*. Taken from Wertheim *et al*.[35] These conditions, amongst others, can all be caused by *S. aureus*. Often, symptoms are the result of the location of infection. Most strains of *S. aureus* are not normally pathogenic, but may cause disease if the immune system of the host is compromised. The most common symptoms of pathogenesis by *S. aureus* are carbuncles and sinusitis which can often be cleared by the host's own defences, without the need for clinical intervention.

1.2.4 Methicillin resistant *S. aureus* – MRSA

MRSA is usually used as a broad term for a large number of strains of *S. aureus* that have acquired resistance not just to methicillin but to a number of different antibiotics often of different classes[36]. Since the advent of the first antibiotics in the 1930s and 1940s bacteria have evolved multiple defensive mechanisms. The ability of bacteria to share genetic information via inter-species and intra-species horizontal gene transfer as well as vertical gene transfer means that as soon as one cell develops resistance to a drug there is potential for this to spread to others.

Methicillin, like other β-lactam-based antibiotics, functions by inhibiting the manufacture of peptidoglycan, the complex macromolecular structure that forms the bacterial cell wall. Before methicillin was introduced it was found that many *S. aureus* strains had started to produce a β-lactamase – an agent that is able to break down these antibiotics, which include penicillin. Methicillin was resistant to this enzyme due to slight alterations within its structure, but soon after its introduction *S. aureus* strains that produced an alternative methicillin-resistant enzyme began to appear, deemed MRSA[37].

S. aureus has traditionally been thought of as a nosocomial infection, often being referred to as healthcare-associated MRSA (HA-MRSA). However, it has been more recently found that a number of strains, unrelated to those isolated from in-patients or those having had a recent stay in hospital, exist apparently in isolation within the community. These strains have been deemed community acquired MRSA (CA-MRSA)[38]. These demonstrate high variability across different communities but frequently it is the case that CA-MRSA carries many more virulence factors than HA-MRSA and has caused the death of some otherwise healthy individuals[39,40]. Questions remain over where such strains have come from. It has been suggested that they may be 'feral descendants' of HA-MRSA strains but it appears as if the genetic differences between strains is too great for this to have occurred in such a short space of time[38].

Figure 1.2 shows the time of introduction of various antibiotics compared with the emergence of various resistant bacteria. Methicillin resistance occurred very quickly after its initial use in the clinic. However, resistance to vancomycin occurred a number of decades after its introduction, firstly in the *Enterococci*, and then in *Staphylococci*. It

has been suggested that the major gene responsible for vancomycin resistance, *vanA*, was transferred from *Enterococci* to *Staphylococci* in the gut of a co-infected individual, and the possibility of such a conjugative event has been confirmed in the laboratory[31].

Vancomycin resistant *Staphylococcus aureus* (VRSA) strains are not yet widespread amongst the population meaning that vancomycin can still often be used as a drug of last resort. However, methicillin resistance is widespread. The mechanism of resistance in this case is based upon acquisition of the *mecA* gene that encodes penicillin binding protein 2a (PBP2a), which methicillin cannot inhibit, in place of PBP2, which is inhibited by methicillin, hence peptidoglycan synthesis is able to continue using PBP2a. Detailed explanations of the mechanisms and regulation of *mecA*-mediated resistance have been provided in reviews written by Stapleton *et al.*[37] and Deurenberg *et al.*[41].

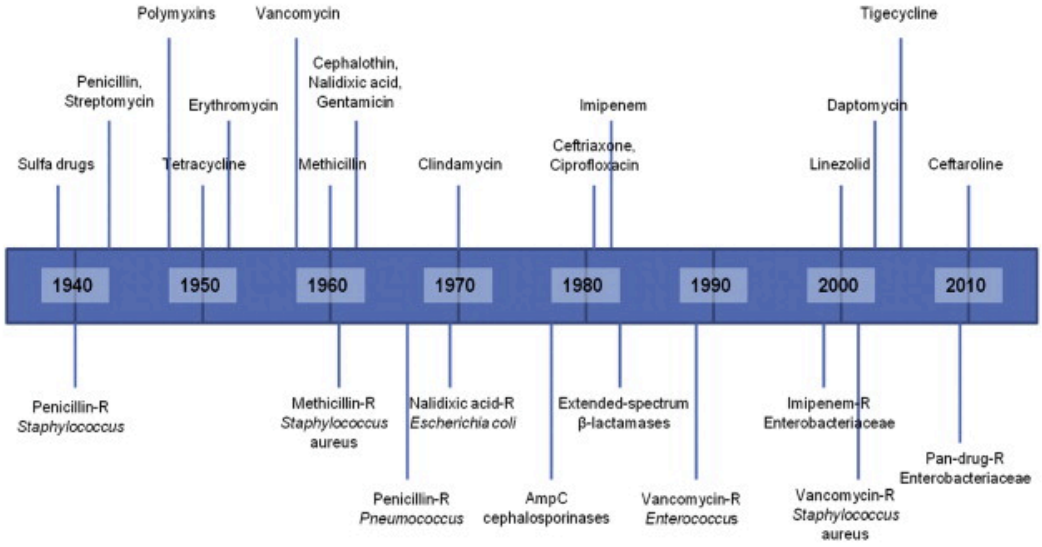

Figure 1.2. Antibiotic and antibiotic resistance development timeline. A timeline showing the years of development of various antibiotic therapies (above the line), and the years that various resistant bacterial strains emerged that were no longer susceptible to treatment with those therapies (below the line). Taken from Tang *et al.* 2014[42].

1.3 Copper homeostasis

In almost all bacteria, metal homeostasis involves the controlled acquisition of essential metals and the detoxification of excess metal ions from cells. For some metals active metal uptake systems are known, but in *S. aureus*, like in almost all bacteria, no copper importer has been found. Thus copper homeostasis appears to involve only the regulated export of excess copper from the cytoplasm.

Research on bacterial copper homeostasis has largely been performed in model organisms such as *Escherichia coli* and *Enterococcus hirae*. Therefore much of what we know about *S. aureus* copper homeostasis has foundations in genome sequence analysis and protein sequence comparisons, although some preliminary biochemical analysis and mutational phenotyping has gone some way in confirming predictions of component functions in some cases.

1.3.1 Copper homeostasis in *S. aureus*: summary of current understanding

S. aureus copper homeostasis is primarily mediated via the *cop* operon, which in most strains encodes two neighbouring genes; the *copA* gene encodes the membrane protein CopA, a copper exporting P-type ATPase, and the *copZ* gene encodes the soluble protein CopZ, a putative copper metallochaperone[43].

Regulation of the transcription of these genes is controlled by CsoR, a copper-responsive transcriptional de-repressor, which is encoded by a locus elsewhere within the genome[44,45]. Transcribed concomitantly with *csoR* are two other genes, *csoZ* and a hypothetical gene (NCBI Reference Sequence: WP_001221404.1).

CsoZ is predicted to share some of the structural features of the copper metallochaperones and was thus proposed to be a second *S. aureus* metallochaperone. Although it does not contain the typical CXXC binding motif found in CopZ and the CopZ-like N-terminal domains of CopA, it does share sequential and structural homology to such heavy-metal associated (HMA) domains.

In addition to these conserved copper homeostasis genes, a few strains also possess a plasmid-encoded system (NCBI Reference Sequence: NC_013322.1)[44], which confers a hyper resistance phenotype to copper; this plasmid locus encodes another copper-

exporting ATPase, CopB, and a multi-copper oxidase, designated *mco*, the precise function in copper detoxification of which is unclear[44,46]. This system is not present in *S. aureus* NCTC8325 or its derivatives..

1.3.2 The *cop* regulon of *S. aureus*

S. aureus, much like the model system *E. hirae*, encodes a *cop* operon; it is less complex genetically than that of *E. hirae*, with just two open reading frames (ORFs), *copA* and *copZ*. The CopA P-Type ATPase protein of *S. aureus* shares 49% sequence identity with CopA of *E. hirae*. It has been initially characterised by Sitthisak *et al.* who found that the *copA* gene in publically available *S. aureus* genomes (including NCTC8325, of which SH1000 is a derivative) had >99% sequence identity, and >75% sequence identity compared with other staphylococcal species at the nucleotide level[43].

Included in the amino-acid sequence of CopA (and more generally in copper-transporting P-type ATPases, including in archaea and eukaryotes) are the characteristic N-terminal, soluble HMA domains, which contain a Cu(I)-binding CXXC amino acid residue motif. The ferredoxin-like structure of these domains, and the presence of the CXXC motif, are also shared by CopZ[43,47]. An individual HMA domain consists of four β-strands and two α helices arrange in a $\beta\alpha\beta\beta\alpha\beta$ sequence (the ferredoxin-like fold), with the CXXC motif placed on the outside of the domain, allowing easy access for metal binding[48]. These domains share high homology to CopZ and also to eukaryotic metallochaperones such as Atx1[49], with which these domains interact *in vitro*. Interestingly, the P-Type ATPases tend to have more HMA domains in organisms that are more complex, with some eukaryotic species having up to six, whilst bacterial have a maximum of two. It is unclear whether the function of the N-terminal domains of CopA is regulatory or if they are involved in metal transfer from metallochaperones, such as CopZ, to the transporter; CopA has been shown to function without the HMA domain, which suggests a regulatory function[50]. An alternative mechanism of copper uptake by the protein has been suggested based upon a recently published crystal structure[47], by which copper enters the channel via a conserved platform region within the 'MA' and 'MB' designated helices of the transmembrane domain of the protein, and is delivered by CopZ, which interacts with this platform region[46]. Replacement of the cysteine residues with alanine residues within a motif known as the CPC (cysteine-proline-cysteine) metal binding motif of the transmembrane domain, renders CopA of *Archaeoglobus fulgidus*

inactive, but still correctly folded[51], implying that the CPC motif is directly involved in transport of the copper ions.

The CopZ metallochaperone of *S. aureus* is largely uncharacterised but shares a high degree of homology with other bacterial CopZ proteins, as well as the eukaryotic Atx1[52]. As in those examples, CopZ shows both sequence and structural homology to the N-terminal HMA domains of CopA, of which there are two in within the structure of the CopA proteins of *S. aureus* and *B. subtilis*[48,53]. The structural similarity between CopZ proteins and the HMA domains of P-type ATPases leads to a strong interaction of CopZ with the HMA domain of CopA *in vitro* and *in vivo*[54]. The role of such an interaction is unclear. Although originally proposed to be involved in delivery of copper from the metallochaperone to the export channel via the HMA domain, it is now thought that this interaction could perform a regulatory role in copper homeostasis[55]. The metallochaperone is also able to interact with a 'platform' region, a charged helical structure on the P-type ATPase, for delivery of copper as stated above[50]. A similar mechanism was suggested recently of the *S. pneumoniae* CupA metallochaperone, which is unrelated to the CopZ family, and the N-terminal domain of the *S. pneumoniae* CopA ATPase, which shares structural similarity with CupA[56,57].

Amongst these studies, none has focussed on the CopA or CopZ of *S. aureus* specifically, apart from a single study conducted by Sitthisak *et al*. which emphasised focus upon the regulation, rather than biochemistry of these components (they did, however, study the HMA domain of the *S. aureus* CopA). Sitthisak *et al*. used comparative genome analysis to propose that CopA of *S. aureus* was structurally similar to CopA proteins from other organisms, including that of *Legionella pneumophila*, in which organism crystal structure CopA was published by Gourdon *et al*[50]. In common with other organisms, the CopA of *S. aureus* has two CopZ-like HMA domains, each containing a CXXC motif, and a transmembrane CPC motif.

Sitthisak *et al*. also showed that expression of the *cop* operon was induced by concentrations of copper in the growth media as low as 5 μM copper, and also to some extent by the presence of lead and ferric ions[43]. Expression of the operon has also shown to be activated by silver in *E. coli*[58]. Concordantly, growth of a Δ*copA* mutant was more

sensitive to copper, ferric and lead ions within the media than the wild-type (WT). The mutant was also more sensitive to hydrogen peroxide, but not to paraquat, both forms of reactive oxygen species (ROS). This was suggested to be due to a build-up of copper and ferric ions within the cell which could both potentially increase levels of ROS within the cytoplasm.

Of the work performed by Sitthisak *et al*. on the HMA domains of *S. aureus* CopA, most notable was the identification of binding of these domains by iminodiacetic acid-agarose (IAA) chromatography to copper ions (as expected), but also to cadmium and cobalt, but not to lead or ferric ions, a result that may have been expected due to the described *in vivo* growth assays. Sitthisak *et al*. suggest that differences in intracellular conditions may mean that such binding may not occur *in vivo* for the same metals. They also suggest that efflux of ferric iron and lead may not require binding of the respective ions to the HMA domain, as they may efflux directly through the transmembrane domain. Sitthisak *et al.* recognise that binding of metals to the HMA domains of CopA is not necessarily linked to expression of the CopA gene (which is now certainly thought to occur via CsoR), although this idea is implied in their work; their investigation does however suggest the potential capacity of CsoR to bind to ferric and/or lead ions.

1.3.3 S. aureus CsoR

In 2010, Baker *et al.* performed transcriptomic analysis upon *S. aureus* (SH1000) and did not identify any putative copper-dependent transcriptional regulator, despite seeing a significant copper-dependent change in transcription of 48 genes (17 were upregulated and 31 downregulated)[59]. A year later, the same group published data indicating that in *S. aureus* (Newman) the *cop* operon, as well as the *cso* operon itself, are under the copper-dependent control of the CsoR transcriptional repressor[44]. This protein shows 24% and 36% amino acid sequence homology to the CsoR proteins of *Mycobacterium tuberculosis* and *B. subtilis* respectively, and 3 residues shown to be important for copper binding are conserved in *S. aureus*[44,45,60].

CsoR constitutes a relatively new family of transcriptional regulators[45], the molecular mechanism of which varies from other copper-dependent transcriptional regulators such as CopY[61]. In *S. aureus*, the CsoR protein has been found to have a Cu(I) dissociation

constant, K_{Cu}, of $10^{18.1}$ M^{-1} in *vitro*, similar to the copper affinities initially determined for the equivalent regulators from *M. tuberculosis* and *B. subtilis*[45,60,62]. Despite *B. subtilis* CsoR showing higher *in vitro* affinities for other metals, these metals did not have any effect upon transcription of *copAZ* compared with copper. The measured stoichiometry of copper binding is one Cu(I) ion per monomer of *S. aureus* CsoR[61]. In *B. subtilis* it has been shown that two CsoR tetramers bind DNA at a specific operator sequence to repress transcription, and that upon binding copper their affinity for DNA is greatly reduced, a feature likely to be conserved in the CsoR from *S. aureus*[60,62].

Notably two further ORFs are encoded on the *cso* auto-regulatory operon, *csoZ* (see above) and a hypothetical protein of unknown function or structure, NWMN_1989. A blast search confirms that these sequences are both present in the genomes of *S. aureus* Newman and 8325. It is currently not known what roles (if any) these ORFs have to play in copper homeostasis or why they are encoded at a different locus to the *cop* operon. CsoZ does not bind copper *in vitro* but it does adopt a ferredoxin-like fold (Gus Pelicioli-Riboldi, Waldron lab, unpublished data), as do CopZ and the HMA domains of CopA[63].

Collectively, the proteins of the *cop* operon maintain copper homeostasis in *S. aureus*. The P-type ATPase CopA effluxes excess copper ions from the cell, maintaining the cellular copper levels below a toxic threshold. The CopZ metallochaperone, based on homology to other systems, is predicted to sequester excess copper ions within the cytosol, and to transfer these bound ions to CopA for transport, thereby maintaining a cytosol devoid of 'free' copper ions. The expression of the *cop* operon is regulated at the transcriptional level by the action of CsoR, ensuring that copper ions are detoxified only when present in excess.

1.4 Copper toxicity

Despite the requirement of almost all organisms for relatively small amounts of copper, above certain concentrations it causes toxicity. Toxicity for the purposes of this project is best defined as a concentration of copper in the growth environment that results in lower levels of bacterial proliferation than occur in its absence. High levels of toxicity may cause cell death and therefore result in a null-growth phenotype, but this is not the only possible outcome of toxicity as cells are often able to divide at lower rates in relatively concentrated copper solutions, and to recover upon its removal (i.e.

bacteriostatic). Moreover, copper can be toxic both in solution and as a solid surface, and the way in which these forms of toxicity take effect may vary. Recently, research into solid nanoparticles has shown these also have a toxic effect, and studies are beginning to show that the innate immune system may utilise the toxicity of copper against pathogenic microorganisms. All of these are relevant for antimicrobial purposes and will be explored here.

1.4.1 Potential mechanisms

Combined knowledge of copper chemistry and bacterial copper homeostasis has led to two main hypotheses regarding the molecular mechanisms of copper toxicity:

1. Via copper-catalysed generation of ROS that subsequently exert toxicity.
2. Through direct binding of copper to proteins, blocking their normal function.

It seems likely that both of these mechanisms contribute to copper toxicity, as they are not mutually exclusive. It is conceivable that a ratio between them and/or an order of occurrence may exist, which may alter depending on copper concentration, atmospheric conditions, and solvent composition in any given system, as well as a specific bacterial species' innate abilities to counter each of these effects and their metabolic state. An excellent example of variability between bacterial species is provided by the comparison of *E. coli* and *S. pneumoniae*. *S. pneumoniae* produces high levels of hydrogen peroxide (which is known to be able to deleteriously react with copper)[64] as part of its normal metabolism, and experiences relatively high levels of ROS exposure during pathogenesis, both of which it is able to cope with effectively. One way in which it has done so is by dispensing with many of its iron-sulphur (Fe-S) cluster containing enzymes, which are thought to be a main targets of damage by ROS[65]. *E. coli* does not face the same onslaught of ROS normally, and therefore has not lost these enzymes, which have been shown to be a major target of copper toxicity in that species[66]. A complex picture of copper toxicity quickly emerges, which varies between species, and the evidence for the occurrence of each of these causes of copper toxicity is discussed below.

Mechanism of cell copper damage	**Reported in contact killing?**	**Reported in solution?**	**Reported in *S. aureus*?**	**References**
Depolarisation of membrane	Yes	No	No	[67], [68]
Copper binding to non-native proteins	No	Yes	This study	This study
Copper induced production of ROS	No	Yes	Yes	[69], [44]
Copper induced DNA damage	No	Yes	No	[70]

Table 1.1. Detailing the various mechanisms of cellular damage caused by copper in contact killing and/or solution, and whether this has been observed in *S. aureus*.

1.4.2 ROS catalysis and membrane depolarisation

In solution, copper may exist as Cu(II) or Cu(I). In water, Cu(I) is almost insoluble under aerobic conditions and forms only fleetingly, if at all, whereas it is the dominant species under reducing conditions. Both ions are extremely reactive and are known to contribute to the Haber-Weiss and Fenton reactions (Figure 1.3), which combine to contribute to ROS generation inside cells, leading to the formation of the highly reactive hydroxyl radical, which in turn has been shown to damage DNA, proteins and lipids[69,71].

For the Fenton reaction to occur intracellularly (and so for Cu(I)-induced ROS damage of chromosomal DNA or intracellular lipid and protein components to occur), reactive Cu(I) needs to be present in the cytoplasm. However, it is widely accepted that within this compartment no free copper exists[72], at least under non-toxic conditions.

This hypothesis has been brought about by the calculation of the approximate number of atoms of copper that exist within an *E. coli* cell to be around 10,000[73,74] and the subsequent finding that the sensitivity of the transcriptional regulator of copper homeostasis in *E. coli*, CueR, is such that it can detect 'free' copper ions present at a concentration several orders of magnitude less than one atom per cell. Thus any deviation from the 'normal' amount of copper within the cell, leading to a single 'free' copper ion, would result in the upregulation of homeostatic systems (CopA and CueO, a postulated copper oxidase, in this case) to remove excess copper.

Indeed, it has been found that CueR is regulated such that it constitutively allows expression of these homeostatic components under normal laboratory culture conditions, but further expression occurs as copper rises[72]. However, it remains possible that cytosolic copper could accumulate when cells are cultured under excess copper conditions, and the copper efflux systems are overwhelmed (i.e. under copper toxicity conditions).

The affinity of copper for CueR in *E. coli* and CsoR of *S. aureus* are similar, meaning that such tight control of copper is probably also present in the latter case. Copper levels within the cell presumably have to go above a threshold concentration before CopA and CopZ of *S. aureus* are unable to cope with the numbers of ions of copper present.

The question remains; if there is no free copper present in the cell then how do transcriptional regulators acquire copper? This is not clear, but it does not appear that

CopZ transfers copper to the regulator[75]; the extremely high affinity of these regulators for copper may mean that they are able to acquire copper from other copper proteins with lower affinity without a specific interaction.

Various studies have been performed to investigate the role of ROS catalysis in the mechanism of copper toxicity[59,76,77], but as of yet no conclusive conclusion has been reached. Indeed, Macomber *et al.* have even gone so far as to state that it is *not* the cause of DNA damage in *E. coli* treated with high copper. They showed that *E. coli* cultured in elevated copper conditions do not upregulate genes known to be responsible for dealing with ROS, even when these cells have been mutated to lack several of their copper homeostasis components[70]. Letelier *et al.* demonstrated that whilst some oxidative damage did occur in cells experiencing elevated copper, as measured by lipid peroxidation, what was much more likely to cause permanent cellular damage was the inhibition of a wide range of enzymes that occurred through indiscriminate binding of copper, and subsequently called for a 're-evaluation of the mechanisms underlying copper-induced toxicity in biological systems'[78].

In *S. aureus* specifically however, Baker *et al.* did find that copper induced a global transcriptional response, which included increased transcription of enzymes that deal with ROS. They did however see less growth in copper in the WT than in mutants of various genes encoding enzymes that catalyse reactions that reduce ROS levels, complicating the copper toxicity phenotype and suggesting that ROS might not be a major factor in copper toxicity in this organism.

Another copper-dependent oxidative effect observed in cells is lipid peroxidation of membranes. However, Weaver *et al.* demonstrated that the damage caused to membranes did not compromise their integrity and concluded that damage to intracellular macromolecules could be what was killing cells[79].

Haber-Weiss Reaction

$$Cu(II) + \bullet O_2^- \rightarrow Cu(I) + O_2$$

Fenton Reaction

$$Cu(I) + H_2O_2 \rightarrow Cu(II) + OH^- + \bullet OH$$

Figure 1.3. The Haber-Weiss and Fenton reactions of copper. These reactions combine to produce the highly toxic species, the hydroxyl radical. Iron can substitute for copper in these reactions, with ferric and ferrous ions replacing cupric and cuprous ions respectively.

1.4.3 Copper binding to non-copper proteins

As stated, copper is able to bind tightly to a wide range of ligands non-specifically. The Irving-Williams series of divalent metals states that Cu(II) will out-compete all other essential divalent metal ions (Mg^{2+}, Ca^{2+}, Mn^{2+}, Fe^{2+}, Co^{2+}, Ni^{2+}, Zn^{2+}) for their native enzyme binding sites, and Cu(I) is also extremely competitive[80,81], especially for binding sites that contain cysteine sidechains. Consequently as we have seen, bacterial cells make use of copper homeostatic systems to limit cytosolic copper abundance (see section 1.4.2) and to confine binding to cuproproteins by copper-trafficking through protein-protein interactions, ensuring delivery to target proteins by kinetic control and thermodynamic affinity gradients[81]. By limiting copper availability in the cytosol and producing a massive overcapacity for copper chelation, proteins compete to bind copper, rather than copper competing with other metals for a given protein, which would lead to widespread mis-metallation.

Toxic copper binding can be classed broadly into two categories: adventitious non-specific binding, which is usually weak and transient within the context of the cytoplasm; and specific copper binding to a non-native copper site, which may be of a relatively high affinity and may or may not displace another, native metal ion.

Despite the risks of toxicity, we know that most cells acquire copper within the cytoplasm at least under some conditions; this, despite the mechanism of copper import being unidentified in most cases (including in *S. aureus*). Thus, it stands to reason that cells contain copper that is bound to intracellular chemical species and that below a certain threshold these and their associated ions do not cause toxicity. Which species these are remains to be precisely answered, but those such as the abundant histidine, glutathione[82,83] or the comparable bacillithiol in Gram-positive bacteria such as *S. aureus*[84], bacterial metallothioneins[85,86] or other known copper metallochaperones or high affinity sites[87,88] are all candidates, as well as the standard copper homeostasis proteins, assumed to deal with the majority of copper present.

In a copper toxicity situation these homeostatic/detoxification binding sites must presumably become saturated as excess copper begins to accumulate in the cell. The chemical properties of copper suggest that it will soon bind to other proteins within the cell, and which proteins it binds to will depend on the same factors of access, allostery and affinity as that which guides binding to native metalloproteins under non-toxic

conditions[81]. Toxicity targets have been identified in some organisms (see below), but it is clear that the entire picture is far from complete[66,89]. Indeed there is also evidence for non-specific adventitious binding[66].

In *S. aureus* initial copper increase leads to the transcription of the *cop* operon (See section 3.4.2.1). Subsequently, a hypothesis can be formed whereby increased copper is dealt with by the copper homeostasis machinery and does not bind to non-native copper ligands, because the affinity of CsoR is sufficiently tight that its metalation (and subsequent de-repression of the *cop* operon) should be an early event under elevated copper conditions.

Under high copper concentrations, are cells able to attain a sufficient concentration of production of CopZ and CopA or other non-toxic copper binding proteins or species that can deal with copper stress? The answer from growth phenotypes is a resounding no[59], as cells are not able to survive in copper conditions above defined concentrations which differ depending on the species and conditions; and this presents a likely selection pressure for copper hyper-resistant mutant strains.

The mixed evidence regarding ROS production (see above) previously thought of as the most likely mechanism of toxicity appears to support another route, namely protein malfunction due to non-specific copper binding, as was first described in *E. coli* by Macomber and Imlay[66].

Here it was found that copper led to the degradation of iron-coordination centres in several enzymes containing iron-sulphur (Fe-S) clusters[66]. An auxotrophy in branched chain amino acid synthesis was observed in cells cultured in the presence of high copper, which implied such Fe-S cluster-containing enzymes are required when cells are cultured in a minimal medium lacking selected amino acids. Upon supplementation with these branched-chain amino acids (isoleucine, leucine and valine), or overexpression of the vulnerable enzymes required for their synthesis, growth is restored. However, even amino acid supplementation was unable to completely restore growth, suggesting that other proteins involved in other metabolic pathways may also be targets of copper toxicity. Other Fe-S cluster containing enzymes involved in carbon metabolism were also affected, such as fumarase A, but in the presence of glucose or other sugars that are able to be metabolised via glycolysis these enzymes are expressed at low levels and thus are

not deemed major targets of toxicity. Throughout their work, ROS generated by copper were detected but were not found to be the cause of toxicity.

Further to this work performed in *E. coli*, Chillappagari *et al.* have also demonstrated that iron sulphur cluster formation is affected by copper toxicity in *B. subtilis*[90]. They demonstrated that an essential Fe-S cluster scaffold protein, SufU, alongside other proteins necessary for Fe-S cluster biosynthesis were upregulated strongly in a probable attempt by the cell to maintain levels of Fe-S cluster containing proteins. They did not see strong upregulation of the *perR* regulon from which they concluded that oxidative stress was not playing a major role in copper toxicity in *B. subtilis*. Djoko and McEwan showed similar effects of copper in *Neisseria gonorrhoea*, demonstrating in this case that the copper-dependent damage of Fe-S clusters mainly affected HemN, an enzyme critical to haem biosynthesis. Copper toxicity thereby gave rise to haem deficiency; haem is necessary for the functioning of catalase and a nitrate reductase that are important in the neutralisation of ROS[91]. These studies contribute to the identification of a strong link between iron and copper homeostasis.

As evidence mounts that copper toxicity cannot be sufficiently explained by the generation of ROS it is becoming clearer that copper binding to cellular proteins are a cause of the toxic effects observed in high copper conditions. The subsequent difficulty for investigators lies in identifying targets and then demonstrating that these targets are consequential *in vivo*. Further complications lie in the specific conditions in which the bacteria are cultured (or are found in the environment). For example, glucose availability alters the abundance and importance of many metabolic enzymes within bacteria, impacting upon how copper may cause toxicity under those conditions relative to low-glucose conditions. Identifying environmentally relevant conditions is also of interest.

1.4.4 Antimicrobial copper surfaces

Thus far, each mechanism has involved copper in solution, which in aerobic conditions will exist as the Cu(II) ion and in anaerobic conditions as the Cu(I) ion which are able to react freely with other solutes and components of a bacterial cell in culture. Within a solid copper surface, whether that is pure copper or an alloy containing copper, the metal ions are locked into an ionic lattice crystal structure that is difficult to disrupt, meaning that interaction of copper with bacteria here may be very different.

A comprehensive review of solid copper surface toxicity was carried out in 2011 by Grass *et al.* which discusses its potential antimicrobial mechanisms[67]. Studies undertaken to test how long it takes to eliminate bacteria from a surface have used various techniques to apply cells, and the biocidal effect of such application has been termed contact killing. Consistently, these experiments have found that when 'dry' material is placed onto a surface, biocidal activity of the surface is exhibited within just minutes. Alternatively, when using 'wet' application, the bacteria were often able to survive for hours. These types of experiments have been carried out on a range of pathogenic bacteria, such as *Salmonella enterica*[92], *E. coli* O157[93,94] (EHEC), *Listeria monocytogenes*[95], *Mycobacterium tuberculosis*[96], *Clostridium dificile*[97,98] and various strains of *S. aureus*[99,100], as well as on various pathogenic fungi including *Candida albicans* and *Aspergillus fumigatus*[101].

Experimentally, 'wet' application provides a solvent in which copper may dissolve and potentially access the cell, as cells are applied suspended in a growth medium to a piece of solid copper or 'coupon'. Consequently, it is likely that these cells experience toxicity by the same mechanism as those in liquid culture, at least to some extent, just of a much reduced volume. Alternatively, 'dry' application aims to remove this solvent component. This is done by using cells concentrated by centrifugation and then applied using a cotton swab. In their 2008 paper, Espirito Santo *et al.* state that approximately 7% of the material applied is in fact liquid (i.e. wet) but that the coupon is completely dry within 5 seconds of application[102]. However, it may be that some residual solvent remains that is undetectable or that 5 seconds is a long enough period of time for the copper surface to exert its toxicity upon dissolution into Cu(II) (cupric ions specifically due to the prevalent aerobic conditions).

Completely dry application seems technically unfeasible or at least extremely difficult to guarantee, as all bacterial cells will be hydrated to some extent or would not be viable. One possibility is that 'dry' application provides such a small volume of solvent that resulting copper ion concentrations are extremely high, resulting in the rapid killing times observed. On the other hand, how solid copper, presumably locked in crystalline form, enters solution (requiring an oxidation event) or is able to react with a 'dry' bacterial cell is not clear mechanistically.

Oxidising membranous enzymes could play a role in releasing copper from dry surfaces, although there is debate concerning the existence of such enzymes at this location. Moreover, research has shown that non-enzymatic media components are often able to complex tightly with copper, and Molteni *et al.* showed recently that biocidal kinetics were strongly affected by the composition of the medium in which resuspended cells were applied to a copper surface[103,104], with water showing the slowest rate. It may be the case that relatively few copper ions are required to exert toxicity, meaning that passive dissolution may be enough to reach this concentration in a matter of hours, and therefore active decomposition of solid copper to its ions is not needed.

A recent study using a honeycomb structure polymer that prevents bacterial contact with a solid surface but allows solvent access, showed that direct bacterial contact with copper did not affect the release of copper ions from a solid copper surface, but that cells not in direct contact experienced reduced biocidal activity[105]. Their observation that the toxicity of copper ions increased with the presence of an iron solid surface compared with glass (without the presence of the honeycomb polymer) led them to conclude that direct contact of the bacteria with an iron surface contributes to membrane permeability which allows subsequent cell damage by copper ions that enter the cell[105]. Neither iron nor glass have been shown to induce contact killing, and other metallic surfaces have yet to be tested for this effect. Notably, *E. coli* cells lacking their *cop* operon copper homeostasis components showed a small but significant decrease in killing time on copper surfaces, suggesting that intracellular copper has a role to play in the mechanism[102].

Thus it is likely that contact killing is mediated, at least in part, via the same mechanisms as that observed in liquid media containing excess copper, but that direct contact of cells with an iron or copper surface contribute to faster killing by allowing these ions to access the intracellular space faster. Such speed of access could perhaps be mediated via membrane depolarisation, yet in light of findings made by Weaver *et al.* mentioned previously, such copper induced depolarisation would not also induce membrane permeability to copper (iron was not investigated here)[79].

Recent studies have indicated that copper-induced cell membrane damage may be a precursor to subsequent intracellular copper toxicity events[105], and peroxidation of membrane lipids and resulting membrane protein malfunction are well documented and are known precursors of increased cell permeability[71,106,107]. These facts, when aligned with evidence that reactive copper is most likely to be found in the periplasm of *E. coli,* point to a potential mechanism whereby copper-induced cell membrane damage facilitates the accumulation of increased levels of cytoplasmic copper, where it can damage intracellular species as shown to occur in the presence of copper *in vitro*[66,107].

1.5 GAPDH enzymes

The focus of this thesis is upon the binding of copper to a cytoplasmic enzyme in *S. aureus*. That cytoplasmic protein is a member of the glyceraldehyde-3-phosphate dehydrogenase (GAPDH) family called GapA, and is referred to as *Sa*GapA throughout this work with regards to the enzyme specific to *S. aureus*. This binding is the first documented case of copper binding to a protein in the cytoplasm in *S. aureus* that is not a metalloprotein (see results). Copper toxicity mediated by damage of Fe-S clusters in *E. coli* did not document copper *binding*, only copper-mediated damage to the function of the Fe-S cluster containing enzymes. Thus this binding is also potentially the first documented case of copper binding to a non-metalloprotein in the cytoplasm in bacteria more generally.

GapA is just one enzyme within the glycolytic pathway, but it performs the rate-limiting step. It is the only enzyme within the glycolysis pathway which produces NADH, producing two NADH molecules for each molecule of glucose that enters the pathway, as each glucose monomer results in two molecules of the substrate of GapA, glyceraldehyde 3-phosphate.

GapA converts glyceraldehyde 3-phosphate (G3P) into 1,3–bisphosphoglycerate. It uses NAD^+ as a cofactor which it reduces to NADH, and the reaction also requires phosphate and releases a proton (Figure 1.4). The enzyme sits within the glycolysis pathway that is evolutionarily conserved throughout all domains of life. The *S. aureus* homologue GapB may perform the reverse reaction, utilising NADPH which it converts to NADP+, in the gluconeogenesis pathway. GapA is not known to require copper or any metal for catalysis.

*Sa*GapA is a member of the GAPDH family of enzymes. This family of enzymes is widely conserved in both prokaryotes and eukaryotes, with some of the ancient genes thought to have been transferred from eubacteria to eukaryotes in the distant past[108]. Although the primary function of GapA is thought to be the reaction that it performs in glycolysis, it has also been documented as having several potential 'moonlighting' functions which are broad-ranging and not fully understood[109,110]. These include binding to and regulation of the function of other proteins, involvement in apoptosis, and interaction with telomeres in eukaryotic cells[109]. The highly conserved nature of the protein would suggest that at least some of these functions may also be conserved across species. Indeed, in *S. aureus* a fraction of *Sa*GapA has been found to be localised to the extracellular surface. The route that this fraction uses to reach such a location is unknown as the *gapA* gene possesses no pre-sequence; likewise the function of this enzyme fraction remains elusive, although it has been shown to be enzymatically active (though presumably lacks access to its cofactor and substrate at this location) and may play a role in adhesion, demonstrating that *S. aureus* GapA may also have additional moonlighting roles[111-113].

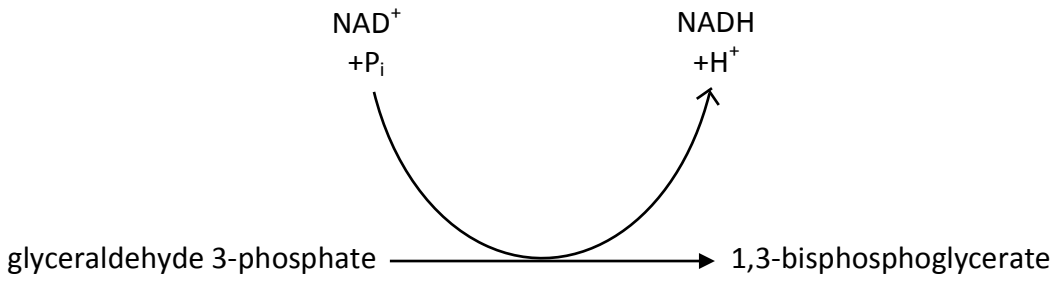

Figure 1.4. The overall reaction performed by *S. aureus* GapA. GapA is a member of the glyceraldehyde-3-phosphate dehydrogenase (GAPDH) family of enzymes, and phosphorylates its substrate, glyceraldehyde 3-phosphate (G3P), producing NADH.

1.6 GapA of *S. aureus*

The GapA enzyme is a key component of the *S. aureus* glycolytic pathway. Its theoretical molecular weight (MW) is approximately 36.29 kDa, and it is thought to form a tetramer with a total mass of ~145 kDa. The reaction that it performs is shown in Figure 1.4, which is the rate-limiting step in glycolysis.

The gene (*gapA*) encoding the GapA protein is part of the glycolytic operon. This operon is controlled by the action of the transcriptional regulator GapR on the operator sequence directly upstream of *gapA*[113], and *gapA* is followed by several other glycolytic genes (shown in Figure 1.5). The enzyme shares around 40% sequence homology with another GAPDH family enzyme expressed by *S. aureus*, GapB, which has been found to be important in gluconeogenesis, performing the opposite reaction to GapA[113].

GapA from *S. aureus* has been previously characterised and crystallised by Mukherjee *et al.* who demonstrated two essential residues within the active site of the enzyme; a histidine (His178) and a cysteine (Cys151) residue[114], the importance of these residues for the subsequently reported interaction of *Sa*GapA with copper is discussed in the following chapters.

This same study focused in detail upon the catalytic mechanism of GapA, inferring from crystal structures of: the apoprotein; the protein with the substrate bound; and the protein with the substrate and cofactor bound. The sequence of conformational changes undergone by the protein as it converts its substrate glyceraldehyde 3-phosphate (G3P) to its product 1,3-bisphosphoglycerate (1,3-BPG)[114] has thus been defined to some extent. It has been demonstrated that G3P binds initially to His178, and then forms a direct, covalent hemithioacetal bond with Cys151. A thioacyl complex is then formed, and the G3P forms a 'flip-flop' maneuvre which releases NADH before a new NAD^+ cofactor enters the active site; a second phosphate group is then added to the substrate and the product 1,3-BPG is formed and released from the enzyme. Further details are provided in Mukherjee *et al.*[114].

Oxidation of the catalytically crucial Cys151 residue of *Sa*GapA has been reported to occur after treatment of *S. aureus* COL with hydrogen peroxide, in a proteomic study by Weber *et al.*[115], which in turn inactivates the enzyme. Oxidation of the thiol group of

Cys151 to a sulfonic acid group was detected by mass spectrometry under these conditions. Notably, Weber *et al.* also found that the oxidised protein was not repaired by cells when the peroxide stress was removed, but that the reduced GapA had to be synthesised *de novo*, nor did it appear that the oxidised protein was degraded. Enzymatic activity, as measured by an *in vitro* assay, demonstrated that the GapA activity was absent when only oxidised protein was present, but returned concomitantly with the reappearance of reduced GapA. A growth arrest was also apparent in the period before new *Sa*GapA was synthesised, whereas when GapA abundance recovered, growth continued. All of these experiments were conducted in the presence of glucose; conditions in which GapA is essential for growth (see below).

One potential difficulty in the study of Weber *et al.* is the stability of peroxide stress conditions. Hydrogen peroxide, when added to growth media in small amounts, is quickly degraded or is converted to water and oxygen by catalase produced by cells. In order to detect the effects of hydrogen peroxide over a longer time period, Deng *et al.*[116] used a steady state system which constantly kept hydrogen peroxide at the same level within the media, which again contained glucose. Using this system they observed increased transcription of glycolytic as well as pentose phosphate pathway (PPP) genes, as well as a host of other genes which had not previously seen to be upregulated in experiments using a single dose of hydrogen peroxide added at the beginning of culture. A steady state system is thought to be more analogous to conditions experienced by bacteria within phagosomes[117].

Due to such studies GapA, and GAPDH enzymes in general, are starting to be considered with more importance than previously, both as central nodes in carbon metabolism and potentially as enzymes with metabolic regulatory functions. In addition, GAPDH enzymes from diverse organisms have been shown to have wider cellular functions as well (termed 'moonlighting' roles). A review from 2012 summarised recent studies that have demonstrated that GAPDH proteins may bind to DNA, be involved in transcription, bind to telomeres in mammalian cells and be involved in apoptosis[109], vastly expanding the potential roles which have previously been considered for GAPDH function.

If GapA is indeed involved in the regulation of carbon metabolism in response to stresses such as hydrogen peroxide, it would be valuable for cells to modulate its activity

in vivo. Several groups have identified that the thiol of Cys151 can be modified *in vivo*. Different outcomes of this modification have been observed which may or may not be regulatory; (1) that the oxidised thiol group of the active site cysteine (Cys149) in rat GAPDH is able to perform a different reaction to the unoxidised form, resulting in the breakdown of 1,3 bisphosphoglycerate (the product of the normal reaction shown in Figure 1.4) to 3-phosphoglycerate[118]; (2) that the S-thiolated active-site cysteine residue of *Saccharomyces cerevisiae* GAPDH would be completely inactivated, but may protect the enzyme from oxidation during ROS stress, allowing eventual dethiolation by glutaredoxin[119,120]; and (3) that the oxidised enzyme is completely inactivated, resulting in growth arrest and loss of ATP production until new enzyme is synthesised by the cell, as has been reported in *S. aureus*[115].

Whether oxidised *S. aureus* GapA is able to catalyse secondary glycolytic reactions, as suggested by Danshina *et al.*[118] in yeast, has not been directly tested. Strikingly however, arrest of growth and ATP production on inactivation of GapA by peroxide would suggest that this enzyme is essential[115]. This is not always the case, as *S. aureus* deletion mutants are still able to grow in glucose-depleted media, in which they are able to metabolise carbon sources that do not require an active glycolytic pathway. Overall, it is clear that oxidation of the active site cysteine residue of GapA does result in metabolic changes within *S. aureus*, the nuances of which have yet to be fully characterised.

With regards to virulence of *S. aureus* it has been demonstrated that GapA *is* essential in a fruit fly model[113]. It has also been suggested that the extracellular fraction of the GapA protein pool is involved in bacterial adhesion to eukaryotic cells[111,112]. Therefore, despite the non-essentiality of GapA under some growth conditions, it can be seen to offer a potential antimicrobial target that attenuates virulence, and its inhibition may function synergistically with other biocidal agents.

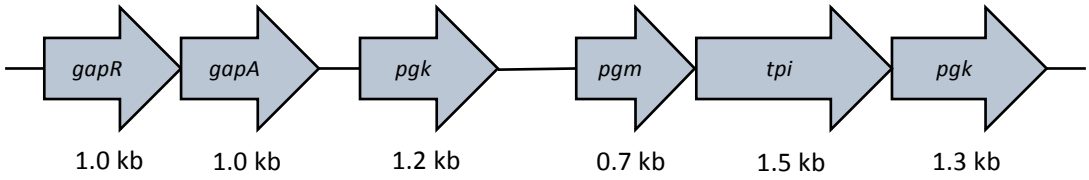

Figure 1.5. The putative glycolytic operon of *S. aureus*. This figure is based upon homologous genomic regions in *Lactobacillus plantarum, Lactobacillus sakei* and *B. subtilis*[121,122] The genes shown are: the operon repressor (*gapR*), glyceraldehyde-3-phosphate dehydrogenase A (*gapA*), phosphoglycerate kinase (*pgk*), phosphoglycerate mutase (*pgm*), triose-phosphate isomerase (*tpi*) and enolase (*eno*). The sizes of the transcripts are shown below each gene to the nearest 0.1 kilo base pairs (kb).

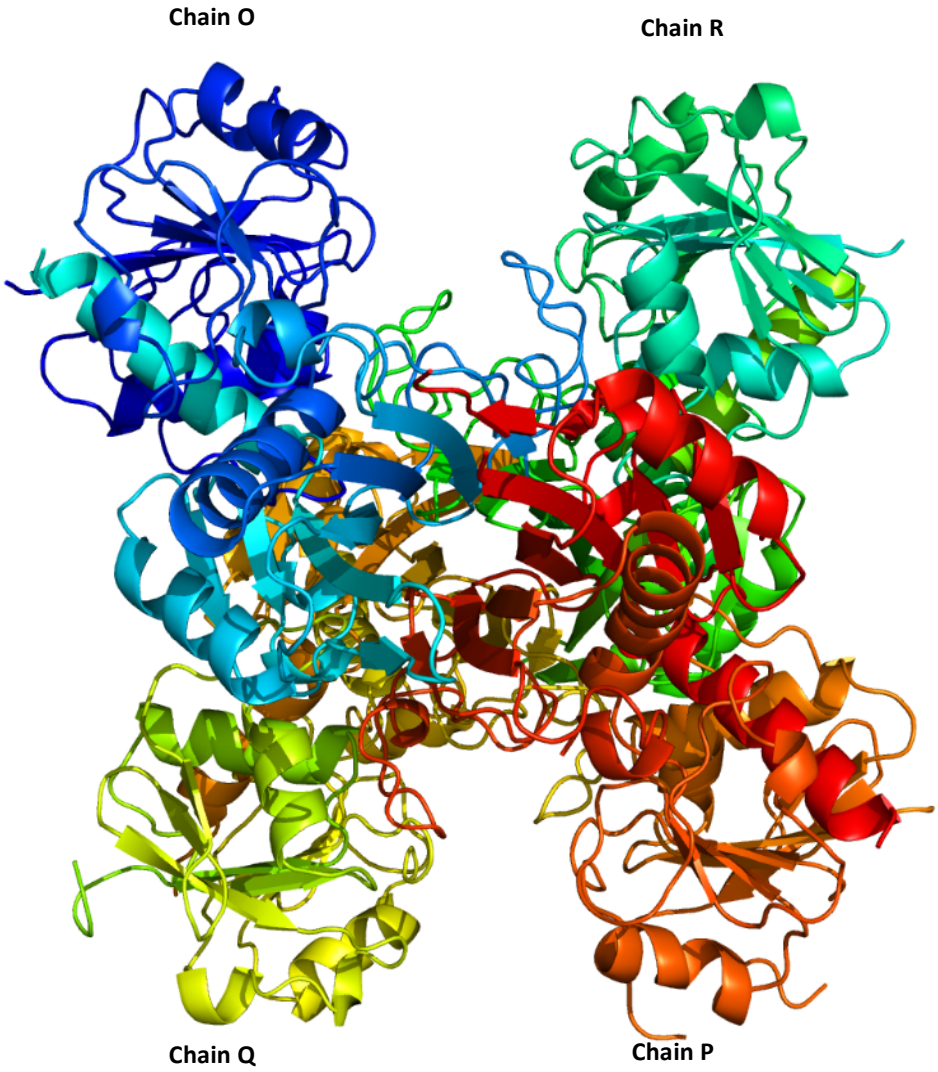

Figure 1.6. The crystal structure of *S. aureus* GapA tetramer. This figure showing the crystal structure of a monomer of *S. aureus* GapA was adapted from published X-ray crystallography data (Protein Data Bank (PDB) ID = 3lc7) acquired by Mukherjee *et al.*[114]. The cartoon representation is coloured by spectrum from N terminal (blue) to C terminal (red). This image was produced using PyMol by Anna Barwinska-Sendra.

1.7 GapA and carbon metabolism in *S. aureus*

Carbon metabolism in any organism is complex and involves many enzyme-catalysed reactions that deal with a vast number of nutrients that are found in the environment. Here we focus upon central carbon metabolism; that is, glycolysis and surrounding pathways including the pentose phosphate pathway (PPP) and the tricarboxylic acid (TCA) cycle. It is through these pathways that *S. aureus* initially produces the main energy-carrying molecules of the cell; ATP, NADH and NADPH. Figure 1.7 demonstrates glycolysis in *S. aureus.* Other potential pathways of energy generation are the phosphoenolpyruvate sugar phosphotransferase system and the methylglyoxal glycolytic bypass (the latter of which may or may not operate within *S. aureus*).

1.7.1 Glycolysis

Glycolysis is a core part of central carbon metabolism. It begins with the phosphorylation of glucose before producing a number of sugar intermediates and eventually feeding its final product, pyruvate, into the TCA cycle. One of the sugar intermediates includes the substrate of GapA, glyceraldehyde 3-phosphate.

During glycolysis energy is produced and stored in the molecules ATP and NADH. For each glucose molecule that is metabolised by the pathway, a net gain of two ATP molecules (2 are consumed and 4 are produced) and two NADH molecules is made. Both ATP and NADH are then utilised by the cell to perform energy-requiring reactions.

When the *S. aureus* cell has access to glucose, glycolysis is the primary catabolic pathway occurring. The presence of glucose has a broad effect upon most bacteria, causing the repression of up to 10% of genes[123]. These repressed genes are mostly those which help the cell to metabolise carbon sources that are not glucose or glucose metabolites. In essence *S. aureus*, along with other bacterial species, has evolved to utilise glucose first and foremost if it is present, and only to activate the genes required to deal with other carbon sources if glucose is absent. This process is known as carbon catabolite repression (CCR).

When glucose is present in the growth medium a *S. aureus* Δ*gapA* mutant will not grow[113]. This is due to CCR. The cell switches off alternative carbon source-utilising

genes and relies exclusively upon glycolysis, which does not function as one of its complement of enzymes, GapA, is not being produced in the mutant. In such a situation alternative carbon metabolism is available, but the cells are preventing themselves from utilising it by prioritising glycolysis.

Conversely, when we grow a *S. aureus* Δ*gapA* mutant in a medium that doesn't contain glucose, it is able to grow using alternative carbon sources. Whilst glucose is recognised as the primary carbon source for cells by this evolved mechanism, a secondary source is not as well established. The regulation of genes is controlled in a less restricted way in this instance than during catabolite repression, making use of whichever other energy sources are available. One study has demonstrated some order of preference, beginning with gluconate and followed by succinate, ribose, lactate and finally acetate, but this was the extent of the carbon sources used[124].

If GapA is inactivated, then alternative routes of carbon metabolism can be used, but only in the absence of glucose. There are numerous other pathways that can be utilised by *S. aureus* in order to survive if glycolysis is not functioning. As mentioned, the PPP, TCA cycle, the phosphoenolpyruvate sugar phosphotransferase system and the methylglyoxal glycolytic bypass are all ways in which the cell can continue to produce energy. Each of these offers the potential to produce at least one of the energy carrying molecules (ATP, NADH or NADPH) which can be used to sustain the cell.

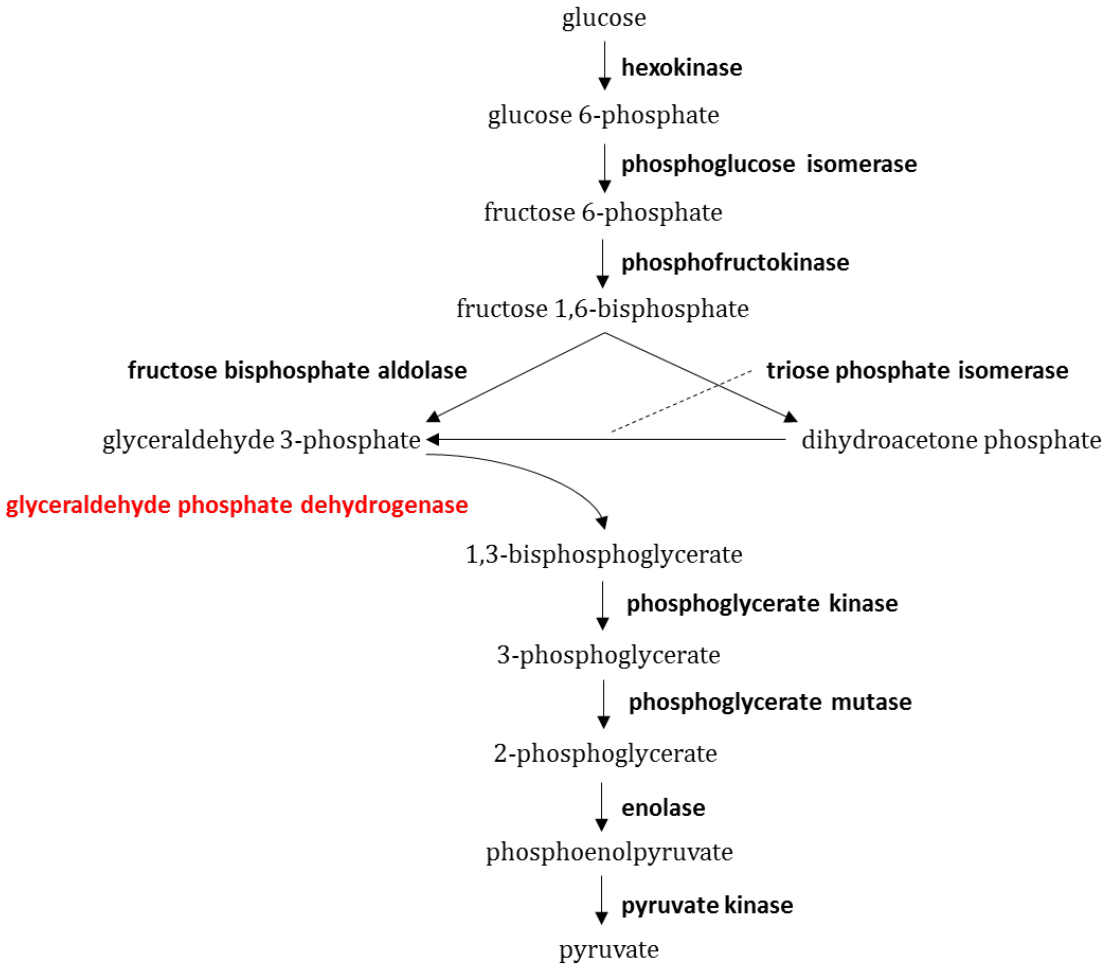

Figure 1.7. The glycolytic pathway. The metabolites and enzymes of glycolysis (shown in bold) given alongside the reaction (with triose phosphate joined to its reaction by a dashed line) that they perform within the glycolytic pathway. GapA (shown here as glyceraldehyde phosphate dehydrogenase and highlighted in red) follows the reaction of fructose bisphosphate aldolase which splits the hexose sugar fructose 1,6-bisphosphate into two triose sugars.

1.7.2 The pentose phosphate pathway

The PPP is a branch of carbon metabolism that is used by cells to produce important metabolites such as amino acid precursors, as well as NADPH, a cofactor utilised by a number of enzymes mainly involved in anabolic pathways[125]. NADPH is also important in maintaining a pool of reduced bacillithiol within the Gram-positive bacterial cell, which is required for dealing with oxidative stress and is the equivalent of glutathione found in many bacteria, acting as one of the main reductant pools with the cell[84,126]. Thus the pathway may be of particular benefit with regards to high levels of copper entering cells in terms of any oxidation caused by copper catalysis of the Fenton reaction. A caveat of the PPP is that it runs concurrently to the first phase of glycolysis, that is, the glycolytic pathway until glyceraldehyde-3 phosphate is produced (the substrate of GapA). Thus it does not provide an alternative route to the latter stages of glycolysis and ultimately into the TCA cycle which is a source of abundant energy to cells, as well as precursors to numerous important metabolites.

1.7.3 The tricarboxylic acid cycle and other energy generating pathways

The TCA cycle is a large and important part of central carbon metabolism. Numerous enzymes are involved in the cycle which provides several intermediates that are important for further biosynthesis of amino acids and other complex molecules. It also provides cells with energy in the form of 4 NADH molecules (it also provides 1 molecule of guanosine triphosphate (GTP), and ATP in some instances, although if ATP is produced then only 3 NADH molecules result) for each pyruvate molecule which enters the pathway. The cycle is repressed under glucose-replete conditions and is activated under growth-limiting conditions and when glucose is not present, under which gluconeogenesis to phosphoenolpyruvate and pyruvate provides routes to biosynthesis of multiple intracellular metabolites derived from glycolytic intermediates[127]. This cycle therefore provides an important energy generation route when glucose is not present.

Other pathways that are a potential source of energy are the phosphoenolpyruvate sugar phosphotransferase system (PTS) and the methylglyoxal glycolytic bypass[128,129].

The PTS is intimately linked to CCR and is able to generate pyruvate from phosphoenolpyruvate which can then feed into other carbon catabolism pathways[130]. It is a system that is used by many bacterial species to sense available nutrients and to

control expression based upon this availability (the essence of CCR) via a phosphorylation cascade. This is an important source of control of metabolism but in terms of energy production, it does not directly generate energy carrying molecules although phosphoenolpyruvate can enter other generating pathways.

The methylglyoxal glycolytic bypass is a potential bypass of the normal glycolytic pathway in *S. aureus*[131,132]. It is unclear if all of the enzymes necessary for the entire pathway to occur in *S. aureus* are present but it does occur in other bacteria such as *E. coli*, and *Bacillus subtilis*[131-133] and methylglyoxal is certainly an inadvertent and spontaneous byproduct of some non-enzymatic reactions within this species[134].

Each of these pathways (PPP, the TCA cycle, PTS and the methylglyoxal glycolytic bypass) has something to contribute to carbon metabolism, allowing the cell to exert flexibility when in a position of nutrient deprivation or when a step in standard carbon metabolism is blocked, such as we have hypothesised with GapA when *S. aureus* is experiencing copper stress.

1.8 Summary of Introduction

A poor understanding of copper toxicity in bacteria in general and more specifically in *S. aureus*, which is an increasingly important pathogen, led to the investigation of copper toxicity within this organism. Preliminary metalloproteomic analysis resulted in the preliminary identification of *Sa*GapA as a potential copper binding non-metalloprotein in the cytoplasm, the first of its kind. This project has undertaken the further investigation of the potential for copper binding of *Sa*GapA.

1.9 Aims and Objectives

*Sa*GapA having been identified as a potential copper binding target via preliminary work, the aims of this study were to confirm this enzyme as a *bona fide* copper binding target *in vivo*. Investigation of copper binding *in vitro* in order to establish understanding of the binding mechanism was a further aim.

1.9.1 Specific objectives

In vivo

- To characterise the effects of copper on the growth of *S. aureus* SH1000.
- To investigate the copper accumulation of cells grown in elevated copper.
- To confirm that *Sa*GapA binds copper *in vivo* under elevated copper conditions.
- To establish whether copper inhibits *Sa*GapA *in vivo*.
- To investigate the consequences of copper binding to *Sa*GapA *in vivo*.

In vitro

- To establish that copper binds to recombinant *Sa*GapA.
- To investigate the binding mechanism of copper binding, if established.
- To establish whether copper inhibits *Sa*GapA *in vitro*.

Chapter 2. Materials and Methods

2.1 Bacterial strains, growth assays and conditions

All of the strains used in this study are listed in Table 1. Cells were grown in lysogeny broth (LB) (10 g L^{-1} tryptone, 5 g L^{-1} yeast extract, 10 g L^{-1} NaCl), tryptic soy broth (TSB) (17 g L^{-1} tryptone, 5 g L^{-1} NaCl, 2.5 g L^{-1} K_2HPO_4, 0.25 % (w/v) glucose), Tris minimal medium (TM) (12.1 g L^{-1} Tris(hydroxymethyl)aminomethane (Tris), 1 x salts (25 x stock: 145 g L^{-1} NaCl, 92.5 g L^{-1} KCl, 27.5 g L^{-1} NH_4SO_4, 3.56 g L^{-1} Na_2SO_4, 6.8 g L^{-1} KH_2PO_4), 5 % (w/v) casamino acids, 0.5 µg ml^{-1} pantothenic acid, 10 µg ml^{-1} biotin, 50 µM thiamine, 500 µM $MgCl_2$, 100 µM $CaCl_2$, 10 µM niacin, 4 µg ml^{-1} tryptophan, 11 µg ml^{-1} cysteine), Townsend-Wilkinson medium (TWM), ($K_2HPO_4.H_2O$, 7000 mg L^{-1}; NaH_2PO_4, 2300 mg L^{-1}; $(NH_4)_2SO_4$, 1000 mg L^{-1}; citric acid, 210 mg L^{-1}; $MgSO_4.7H_2O$, 493 mg L^{-1}; $MgCl_2$, 50 mg L^{-1}; thiamine, 1 mg L^{-1}; niacin, 1.2 mg L^{-1}; pantothenic acid, 2.5 mg L^{-1}; biotin, 0.005 mg L^{-1}; L-amino acids; alanine, 60 mg L^{-1}; arginine, 50 mg L^{-1}; aspartic acid, 90 mg L^{-1}; cysteine, 20 mg L^{-1}; glutamic acid, 100 mg L^{-1}; glycine, 50 mg L^{-1}; histidine, 20 mg L^{-1}; isoleucine, 30 mg L^{-1}; leucine, 90 mg L^{-1}; lysine, 50 mg L^{-1}; methionine, 10 mg L^{-1}; phenylalanine, 40 mg L^{-1}; proline, 10 mg L^{-1}; serine, 30 mg L^{-1}; threonine, 30 mg L^{-1}; tryptophan, 10 mg L^{-1}; tyrosine, 50 mg L^{-1}; valine, 80 mg L^{-1}) or Tris-succinate medium (TSM) (as TM with the addition of the desired concentration of succinate).

Additional carbon sources were added to a final concentration of 1% (w/v) unless otherwise stated (see results). All media was adjusted to a pH of 7.5 prior to autoclaving. *E. coli* strains were grown in LB. When required, ampicillin (100 µg ml^{-1}), kanamycin (50 µg ml^{-1}) or tetracycline (10 µg ml^{-1}) were added to bacterial growth media. Bacterial cultures were grown at 37°C with shaking (180 rpm) unless otherwise stated. Growth analysis was performed in a plate reader. Cultures were prepared by diluting overnight starter cultures to a starting OD_{595} of 0.05 and then adding 300 µl of each culture to a sterile 96 well plate with a lid, placed in a plate-reader (Fluorostar Optima, BMG Labtech) and analysed at 595 nm, at 37 ˚C with orbital shaking.

2.2 Overexpression and Purification of r*Sa*GapA

Cloning of the open reading frame (ORF) of *gapA* into pLEICS-03, which introduces a hexa-histidine tag (His-tag) to the N-terminal of the protein, has been described previously[113]. The vector was purified using a plasmid miniprep kit (Sigma) and transformed into the *E. coli* strain BL21. The transformants were cultured in LB at 37 °C,

and expression was induced when an optical density at 595 nm (OD_{595}) of 0.6 was reached using 1 mM isopropyl-β-D-thiogalactopyranoside (IPTG) for 6 hours in an orbital shaker (180 rpm) at 37 ˚C (different expression conditions were tested, see Chapter 4)

Cells were harvested by centrifugation (3,939 *g*, 30 mins, 4 ˚C), resuspended in buffer (150 mM NaCl, 40 mM 4-(2-hydroxyethyl)-1-piperazineethanesulfonic acid (HEPES), 5 mM dithiothreitol (DTT), pH 7.5 in de-ionised (DI) water) before lysis by sonication. Insoluble material was removed by centrifugation (48,384 *g*, 30 mins, 4 ˚C). Protein was purified by Ni-nitrilotriacetic acid (NTA) affinity chromatography (5 ml His-Trap column, GE). The column was equilibrated initially with 5 column volumes of buffer (150 mM NaCl, 40 mM HEPES, 5 mM DTT, pH 7.5 in DI water) containing 20 mM imidazole and once the soluble lysate had been loaded onto the column it was washed with 5 column volumes of the same buffer containing 20 mM imidazole. The tagged enzyme was eluted using buffer (as previous) containing 300 mM imidazole, elution was halted after protein concentration had fallen, as measured the by UV-vis trace on AKTA fast protein liquid chromatography (FPLC) equipment.

The His-tag was cleaved from GapA using tobacco etch virus (TEV) protease (Sigma) added at a quarter of the final concentration of protein (as measured by Bradford) and another step of NTA affinity chromatography performed to remove TEV protease and any un-cleaved protein, which bound to the column. The cleaved protein did not bind using buffer containing 20 mM imidazole.

Further purification of GapA was achieved by size-exclusion (SE) chromatography (Superdex 200 Increase 10/300 GL column) using buffer (as previous) on an AKTA FPLC (flow-rate 1 ml min^{-1}). This was carried out upon pooled fractions from the second stage of Ni-NTA affinity containing r*Sa*GapA.

Size exclusion chromatography was followed by a final step of anion exchange chromatography (1 ml Q-HP column, GE), which was carried out under rigorously anaerobic conditions in an N_2 glovebox, to remove the reductant DTT from the final purified sample prior to copper binding experiments. The wash buffer (150 mM NaCl, 40 mM HEPES, pH 7.5 in DI water) and the final elution buffer (600 mM NaCl, 40 mM

HEPES, pH 7.5 in DI water) did not contain DTT. Before application to the anion-exchange column, the protein was treated with 1 mM (bathocuproine disulphonate) BCS to ensure the removal of any residual copper and 1 mM tris(2-carboxyethyl)phosphine (TCEP) to ensure that the protein was completely reduced. Protein was quantified where necessary using Bradford reagent using a (bovine serum albumin) BSA protein standard for construction of a standard curve from 0 to 20 μg ml^{-1} in 2.5 μg ml^{-1} graduations [135] (Thermo Scientific), or using absorbance at 280 nm using a spectrophotometer (Perkin Elmer) and an ε value of 22,920 (obtained using ExPasy ProtParam open source software).

2.3 DTNB reaction

A stock solution containing 100 mM sodium phosphate and 1 mM ethylenediaminetetraacetic acid (EDTA) at pH 8.0 was prepared and 20 mg 5,5'-dithio-*bis*-(2-nitrobenzoic acid) (DTNB) was dissolved in 5 ml of the stock under anaerobic conditions. An aliquot (50 μl) of r*Sa*GapA of unknown concentration was added to 900 μl of buffer (150 mM NaCl, 40 mM HEPES), containing 6 M guanidine hydrochloride when required, and mixed well within an anaerobic quartz cuvette (Hellma). A blank was prepared with no added protein, using 50 μl of sample buffer instead. To each of these tubes, 50 μl of the DTNB stock solution was added, again under anaerobic conditions. Spectra of the sample were then obtained using a UV/visible spectrophotometer (Perkin Elmer), with the concentration of thiols calculated using the value of the absorbance at 412 nm. If the absorbance was not constant then samples were incubated at room temperature until a further increase in absorbance was not observed. The sample of recombinant protein without added DTNB or guanidine were also analysed in this way, with an entire spectrum being taken for protein quantification at 280 nm, allowing the two protein concentration values to be compared.

2.4 Copper quantification

A solution of approximately 100 mM tetrakis(acetonitrile)copper(I) hexafluorophosphate (Sigma) was prepared anaerobically in acetonitrile and serially diluted into buffer (150 mM NaCl, 40 mM HEPES, in DI water, pH 7.5) to a final concentration of 1 mM Cu(I). A solution of 100 mM bathocuproine disulphonate (BCS) was prepared anaerobically into buffer (150 mM NaCl, 40 mM HEPES, in DI water, pH 7.5) and serially diluted in the same buffer to a final concentration of 20 μM BCS. An aliquot (1 ml) of 20 μM BCS was pipetted into an anaerobic quartz cuvette and a

UV/visible spectrum obtained in a spectrophotometer (Perkin Elmer). The solution of 1 mM tetrakis(acetonitrile)copper(I) hexafluorophosphate was placed in an anaerobic syringe, and then injected in 2 µL aliquots into the BCS solution and mixed by inversion. Spectra were taken after each injection, and the process continued until the observed maximum at 483 nm reached a peak value, i.e. the BCS was saturated with Cu(I). The change in absorbance at 483 nm with each injection of Cu(I) was used to calculate the concentration of $[Cu(I)(BCS)_2]$ complex formed using the published extinction coefficient (ε = 13,300 M^{-1} cm^{-1})[136].

2.5 Unfolding of r*Sa*GapA and fluorescence spectroscopy

Three protein samples, each of final concentration 10 µM r*Sa*GapA, were prepared from a concentrated stock in buffer (150 mM NaCl, 40 mM HEPES); one containing 8 M urea; another containing 6 M guanidine hydrochloride; the third containing only buffer. Each was placed into a fluorimetry cuvette in turn and a fluorescence spectrum acquired in a spectrofluorometer (Eclipse Model, Cary) using an excitation wavelength (λ_{ex}) of 280 nm and detection of emission at 300 to 450 nm. Data was collated for comparison of the wavelength and intensity of emission maxima.

2.6 Cu(I) titration of r*Sa*GapA and competition assay with BCS

A solution of r*Sa*GapA was prepared anaerobically in buffer (150 mM NaCl, 40 mM HEPES, pH 7.5) and placed in an anaerobic quartz cuvette (Hellma). A Cu(I) solution of 20 µM, prepared and quantified as described (Section 2.4), was titrated in 2 µl aliquots from an anaerobic syringe and the solution mixed by inversion. A UV/visible spectrum was taken using a spectrophotometer (Perkin Elmer) immediately after each addition.

For BCS competition, two solutions were prepared anaerobically. One contained 16.66 µM µM BCS in buffer (150 mM NaCl, 40 mM HEPES, pH 7.5 in DI water), the other contained 16.66 µM BCS and 5.9 µM r*Sa*GapA in the same buffer. Each of these were placed in anaerobic quartz cuvettes and titrated with a stock solution of Cu(I), with spectra obtained after each addition as described above, each addition adding to 1.79 µM Cu(I) to the solutions. Spectra collected could be analysed and concentrations of the $[Cu(I)(BCS)_2]$ quantified as described from the absorbance at 483 nm.

2.7 *Sa*GapA and r*Sa*GapA activity assay

The enzyme activity of GapA was measured using an assay adapted from Purves *et al.*[113]. A stock reaction buffer containing 2 mM nicotinamide dinucleotide (NAD^+), 2 mM glyceraldehyde 3-phosphate (G3P) (Sigma), 50 mM sodium phosphate, 1% (w/v) triethanolamine, 150 mM NaCl, 40 mM HEPES, pH 7.5 was prepared. Aliquots in which individual reagents were omitted were also prepared as required for controls. The protein sample (either cell lysate or purified recombinant protein) was added to initiate the reaction, which was measured spectroscopically using absorbance at 340 nm. The concentration of NADH produced after a given time was calculated using the extinction coefficient of NADH at 340 nm (ε = 6,220 M^{-1} cm^{-1})[137].

In the case of assaying *Sa*GapA activity within a *S. aureus* cell lysate, the soluble fractions were prepared using a bead beater (3 x 40 seconds, with 1 minute on ice in between each cycle), followed by centrifugation (10 mins, 12,000 *g*, at 4˚C) to remove insoluble material. Total protein in the lysates was quantified by Bradford assay, and then each sample was diluted into buffer (150 mM NaCl, 40 mM HEPES, pH 7.5) as required to equalise the amount of protein for the assay, protein was diluted to a concentration of 50 µg ml^{-1} in the case of lysate assays, before addition of 185 µl of reaction buffer, unless stated otherwise.

When using the plate reader spectrophotometer (Biotek), 15 µL of soluble lysate was added to each well, and 185 µl of reaction buffer added immediately before the readings were taken. The path length of the reaction in the plate was accounted for via use of a conversion factor attained through construction of standard curves of NADH in the plates (see Chapter 3).

In the case of measuring activity of purified r*Sa*GapA, protein concentration was calculated via absorbance at 280 nm or by Bradford assay, and the protein was diluted as required into buffer (150 mM NaCl, 40 mM HEPES, in DI water, pH 7.5). Aliquots (15 µl) of r*Sa*GapA were placed into the multi-well plates and the final volume brought up to 200 µl with reaction buffer immediately before the commencement of readings by the spectrophotometer. In the case of r*Sa*GapA activity assays performed in the cuvette spectrophotometer (Perkin Elmer), a quartz cuvette was used (Hellma). The r*Sa*GapA protein was added to the cuvette initially, with reaction buffer bringing the final volume

to 1 ml immediately before readings were taken. The path length of the cuvette was 1 cm. All readings were taken at 340 nm.

2.8 Mutagenesis of the *gapA* gene in construct pLEICS-03

The *gapA* gene, in plasmid pLEICS03-*Sa*GapA, was modified using a variant of QuikChange Mutagenesis (Stratagene) by polymerase chain reaction (PCR) (PCR number 1, Table 2.2), using primers that introduced a codon mutation at Cys151, His178 and Cys96 to create the plasmids (primer pairs shown in brackets after respective vectors) pLEICS03-*Sa*GapA(C151A) (QC PL03-GapA C151A For, QC PL03-GapA C151A Rev), pLEICS03-*Sa*GapA(H178A) (QC PL03-GapA H178A For, QC PL03-GapA H178A Rev) and pLEICS03-*Sa*GapA(C96A) (QC PL03-GapA C96A For, QC PL03-GapA C96A Rev) respectively. PCR conditions and primers are shown in Tables 2.2 and 2.3 respectively. After PCR, the template plasmid was digest using the *Dpn*I enzyme that digests methylated DNA but leaves un-methylated DNA intact. The digested plasmid was transformed into *E. coli* DH5α and transformants selected on LB plates containing kanamycin after overnight incubation at 37 °C. Transformants were cultured in LB overnight, and plasmid was purified from these cultures using a miniprep kit (Sigma). Confirmation of the correct mutation being present was by restriction digest using *Rsa*I (according to the protocol described in the NEB manual) of pLEICS03-*Sa*GapA(C151A) and pLEICS03-*Sa*GapA(C96A) followed by agarose gel electrophoresis, and subsequently by DNA sequencing (performed by GATC). The verified plasmids were later transformed into *E. coli* BL21 cells for overexpression.

2.9 Genotypic verification of SH1000 vs 8325-4 *rsbU* and SH1000 vs SH1000 Δ*gapA* (*gapA* mutated by insertion of a tetracycline resistance cassette)

Cultures of wild type SH1000 and 8325-4, and of the SH1000 Δ*gapA* mutant, were cultured overnight in TM medium. Tetracycline (10 mg ml^{-1}) was included in the growth medium of the SH1000 Δ*gapA* culture to select for the mutant. Cultures were centrifuged (10 minutes, 4000 *g*, 4 ˚C) and cells resuspended in 500 µl of buffer (150 mM NaCl, 40 mM HEPES, pH 7.5). Glass beads (0.1 g) were added to each cell suspension in a 2 ml screw cap tube. Cells were agitated in a bead beater (3 x 40 seconds, with 1 minute on ice in between each cycle) to lyse cells. Insoluble material was removed by centrifugation (5 minutes, 12,000 *g*, 4 ˚C, x 2). Soluble lysates were diluted in the same buffer and treated with a PCR clean-up kit (Sigma) before being used as template in the

relevant PCR reaction (Table 2.1). PCR products of the amplified gene (*rsbU* or *gapA*), generated using PCR conditions shown in Table 2.2 and primers shown in Table 2.3, were separated on 1 % (w/v) agarose gels containing GelRed (Biorad) staining agent for visualisation and imaging of bands under UV light. The amplified *rsbU* gene was further treated with restriction enzyme *Apo*I (according to the protocol described in the NEB manual), and the digested sample analysed in the same way on an agarose gel.

2.10 Size exclusion analysis of r*Sa*GapA copper binding

Aliquots of the purified r*Sa*GapA, with and without addition of Cu(I), were applied to a size exclusion column attached to an AKTA pump system (Superdex 200 Increase 10/300 GL column). Three samples of approximately 17.5 µM r*Sa*GapA, see results for precise concentrations, in 150 mM NaCl, 40 mM HEPES, pH 7.5 in DI water were prepared anaerobically, with addition of 0, 0.9 or 1.5 mole equivalents of Cu(I) (prepared as described in section 2.4). Each sample (0.5 ml) was loaded onto the column, and resolved at 1 ml min^{-1} in 150 mM NaCl, 40 mM HEPES, pH 7.5. Fractions (0.5 ml) were collected and analysed for protein content by Bradford assay, alongside the automated A_{280} analysis performed by the AKTA. Fractions were assayed for *Sa*GapA activity as required (section 2.7) and by ICP-MS for metal content as required (section 2.11).

2.11 Inductively-coupled-plasma mass-spectrometry (ICP-MS)

ICP-MS is a method for the quantification of metals and some non-metals within a sample at extremely low concentrations. It involves automated uptake of prepared samples which are then ionised within a plasma before the quantities of the ions present are assessed via mass spectrometry.

Samples were prepared by 30 x dilution in 2.5 % high-purity nitric acid (Merck) containing internal metal standards at a constant concentration of 20 parts per billion (ppb) (metals used as standards: Ag, Pt). Standards curves of the target metals (Cu, Zn, Mn, Co, Ni) were prepared using metal standard solutions (BDH) at concentrations of 0, 1, 5, 25, 50 and 100 ppb (Cu, Zn, Mn, Co, Ni), matrix-matched by addition of identical buffer to that present in the samples, and analysed alongside each set of samples. Cell lysates of *S. aureus* cells grown in varying copper concentrations were prepared as described in their preparation for the GapA activity assay (section 2.7), and were digested directly in high concentration (65%) nitric acid before dilution prior to ICP-MS

analysis. Samples from size exclusion analysis were prepared as described in their respective method sections (sections 2.14 and 2.10).

2.12 Glycerol Stocks

All bacterial strains were stored as glycerol stocks at -80°C. Glycerol stocks were produced by resuspension of overnight liquid cultures in 1 ml sterile TSB or TM (for Δ*gapA* strains) + 20% (v/v) glycerol, and stored in 2 ml screw top tubes. Strains were recovered from storage by plating onto appropriate solid medium containing required antibiotics and grown overnight at 37°C.

2.13 SDS Polyacrylamide gel electrophoresis (SDS-PAGE)

Samples were prepared with the addition of 4 x SDS-PAGE loading buffer (400 mM DTT, 8 % (w/v) sodium dodecyl sulphate (SDS), 0.4 % (w/v) bromophenol blue, 40% (w/v) glycerol) and boiled for 10 minutes. Samples were adjusted for protein concentration by Bradford assay as required.

Gels were prepared containing 12% or 15% (w/v) acrylamide in the case of the running gel (one 5 % acrylamide stacking gel contained; 2.85 ml dH_2O, 0.57 ml 1 M Tris, pH 6.8, 20 µl 20% SDS, 0.35 ml 29:1 40% acrylamide:bis-acrylamide solution, 38 µl 10% ammonium persulphate (APS), 5µl tetramethylethylenediamine (TEMED); one 12% acrylamide running gel contained; 2.9 ml dH_2O, 4.0 ml 1M Tris, pH 8.8, 54 µl 20% SDS, 3 ml 29:1 40% acrylamide:bis-acrylamide, 54 µl 10% APS, 10 µl TEMED; water and acrylamide concentrations were adjusted accordingly for 15% acrylamide gels). Electrophoresis took place in a gel tank (Biorad, 180 V, 60-90 minutes) filled with 1 x running buffer (248 mM Tris, 1.92 M glycine, 1% w/v SDS).

2.14 Metalloproteomics

Cultures (1 L each) of SH1000 and SH1000 Δ*gapA* were grown in TM medium containing 50 µM $CuSO_4$ for 6 hours at 37 ˚C with shaking (180 rpm). Cells were collected by centrifugation (3,939 *g*, 30 mins, 4 ˚C) and then resuspended in buffer (150 mM NaCl, 40 mM HEPES, pH 7.5). Cells were lysed by freeze grinding under liquid nitrogen in a pestle and mortar before being transferred to an anaerobic chamber. Once thawed anaerobically, samples were centrifuged (48,384 g, 30 mins, 4 ˚C) and returned to the chamber, and the soluble fraction was anaerobically ultra-centrifuged (80, 000 rpm, 30 mins, 4 ˚C) to remove all insoluble material.

Each resulting lysate was applied to a fresh anion exchange column (Q-HP, 1 ml column, GE), washed in buffer for 5 column volumes (40 mM HEPES, pH 7.5), and then bound proteins were eluted with 2 x 1 ml each of buffers (40 mM HEPES, pH 7.5) containing increasing concentrations of NaCl (0, 100, 200, 300, 400, 600, and 1000 mM, sequentially). Each resulting fraction of eluent was assayed for GapA activity and tested for metal concentration by ICP-MS at a dilution of 1 in 30 (see sections 2.7 and 2.11).

The first 1 ml fraction that was eluted by 400 mM NaCl was found to contain the majority of GAPDH activity in the wild type extract, and therefore this fraction (from both wild type and mutant extract) was further separated by size exclusion chromatography (flow rate, 1 ml min^{-1}; buffer, 150 mM NaCl, 40 mM HEPES, pH 7.5 in DI water; column, Superdex 200 Increase 10/300 GL, GE). All resulting fractions (0.5 ml) were again tested for metal concentration by ICP-MS at a dilution of 1 in 30 and the fractions around the *Sa*GapA peak were tested for GapA activity and for protein concentration by Bradford assay. Fractions around the *Sa*GapA peak were also analysed by SDS-PAGE in both chromatography steps as described.

2.15 DNA analysis using agarose gel electrophoresis

DNA samples (PCR product, restriction digests, etc.) were mixed with 6 x DNA loading buffer (Thermo Scientific) and loaded onto a 1% (w/v) agarose gel composed of TAE buffer (40mM Tris, 20mM acetic acid, and 1 mM EDTA in distilled water, pH 8.0). Electrophoresis of samples, and a DNA marker ladder (Thermo Scientific), took place in a gel tank (BioRad, 70 V, 45-80 mins).

2.16 Transduction of 8325-4 Δ*gapA* and verification

Transduction of the Δ*gapA* mutation from *S. aureus* 8325-4 was transduced into SH1000 to create the novel strain SH1000 Δ*gapA* using the method described by Krausz *et al*.[138]. The strain was verified by amplification of the *gapA* gene region within both the WT and mutant strains of 8325-4 and SH1000. The SH1000 *rsbU* background was also confirmed as described in section 2.9. PCR protocols and primers used are described in Tables 2.2 and 2.3 respectively. Amplification was followed by analysis by agarose gel electrophoresis.

2.17 Atomic Absorption Spectroscopy (AAS)

After preparation of a 1 mM stock of Cu(I) (section 2.4), 10 injections of 2 µl (20 µl in total) were injected from the anaerobic syringe into a 1,980 µl solution of 2 % nitric acid. This was analysed by atomic absorption spectrophotometry (Thermo Scientific). A standard curve was constructed using a metal standard (BDH) for accurate quantification, in 2 % nitric acid, with concentrations from 0 – 2 ppm copper in 0.2 ppm increments used.

2.18 Transformation of bacterial strains

DNA concentrations were acquired using a NanoDrop (Thermo Scientific). The desired plasmid (prepared using a miniprep kit, Sigma) was diluted as required to a concentration of between 20 and 120 ng μl^{-1} as measured by NanoDrop. An aliquot (2 µl) of the plasmid solution was added to a 50 µl aliquot of competent cells in a 1.5 ml tube. Competent cells were prepared as described previously using the rubidium chloride method[139]. The cells and plasmid were gently mixed and then incubated on ice for 20 minutes before being heat shocked, using a heat block, for 1 minute at 42 ˚C. The cells were placed immediately on ice for 2 minutes before 950 µl LB was added. Tubes were incubated with shaking at 37 ˚C for 1 hour, and then 200 µl spread, using sterile glass beads, onto the desired solid medium containing required antibiotics on a Petri plate (recipes as stated in section 2.1) except with the addition of 15 g L^{-1} bacterial agar in all cases, antibiotics added after sufficient cooling of the liquid agar had occurred). Plates were incubated at 37 ˚C overnight or until colonies appeared.

Strain Name	Genotype	Reference
E. coli DH5α	*fhuA2 lac(del)U169 phoA glnV44 Φ80' lacZ(del)M15 gyrA96 recA1 relA1 endA1 thi-1 hsdR17*	Taylor *et al.*, 1993
E. coli BL21	*F – ompT gal dcm lon hsdSB(rB - mB -) λ(DE3 [lacI lacUV5-T7 gene 1 ind1 sam7 nin5])*	Studier & Moffatt, 1986
S. aureus SH1000	8325-4 with rsbU mutation repaired	Horsburgh *et al.*, 2002
S. aureus 8325-4	NTCC8325 cured of prophages	Horsburgh *et al.*, 2001
S. aureus 8325-4 Δ*gapA*	NTCC8325 cured of prophages, Δ*gapA*	Purves *et al.*, 2010
S. aureus SH1000 Δ*gapA*	8325-4 with rsbU mutation repaired, Δ*gapA*	this study

Table 2.1. Strains used in this study, with their genotype and reference of origin.

PCR Number	Program	Description
1	95 ˚C, 10 mins; (95 ˚C, 30 s; 60 ˚C, 30 s; 72 ˚C, 5 mins) x 30; 72 ˚C 10 mins	used for amplification of the pLEICS03-GapA plasmid in mutagenesis
2	95 ˚C, 10 mins; (95 ˚C, 30 s; 60 ˚C, 30 s; 72 ˚C, 3 mins) x 30; 72 ˚C 10 mins	used for amplification of the *gapA* gene for mutant verification and sequencing of mutated pLEICS03-GapA open reading frame regions
3	95 ˚C, 10 mins; (95 ˚C, 30 s; 55 ˚C, 30 s; 72 ˚C, 5 mins) x 30; 72 ˚C 10 mins	used for amplification of *rsbU* for SH1000 strain verification

Table 2.2 PCR reactions listed by number with the program used and description of the purpose of each reaction. All reactions were carried out using a C1000 Touch Thermo Cycler from Biorad.

Primer name	Sequence	Application
gapA F	GGTAGAATTGGTCGTTTAGC	confirm Δ*gapA* mutant
gapA R	GAAAGTTCAGCTAAGTATGC	confirm Δ*gapA* mutant
QC PL03-GapA H178A For	GGTTTAATGACTACAATTGCTGCTTACAC AGGTGATC	quick-change of p-Leics-03 GapA overexpression vector
QC PL03-GapA H178A Rev	GATCACCTGTGTAAGCAGCAATTGTAGTC ATTAAACC	quick-change of p-Leics-03 GapA overexpression vector
QC PL03-GapA C151A For	GTTTCAGGTGCTTCAGCTACTACAAACTC ATTAG	quick-change of p-Leics-03 GapA overexpression vector
QC PL03-GapA C151A Rev	CTAATGAGTTTGTAGTAGCTGAAGCACCT GAAAC	quick-change of p-Leics-03 GapA overexpression vector
QC PL03-GapA C96A For	CGATGTAGTATTAGAAGCTACTGGTTTCT ACACTG	quick-change of p-Leics-03 GapA overexpression vector
QC PL03-GapA C96A Rev	CAGTGTAGAAACCAGTAGCTTCTAATACT ACATCG	quick-change of p-Leics-03 GapA overexpression vector
pL-03 gapA seq for	ATGGCAGTAAAAGTAGCAATTAAT	sequencing of pLEICS03 gene expression region
pL-03 gapA seq rev	TTATTTAGAAAGTTCAGCTAAGTA	sequencing of pLEICS03 gene expression region
RsbU Amp For	TCAAATTATTATATACCCATC	amplifying and sequencing *rsbU*
RsbU Amp Rev	CCTTGCTTAAGCATTTGC	amplifying and sequencing *rsbU*

Table 2.3 Primers used in this study, with sequence and application shown.

Plasmid	Description	Reference
pLEICS03-*Sa*GapA	pLEICS03 containing *gapA* open reading frame for protein expression	Purves *et al.* , 2010
pLEICS03-*Sa*GapA(C151A)	pLEICS03 containing *gapA*(C151A) open reading frame for protein expression	this study
pLEICS03-*Sa*GapA(H178A)	pLEICS03 containing *gapA*(H178A) open reading frame for protein expression	this study
pLEICS03-*Sa*GapA(C96A)	pLEICS03 containing *gapA*(C96A) open reading frame for protein expression	this study

Table 2.4. Plasmids used in this study, with description of application and reference of origin shown.

Chapter 3: *S. aureus* GapA binds to copper, and is inhibited by copper *in vivo.*

3.1 Introduction to Chapter 3

As discussed in the introduction (section 1.4), copper is toxic to *S. aureus*, whilst also being required in trace amounts for growth. In this chapter the range of copper concentrations that inhibit growth of this species was investigated in a number of different growth media and using different carbon sources.

Preliminary data from the Waldron laboratory, using chromatography-based metalloproteomics approaches, identified several candidate proteins as being associated with copper within *S. aureus* cells exposed to high copper concentrations during growth. One of these proteins was GapA. Herein, the correct identification of GapA was confirmed by comparison of copper distribution in chromatographic fractions from a Δ*gapA* mutant with wild type *S. aureus*. Furthermore, by testing the effects of copper on the activity of *Sa*GapA, we demonstrate that copper inhibits its activity and propose that this inhibition is likely mediated by direct binding of copper ions to the enzyme.

Despite there being no known copper importers in *S. aureus*, copper is present in many bacterial cells in higher concentrations than in the surrounding media, implying that copper does enter the cells by some active mechanism (Figure 3.7)[73]. Such an implication sits well with the existence of a *S. aureus* copper homeostasis system[43], conserved in many staphylococcal genomes, with the function of exporting copper from cells[140].

Intracellular reducing conditions are expected to lead to the predominant form of copper in the cytosol being the Cu(I) ion, which binds strongly to a range of ligands but particularly to cysteine thiolates, exhibiting some of the highest affinities found in any biological metal-ligand interactions[45,85]. Within the cytoplasm, copper is expected to bind overwhelmingly to the copper homeostatic proteins (CopA, CopZ and CsoR), which each demonstrate very high Cu(I) binding affinities and have evolved to suit this function[43]. However, when copper first enters the cell, or when exogenous copper levels (and thus rate of copper influx) is overwhelming, it may be assumed that the metal does not immediately bind to the usual binding ligands and may in fact bind to non-native copper proteins before being passed to proteins with higher affinities, thus having the

potential to damage non-native proteins and affect the processes in which they are involved; perceived experimentally as toxicity.

A fully effective copper homeostatic system may be expected to keep copper concentrations within cells at a concentration that does not inhibit growth. A growth defect would therefore suggest that this system is overwhelmed somewhat as intracellular copper concentrations increase; when a certain intracellular concentration is reached cells fail to grow, and above this cell death may occur.

As copper homeostasis is overwhelmed, what is copper doing that leads to the observed growth defect? Several intracellular targets of copper toxicity have been suggested, the main candidates being iron-sulphur (Fe-S) cluster containing proteins[66] (see Introduction; section 1.4.1). The indirect effects of high levels of copper have also been suggested as causative of copper toxicity, such as the catalysis of the Fenton reaction within cells, leading to oxidatively damaged macromolecules, but this has been disputed by others[70,141]. It may well be that more than one process is responsible for toxicity, and these may even differ depending on the environment that the cells are in.

It is likely that as the intracellular copper concentration rises, the damage that copper causes within cells also increases. Adventitious binding of copper to incorrect metal binding sites (and potentially displacement of the native metal ions from metalloproteins) may lead to a damaging cascade of incorrect metal binding and macromolecule oxidation that exacerbates toxicity and is an effect of the presence of overwhelming copper levels.

Identification of such non-native copper targets within cells is fraught with complexity, not least as it is difficult to isolate proteins in the same state as one would expect to find *in vivo*. The reducing potential of the intracellular environment is different to extracellular conditions; such a reducing environment is critical to the maintenance of homeostasis of all biometals as well as many other cell regulatory processes, and cell lysis may well result in a rapid change in metal occupancy sites; if such a scenario is not minimised or avoided experimentally it may lead to the artefactual identification of proteins bound to metals (false positives) or a lack of identification of protein-metal complexes that *do* occur *in vivo* (false negatives).

In order to identify potential targets, our approach has been to grow cells in media containing copper and to prepare their cytosolic extracts under rigorously anaerobic conditions to prevent oxidation of metal ions or binding protein residues, and then to minimally separate the extracts by native multi-dimensional chromatography (again using anaerobic conditions). Chromatography fractions are then analysed for protein and for metal concentration, and these two values then correlated to match the abundance of individual proteins within a sample to the abundance of metal in order to identify which proteins are associated with the copper[87,142]. In this manner one particular protein, GapA, was identified amongst others from preliminary data gathered prior to this project.

S. aureus GapA (*Sa*GapA) is thought to be primarily cytosolic where it participates in central carbon metabolism (the glycolytic pathway), but a proportion of it has been shown to be localised to cell wall fractions[143]. How it gets to this location is unclear as it has no pre-sequence; cell autolysis could be a potential route[111]. The only other previous detailed study of *Sa*GapA function focused on the enzyme localised to the cell wall, via utilisation of a whole cell GapA activity assay, and not upon the intracellular enzyme[113]. Here, we focus exclusively on *Sa*GapA within the cytoplasm of the bacteria.

3.2 The growth of *S. aureus* is inhibited in liquid media by copper in a dose-dependent manner

Initially we were interested in determining the inhibitory effect of copper on *S aureus* cells in different concentrations and in different media. This would allow for selection of a suitable concentration of copper in which to grow cells for subsequent metalloproteomics experiments. This concentration is important, as if too high a concentration is used, leading to intense growth inhibition, the effects of copper may change the metabolism of the cells to such a degree that our observed result would be an artefact of such conditions, due to changes in expression patterns or other effects. Furthermore, it was required that sufficient bacterial biomass could be acquired with which to perform metalloproteomics experiments, requiring significant cell growth, and therefore too great an inhibition of growth by copper was not desired.

Figures 3.1 and 3.2 demonstrate growth inhibition over a wide range of copper concentrations (0 – 10,000 μM $CuSO_4$) in four different types of growth media. Growth in TSB, a complex, rich medium which contains 0.25% (w/v) glucose as primary carbon source, as well as soytone (a lysate of soya) and abundant casamino acids, shows an unexpected phenotype as growth appears to be stimulated by the addition of copper up to 1,000 μM after 5 hours, with this difference being less pronounced after 16 and 24 hours. Growth was observed in TSB medium supplemented with 1,000 μM, but no growth was observed in TSB medium supplemented with 10,000 μM copper. This same trend (i.e. growth up to 1,000 μM, but no growth at 10,000 μM) was also observed in another rich medium, LB (which contains tryptone and yeast extract) and also in TSM (which contains a high level of the carbon source succinate). In these cases however the addition of copper at concentrations between 0 μM and 1,000 μM did not make a notable difference to growth.

A notable exception to the trends observed in TSB, LB and TSM media was observed in the TWM medium, which shows no growth at 1,000 μM or 10,000 μM, with no major differences in growth seen at concentrations below these. The major differences between TWM and TSM is that TSM contains succinate as a carbon source in addition to the amino acids added to it as part of a casmino acid digest, whilst TWM contains amino acids added individually (and at lower concentrations) with no additional carbon

source; in the case of TWM, cells are therefore using amino acids as their major carbon source.

TSM minus succinate was chosen, herein referred to as TM, as a standard medium in which to grow *S. aureus* due to it being a minimal, well-defined medium in which we could manipulate concentrations of metals and carbon sources and one in which *S. aureus* shows a high sensitivity to copper, allowing us to focus on relatively fine changes in growth brought about by differing copper concentrations. The primary source of amino acids in TM is a casamino acid digest (as in TSM), supplemented with added cysteine and tryptophan. This addition of just three reagents as opposed to 18 individual amino acids (as in TWM) gave less room for error during preparation of the media (several of the individual amino acids display poor solubility, leading to batch-to-batch variability) and meant that this medium was more highly standardised between batches.

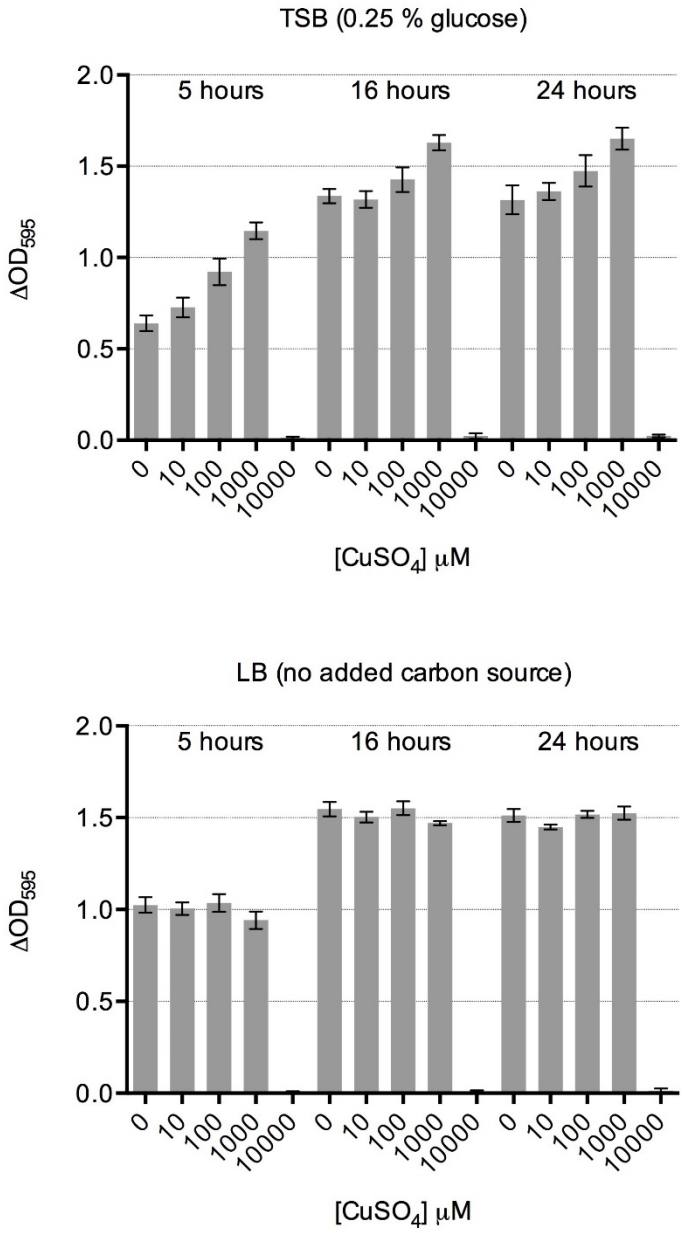

Figure 3.1. Copper inhibits the growth of *S. aureus* in a dose- and medium-dependent manner. *S. aureus* was inoculated into sterile TSB and LB containing 0, 10, 100, 1,000 and 10,000 μM $CuSO_4$ to a starting OD_{595} of 0.05, and incubated at 37°C with 180 rpm orbital shaking. OD_{595} readings were taken at 5, 16 and 24 hour time points. The change in density (ΔOD_{595}) readings are shown, i.e. with the OD_{595} at 0 hours being equivalent to 0.

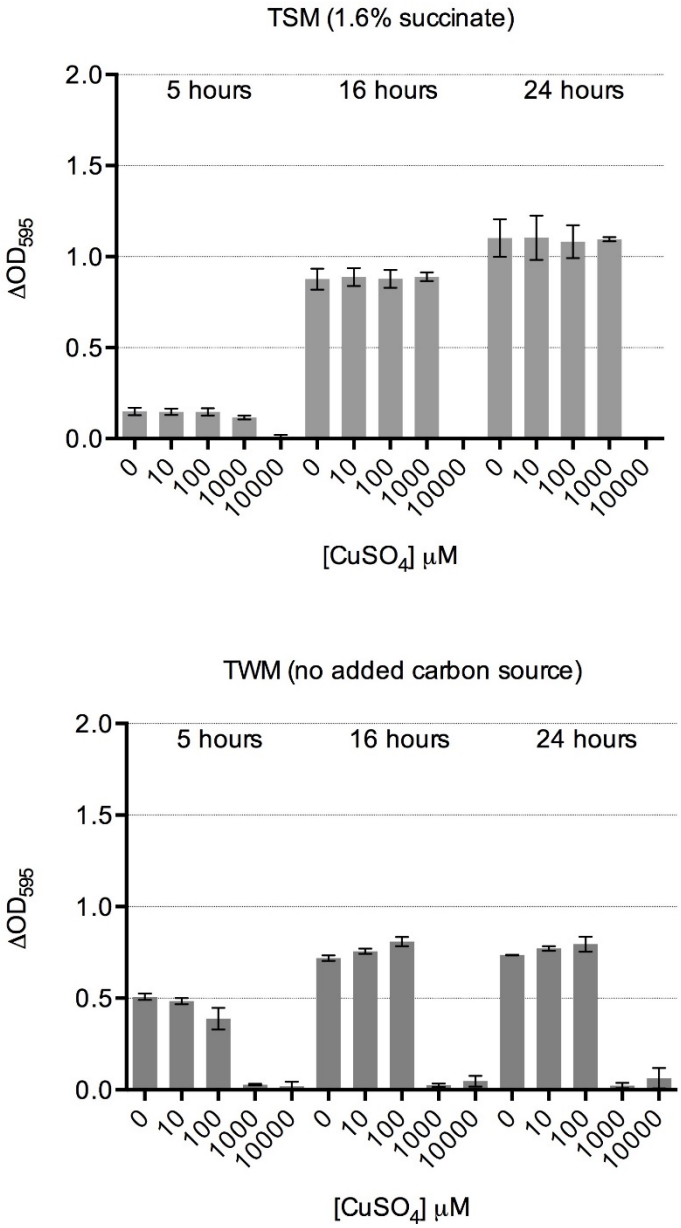

Figure 3.2. Copper inhibits the growth of *S. aureus* in a dose- and medium-dependent manner. *S. aureus* was inoculated into TWM and TSM containing 0, 10, 100, 1,000 and 10,000 μM copper to a starting OD_{595} of 0.05, and incubated at 37°C with 180 rpm orbital shaking. OD_{595} readings were taken at 5, 16 and 24 hour time points. The change in density (ΔOD_{595}) readings are shown, i.e. with the OD_{595} at 0 hours being equivalent to 0.

Growth inhibition of *S. aureus* by copper was also established at a lower range of concentrations than used in Figures 3.1 and 3.2 in TM without the addition of an additional carbon source (Figure 3.3) and then with the addition of glucose and succinate to the media (Figure 3.4).

It was observed that in the absence of an added carbon source (i.e. utilising amino acids from casamino acids alone), *S. aureus* is not able to grow to as high a density as in the presence of a carbon source. Indeed, even in the presence of 1 mM copper, *S. aureus* is able to grow significantly in TM containing glucose or succinate, whereas when those carbon sources are omitted, *S. aureus* fails to grow in this medium with 500 μM added copper. The fact that *S. aureus* does not grow to the same density as that observed in the presence of glucose is consistent with the fact that the carbon source present in TM is amino acids, which are less rich in energy than glucose, being utilised within the TCA cycle when the CCR is not occurring, as opposed to glucose, the initial metabolite of glycolysis which allows energy generation via glycolysis as well as producing useful metabolites which feeds into the TCA cycle and other pathways (see introduction).

Figure 3.5 demonstrates some of the higher concentrations of copper that *S. aureus* is able to grow in when glucose is available. It appears that between 0.5 and 2.5 mM copper, the effect of increasing copper upon growth is minor whilst remaining dose-dependent in TM containing glucose. At 3 mM copper, a large decrease in growth compared to the 2.5 mM sample, as well as the control, can be observed. As demonstrated in Figure 3.1 (top panel), cells grown in 10 mM copper do not grow, even in the presence of glucose and other complex media reagents (present in TSB). The upper limit of the copper concentration in which *S. aureus* may grow in the presence of 0.25 % (w/v) glucose is between 5 and 10 mM copper (data not shown).

It was possible from these data that high levels of glucose may be acting as a copper chelator, effectively reducing the copper concentration available to cells. As stated, copper has non-specific high affinity for many varied ligands. To explore possible chelation of copper by glucose it was demonstrated that when *S. aureus* was grown in a 3 mM inhibitory dose of copper, increasing the level of glucose present made little difference to growth (Figure 3.6). If the effect that glucose has of increasing the amount of copper required to inhibit the growth of *S. aureus* was caused by copper chelation by

glucose itself in the medium, the expected result would be that, as glucose increased, copper exerted less inhibition upon growth. In fact, copper in the presence of 5 % (w/v) glucose seems to have a greater inhibitory effect than lower concentrations of glucose, which is probably due to the osmotic pressures that such a high level of glucose would exert.

If glucose does not rescue *S. aureus* growth from copper inhibition by chelation, then possibilities remain that it does so because of the energy it provides to cells or through alterations to cellular metabolism which heighten the resistance of the cells to copper. The copper exporter in *S. aureus* (CopA) is an ATPase, therefore utilising energy released by hydrolysis of ATP to transport copper across the cell membrane, with the most efficient ATP generation occurring in the presence of glucose. This is the most obvious way that can explain the ability of cells to survive much higher concentrations of copper in the presence of glucose compared to in its absence. More energy may also be useful for cells attempting to repair intracellular damage that copper has caused. Another possibility is that the presence of glucose causes heightened expression of proteins which protect the cell from copper damage, for example through a chelating mechanism. An example of such a protein to be highly expressed in the presence of glucose is *Sa*GapA.

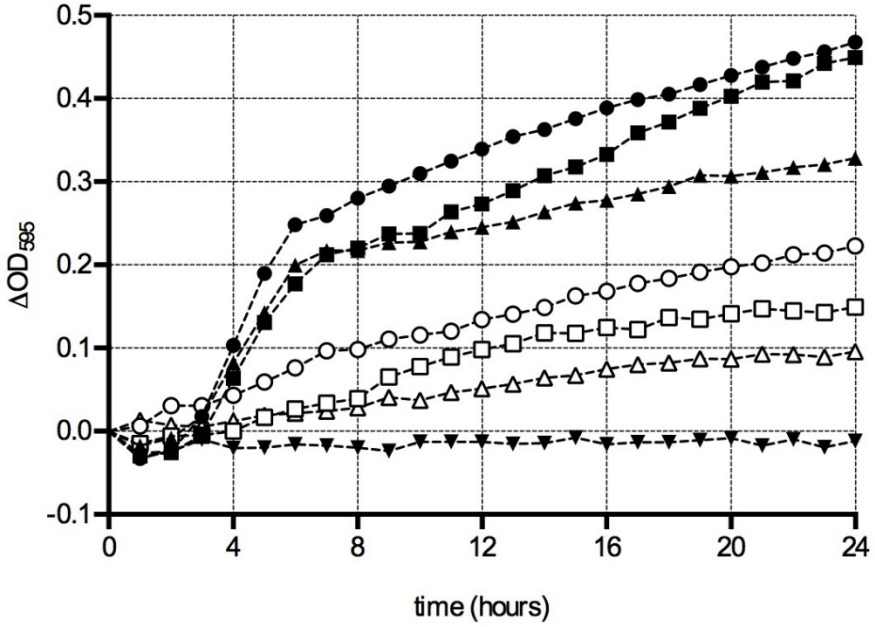

Figure 3.3. *S. aureus* grown in TM without the addition of a carbon source has its growth completely inhibited in the presence of 500 µM copper. *S. aureus* was inoculated to an initial OD_{595} of 0.05 in TM medium containing varying copper concentrations. An aliquot (300 µl) of each culture was grown for 24 hours in an orbital shaking plate reader (180 rpm) at 37 ˚C. Each data point represents the average change in OD_{595} of 3 readings from 3 individual experiments, error bars have been omitted for clarity. Concentrations of copper used were; 0 µM, closed circles; 50 µM, closed squares; 100 µM, closed triangles; 250 µM, open circles; 300 µM, open squares; 400 µM, open triangles; 500 µM, closed inverted triangles.

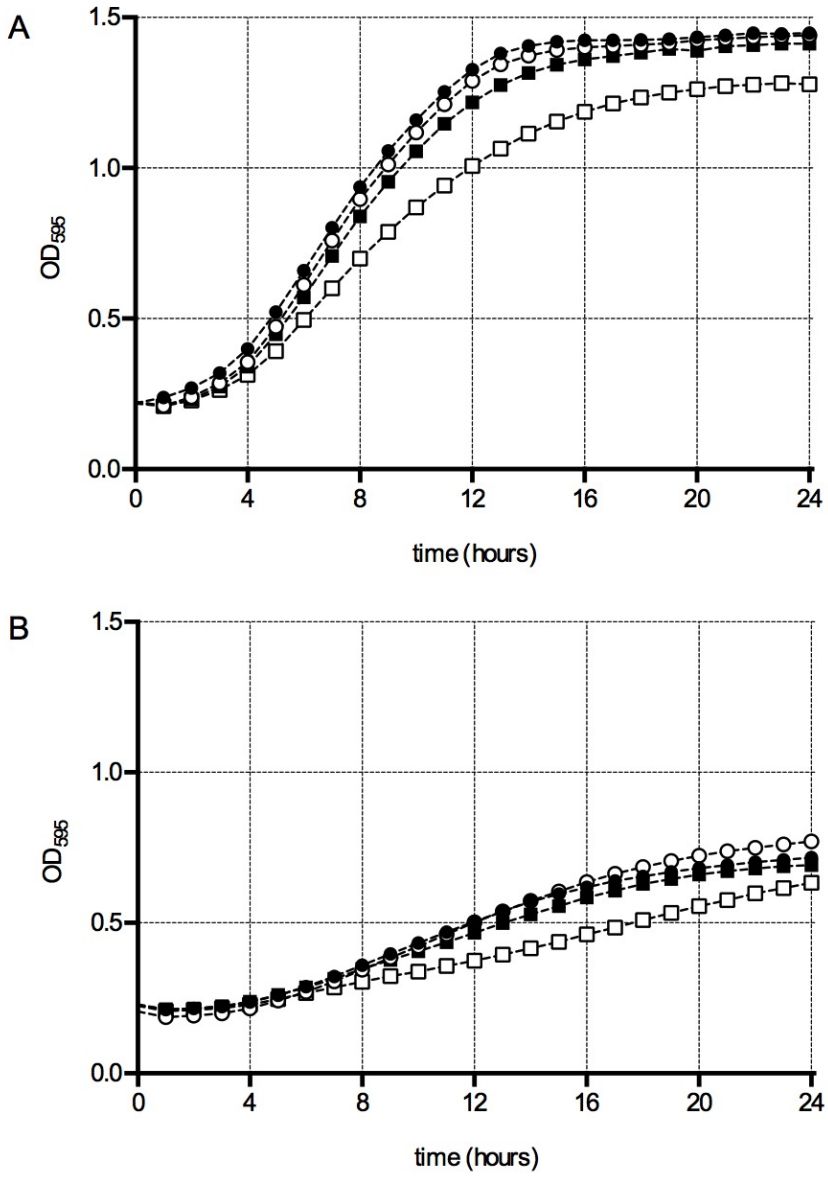

Figure 3.4. *S. aureus* can grow in at least 1,000 µM copper in TM in the presence of glucose or succinate. *S. aureus* was inoculated to an initial OD_{595} of 0.05 in TM medium containing varying copper concentrations. Aliquots (300 µl) of each culture were grown for 24 hours in an orbital shaking plate reader (180 rpm) at 37 ˚C. Panel A shows cells grown in TM with the addition of 1% (w/v) glucose, whereas Panel B shows cells grown in TM with the addition of 1% (w/v) succinate. Each data point represents the average OD_{595} of 3 readings from 3 individual experiments, error bars have been omitted for clarity. Concentrations of copper used were; 0 µM, closed circles; 10 µM, open circles; 100 µM. closed squares; 1000 µM, open squares.

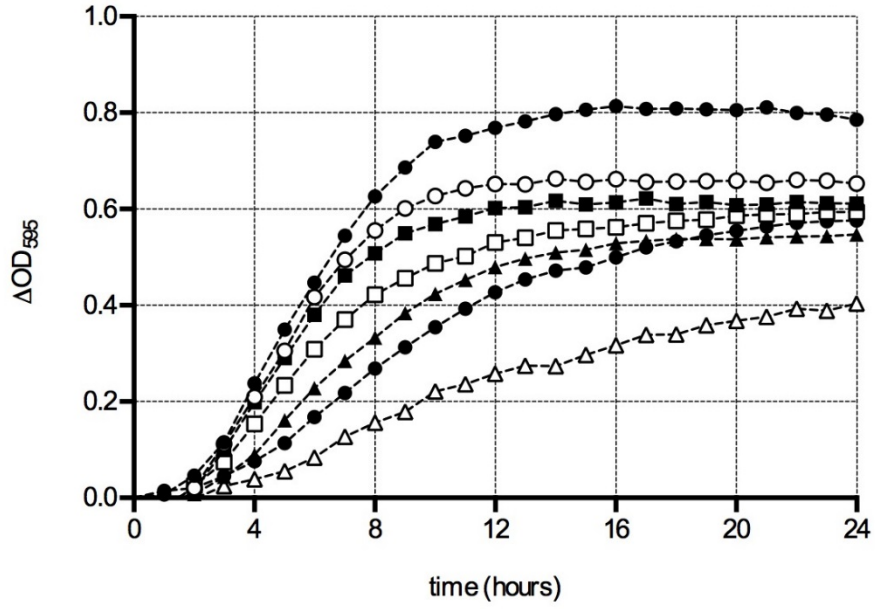

Figure 3.5. *S. aureus* is able to grow in the presence of 3 mM copper in the presence of 0.25 % (w/v) glucose. *S. aureus* was inoculated to an initial OD_{595} of 0.05 in TM medium with added glucose (0.25 % w/v) containing varying copper concentrations. Aliquots (300 µl) of each culture were grown for 24 hours in an orbital shaking plate reader (180 rpm) at 37 ˚C. Concentrations of copper used were; 0 mM, closed circles; 0.5 mM, open circles; 1 mM, closed squares; 1.5 mM, open squares; 2 mM, closed triangles; 2.5 mM, closed circles; and 3 mM, open triangles.

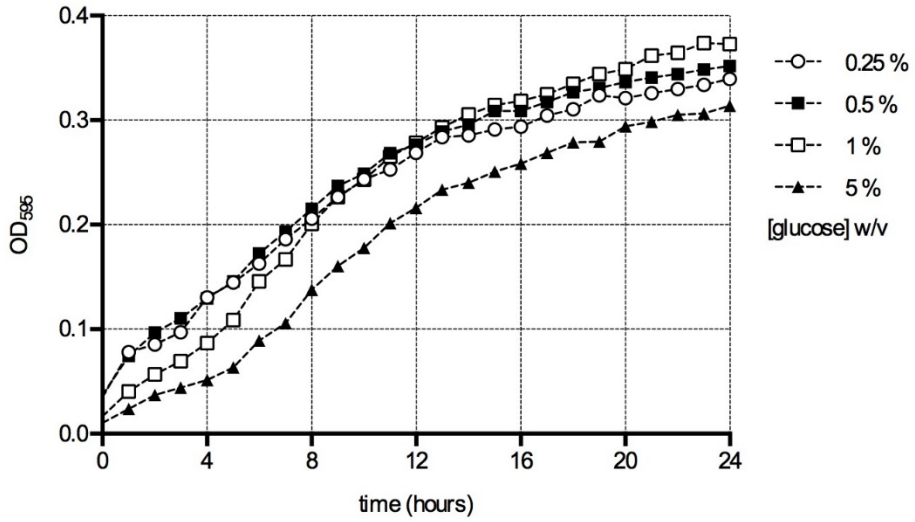

Figure 3.6. Increasing the glucose concentration in TM does not increase the growth of *S. aureus* in the presence of 3 mM copper. *S. aureus* was inoculated to an initial OD_{595} of 0.05 in TM medium. Aliquots (300 µl) of each culture were grown for 24 hours in an orbital shaking (180 rpm) plate reader at 37 ˚C. Each data point represents the average change in OD_{595} of 3 readings from 3 individual experiments, error bars have been omitted for clarity. Concentrations of glucose used were (% w/v); 0.25, open circles; 0.5, closed squares; 1, open squares; 5, closed triangles.

3.3 *S. aureus* cells grown under elevated copper conditions increase their intracellular levels of copper, but not of other metals

As we were interested in the effects of copper within the cytoplasm of *S. aureus* we next determined whether those cells accumulated cytoplasmic copper copper. Figure 3.7 demonstrates that cells cultured in TM containing no added carbon source, with the addition of 0, 10 and 100 μM, accumulate copper with an increase in the amount of cellular copper observed in all of these conditions.

As observed in Figure 3.3 of *S. aureus* grown in TM without added carbon, the OD_{595} of *S. aureus* does not increase as much as when 100 μM copper is added to the media. It should be noted that the data shown in Figure 3.7 has not been adjusted for cell count, thus the apparent reduction in uptake of copper as copper concentration in the media rises to 10 μM from 100 μM is most likely a product of a lower of number of cells within the sample.

From these results we can also observe that the import of other biometals (manganese, iron, cobalt and zinc) is not affected by the addition of copper to the medium, with no observed increase or decrease in any other metal recorded in this experiment. As mentioned in the introduction, the route by which copper enters *S. aureus* cells remains unknown, and it remains possible that copper accesses cells by hijacking the known importers of other transition metal, but such a scenario has yet to have been demonstrated. The results here are as expected, a change in the presence of another metal due to the addition of copper was not hypothesised.

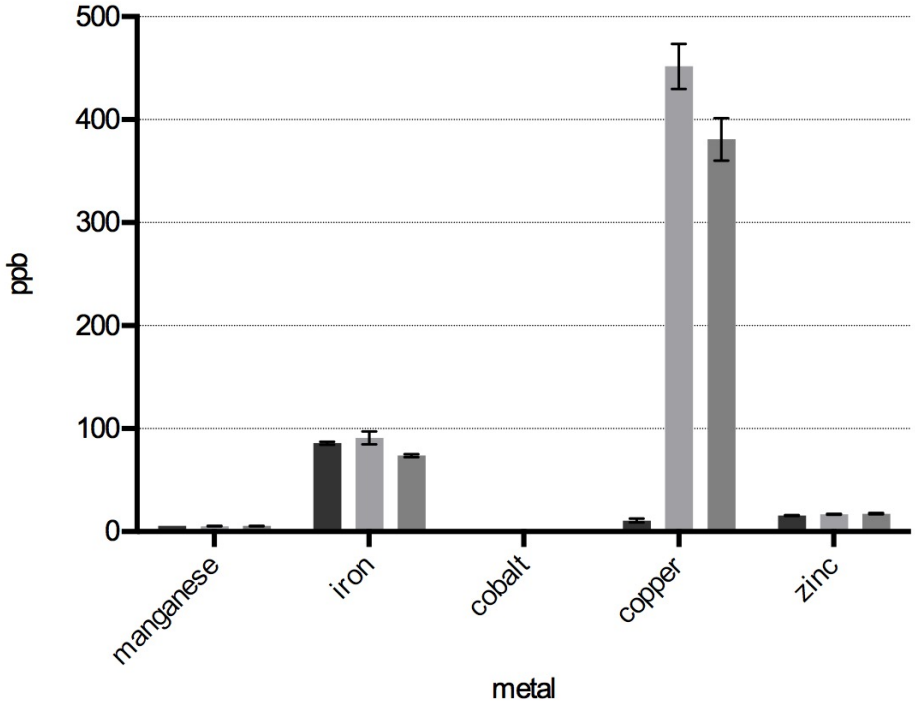

Figure 3.7. Increased copper can be detected by ICP-MS in the cytosolic extracts of cells grown in copper. *S. aureus* SH1000 was grown from a starting OD_{595} of 0.05 in TM with glucose (0.25% w/v) with shaking (180 rpm) at 37 ˚C for 6 hours. $CuSO_4$ was added to the media at concentrations of 0 µM (black bars), 10 µM (light grey bars) and 100 µM (dark grey bars). Cells were washed with and then without EDTA to remove excess copper and then lysed using a bead beater. The lysate was diluted 30 fold in 2.5 % nitric acid and the sample tested for metal content by ICP-MS.

3.4 GapA co-migrates with copper in chromatographic fractions from copper-treated *S. aureus* cells

As stated in the introduction to this chapter, preliminary data obtained in the Waldron lab prior to the start of this project had suggested that the enzyme *Sa*GapA might associate with copper in cells cultured under elevated copper conditions. Data from one example of such an experiment, conducted by Dr Emma Tarrant (Waldron Group, Newcastle University), is shown in Figure 3.8 and Figure 3.9.

After growing SH1000 *S. aureus* cells in elevated copper medium (500 μM in TSB), the cell pellet was lysed and cytoplasmic extract was prepared and separated under rigorously anaerobic conditions by multi-dimensional liquid chromatography. Two rounds of chromatography was necessary as the mixture of proteins in single fractions after one round was still too complex for effective analysis. Fractions derived from the chromatography were analysed by ICP-MS, as well as being resolved by SDS-PAGE for protein analysis. This allowed allocation of one of the copper pools identified by ICP-MS to protein bands resolved by SDS-PAGE.

Figure 3.8 shows one example of this preliminary data whereby GapA was identified in the same fractions as copper. The corresponding SDS-PAGE gels for selected fractions are also shown (Figure 3.9). Bands upon the gel that were deemed to be of interest, which peaked in the same chromatographic fractions as the copper, were identified using MALDI-TOF analysis of a slice of the gel. These bands were selected by statistical analysis of the ICP-MS data and densitometry analysis of SDS-PAGE gels, specifically principal component analysis and correlation analysis (data not shown).

This experiment was performed several times, and GapA was identified in copper-containing fractions on each occasion (data not shown).

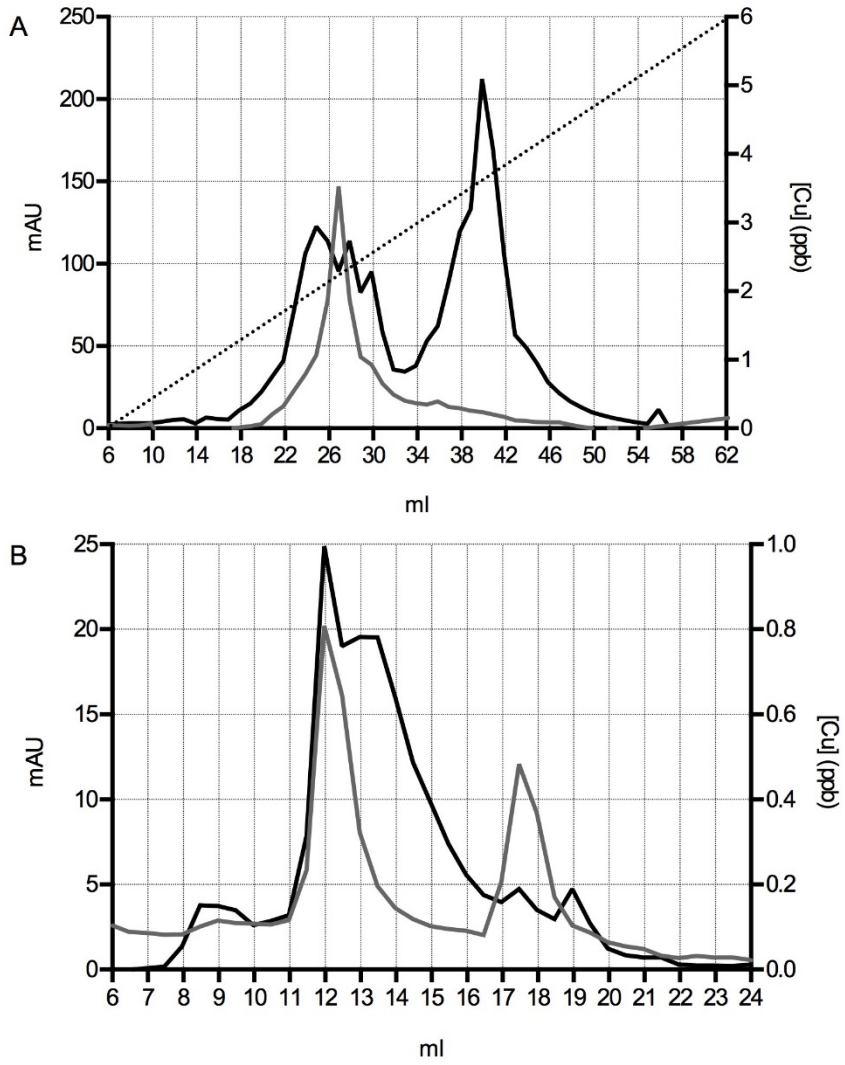

Figure 3.8. Metalloproteomics analysis of cytoplasmic extracts from *S. aureus* SH1000 cells grown in 50 µM copper. *Panels A and B*: Protein concentration is displayed in mAU (left Y-axis, black line), copper concentration in ppb (right y-axis, grey line) and elution volume in ml (x-axis). *Panel A*: A cytoplasmic extract of SH1000, grown in TSB containing 50 µM copper, was initially applied to a hydroxyapatite column. The flow-through from this column contained a copper peak identified by ICP-MS (data not shown). This flow-through material was applied to an anion exchange (Q-HP) column using a NaCl gradient (panel A, black dashed line, 0 – 1 M NaCl), the analysis of which is shown in panel A. The fraction eluting at 27 ml from this separation contained a relatively high amount of copper, and was subsequently applied to a size-exclusion column (Superdex 200 Increase 10/300 GL, GE; flowrate, 1 ml min^{-1}; buffer, 150 NaCl, 20 mM Tris, pH 7.5), the analysis of which is shown in panel B. Eluent from both anion exchange and size exclusiojn chromatography was then analysed by ICP-MS. Data acquired by Dr Emma Tarrant (Waldron Group, Newcastle University).

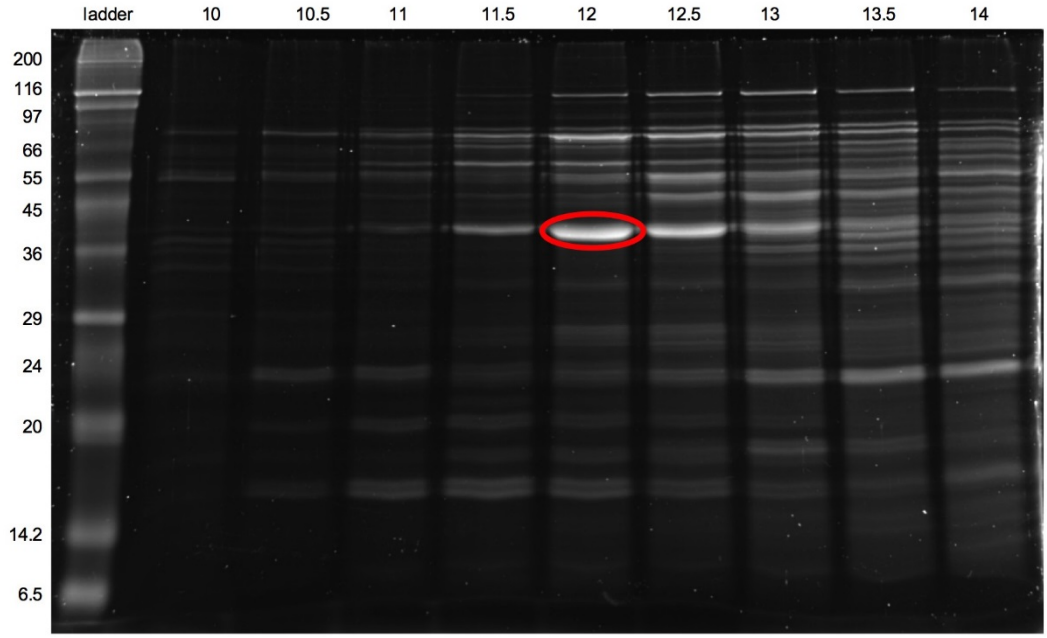

Figure 3.9. Oriole stained SDS-PAGE gel of cell lysates after separation using multi-dimensional liquid chromatography. SDS-PAGE analysis of size exclusion fractions from Figure 3.8; panel B, demonstrated a prominent band, identified as GapA, eluting in the fraction corresponding to 12-12.5 ml identified by MALDI-TOF PMF, where copper also peaks. *Sa*GapA is highlighted in red in 12-12.5 ml; it is by far the most abundant protein in this fraction. Data acquired by Dr Emma Tarrant (Waldron Group, Newcastle University).

3.5 Confirmation of a Δ*gapA* mutant of *S. aureus* and its successful transduction into SH1000 from 8325-4

As preliminary data showed that *Sa*GapA was potentially bound to copper after it was extracted from cells grown in elevated copper conditions, a Δ*gapA* mutant of SH1000 was costructed in order to confirm this identification and to compare the effects of copper on WT *S. aureus* with those upon a Δ*gapA* mutant *in vivo.*

We obtained a *S. aureus* 8325-4 Δ*gapA* mutant from the University of Leicester (a kind gift from Dr Julie Morrissey). Before undertaking experimental work with this mutant, we confirmed the existence of the correct mutation (data not shown) using PCR amplification of the gene in the WT and in the mutant, the latter of which contains an inserted tetracycline resistance cassette (Figure 3.10).

As discussed in the introduction, *S. aureus* 8325-4 has a mutation in the *rsbU* gene which prevents it from being able to cope effectively with oxidative stress. As this project utilises copper which is purported in some cases to lead to a rise in oxidative stress, it was important to work with a strain that was able to cope with this stress in a manner resembling a WT strain. Therefore, after confirming the correct mutation in 8325-4, we transduced the Δ*gapA* mutation from 8325-4 (transduction was performed by A. Barwinska-Sendra, Waldron group) into SH1000, which has had its *rsbU* mutation corrected[24], utilising a standard φ11 phage transduction technique (see methods).

The mutation of *rsbU* in 8325-4 is an 11 base pair deletion within the gene. It is therefore difficult to see the difference in size between amplicons generated from this gene in SH1000 versus 8325-4 when visualised on an agarose gel. We therefore designed a DNA digest using the enzyme *Apo*I which cuts differentially within these amplicons due to the 11 base pair difference, with a site present in the mutated *rsbU* gene but not in the repaired gene of SH1000. A digest of the amplicons generated from the two strains separated by agarose gel electrophoresis demonstrated that our SH1000 Δ*gapA* mutant strain was indeed within an SH1000 genetic background with regard to *rsbU* two bands appeared in the case of mutant gene and only one in the case of the WT(data not shown).

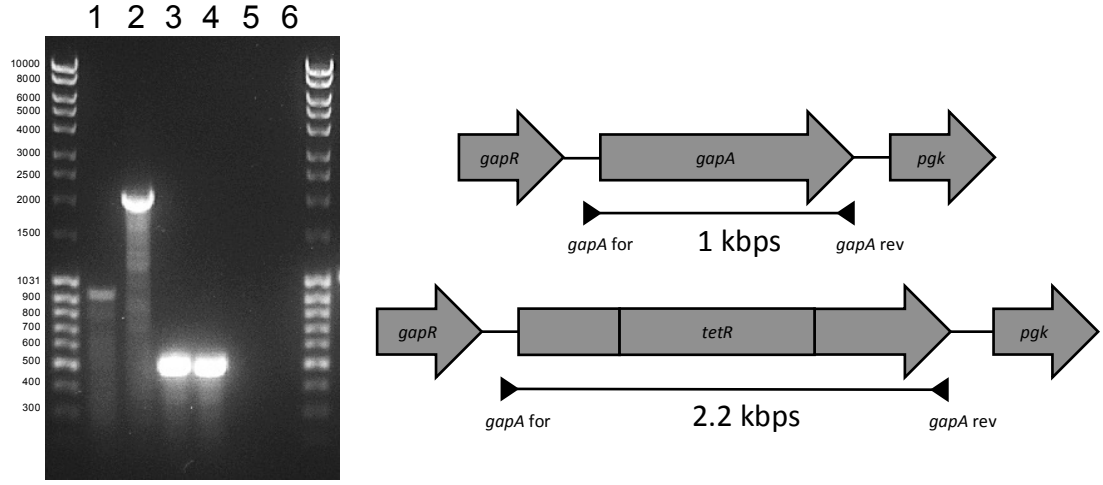

Figure 3.10. **DNA gel demonstrating the presence of a tetracycline resistance cassette within the *gapA* gene of the SH1000 Δ*gapA* strain.** Left) agarose gel showing PCR products amplified from genomic DNA from SH1000 WT (lane 1) and SH1000 Δ*gapA* (lane 2) using primers flanking the *gapA* gene. The larger product produced using the mutant DNA is diagnostic of the presence of a tetracycline resistance cassette within the gene, removing its functionality. Lanes 3 and 4 are positive controls (amplification of a region of genomic DNA upstream of the *copZ* gene) and lanes 5 and 6 are negative controls (no template DNA present) using identical template DNA as in 1 and 2 respectively. Right) schematic diagram of tetracycline resistance cassette insertional inactivation of *gapA*, demonstrating the position of the cassette and primers used. The precise size of the SH1000 WT product is 1053 bp and of the SH1000 Δ*gapA* mutant product is 2189 bp. Primers were designed by researchers at the University of Leicester (Morrissey group).

3.6 Phenotypic analysis of SH1000 Δ*gapA* confirms inability to grow in the presence of glucose

After successful transduction of the Δ*gapA* mutation into SH1000, we confirmed the same growth phenotype for SH1000 Δ*gapA* in TM as has been shown for 8325-4 Δ*gapA* (Figure 3.11), i.e. that the WT will grow in glucose, but the SH1000 Δ*gapA* will not. The phenotype shown by the *ΔgapA* mutant in glucose is due to the mechanism of carbon catabolite repression (CCR) via the CrpA protein. CCR is a mechanism that represses expression of genes required for *S. aureus* to grow in the absence of glycolytic conditions[144,145], which is discussed at length in the introduction to this work. When glucose or other specific metabolites (such as lactose) are present, the enzymes required for growth under other carbon source limited conditions are not required; expression of their genes is therefore repressed in order to save energy and nutrients. In glucose replete conditions, GapA is utilised as part of the glycolysis pathway and is therefore required for cells to grow under these conditions.

In a Δ*gapA* mutant, glycolysis does not function. Therefore the Δ*gapA* mutant will fail to grow in the presence of glucose, even if there are other carbon sources available. This is because catabolite repression continues to function in the mutant, meaning that cells are effectively forcing themselves to utilise the glycolysis pathway despite its malfunction due to the absence of the GapA enzyme.

When glucose is not present, as in TM alone and TM with the addition of pyruvate, catabolite repression does not occur and cells are able to utilise secondary carbon sources such as those shown in Figure 3.11; pyruvate and amino acids.

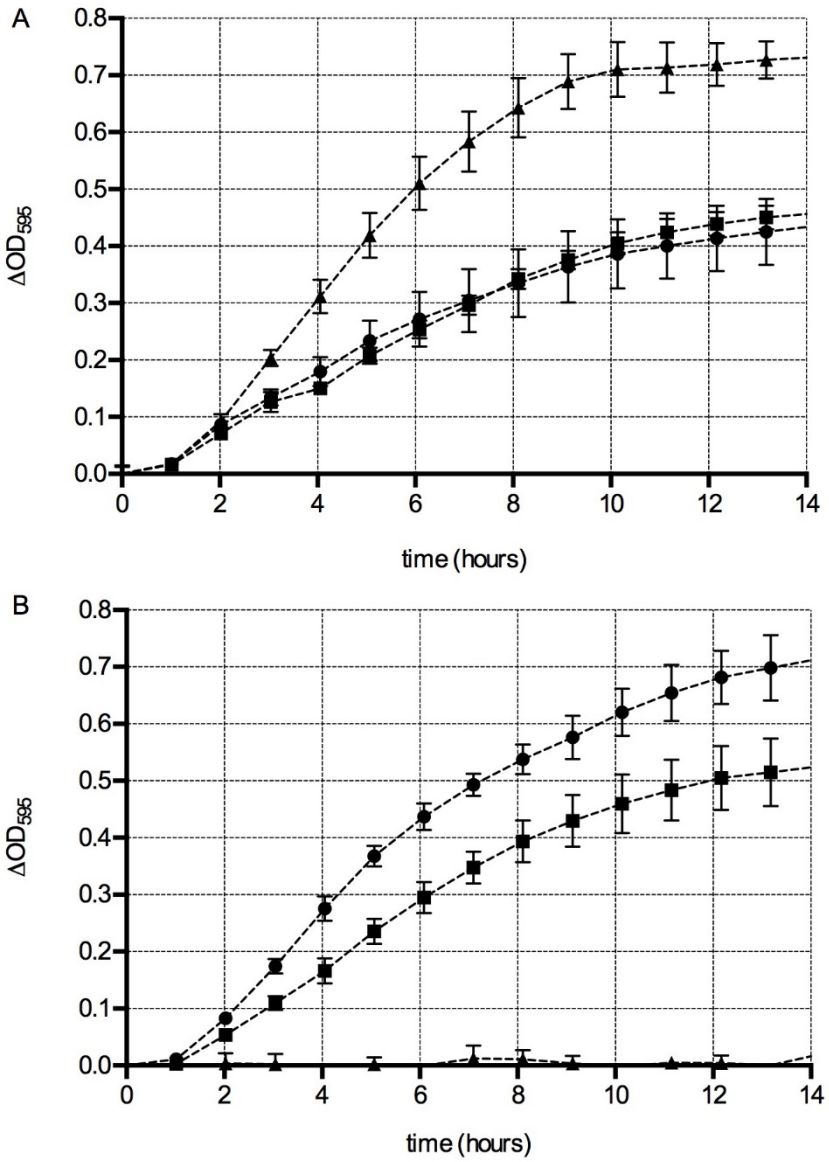

Figure 3.11. **SH1000 WT grows in glucose whereas a SH1000 Δ*gapA* mutant does not.** Starter cultures of *S. aureus* SH1000 WT (A) and SH1000 Δ*gapA* (B) cells grown in TM were diluted 100-fold into TM containing various carbon sources (1 % glucose, triangles; 5 mM pyruvate, circles; no added carbon source, squares). Change in OD (ΔOD_{595}) was measured every hour for 14 hours. Data shown are an average of three independent data sets, each performed in triplicate, error bars have been removed for clarity. This growth assay was performed in a CoStar® 96 well, flat-bottomed plate, shaking (180 rpm) at 37°C. Data shown is representative of 3 independent experiments.

3.7 SH1000 Δ*gapA* shows the same growth phenotype in copper as the WT

It was thought that if copper was binding to *Sa*GapA then the enzyme may be providing some protective effect to the cell, effectively acting as a copper sink, even if just a fraction of the total amount of *Sa*GapA present was doing this. If this was the case then one would hypothesise a decreased resistance to growth in copper in a Δ*gapA* mutant.

To investigate this, the SH1000 WT and SH1000 Δ*gapA* mutant were grown in TM without any added carbon source, containing varying concentrations of copper. Contrary to the hypothesised outcome of this experiment, no significant difference was seen between growth of the WT versus the mutant (Figure 3.12) under these conditions.

Both strains showed no growth in 500 μM copper, as seen previously (Figure 3.3). Whilst the strains showed similar growth in all other concentrations of copper used.

3.8 SH1000 Δ*gapA* shows poorer growth in succinate than the WT in the absence of copper

Due to the inability of *S. aureus* to grow in glucose, and no difference in the growth of the SH1000 Δ*gapA* mutant compared to the WT in copper, the growth of the two strains were compared in TM with the addition of succinate. Under such conditions the glycolytic function of *S. aureus* should not be required and therefore it was hypothesised that the two mutants would grow identically without the addition of copper.

In fact, the Δ*gapA* mutant grew much less in succinate than the WT. This result is difficult to explain, but it may be that some of the hypothesised regulatory functions of *Sa*GapA have a role to play in the metabolism of glucose. In addition, the presence of glucose in the media did not have a significant effect upon the growth of either strain, relative to their controls (Figure 3.13).

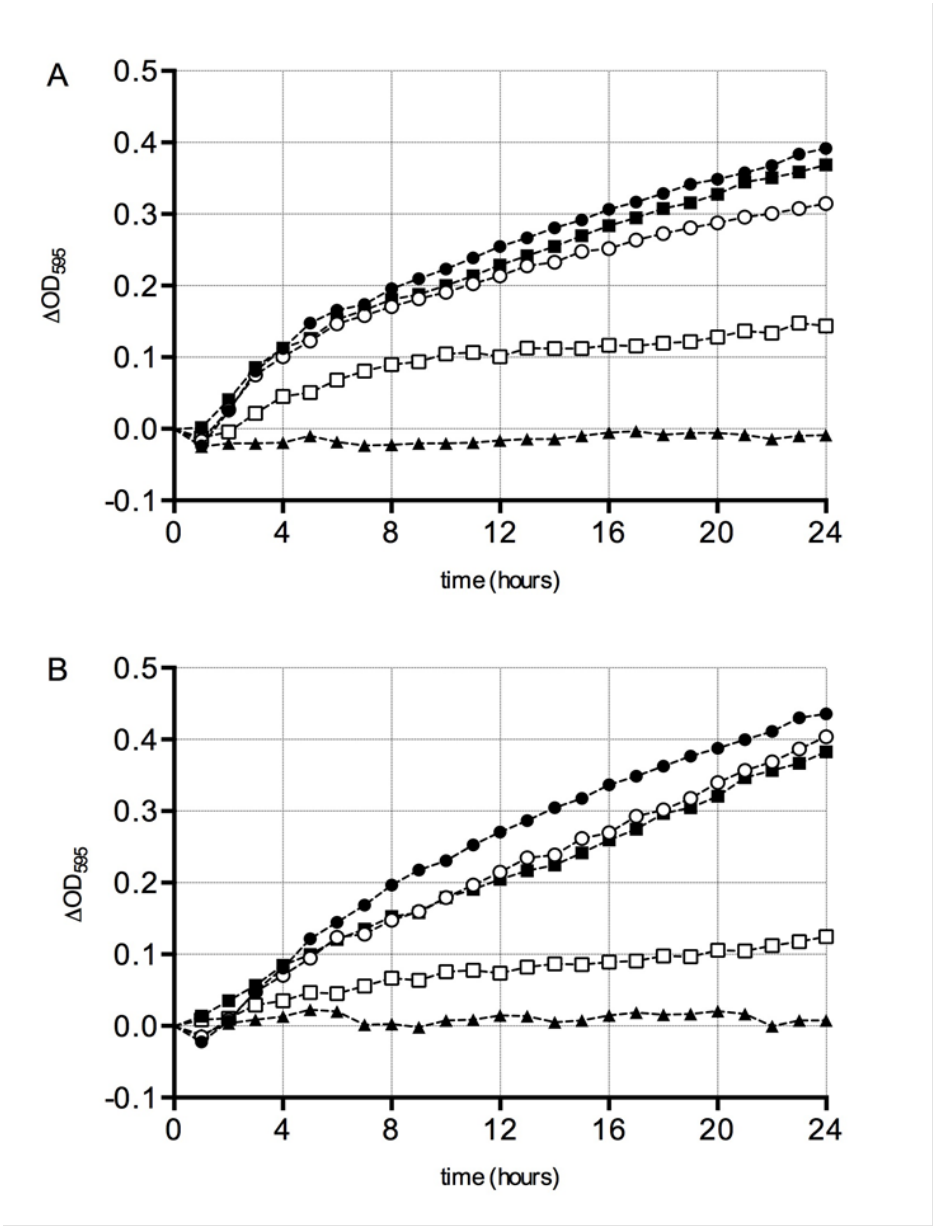

Figure 3.12. Growth analysis of SH1000 WT versus SH1000 Δ*gapA*. Cultures (300 µl) of SH1000 WT (Panel A) and SH1000 Δ*gapA* were grown from a starting OD_{595} of 0.05 in TM (without an additional carbon source) at 37 ˚C shaking (180 rpm) in an orbital plate reader. Concentrations of copper used in the media were; 0 µM, black circles; 50 µM, white circles; 100 µM, black squares; 250 µM, white squares; 500 µM, triangles.

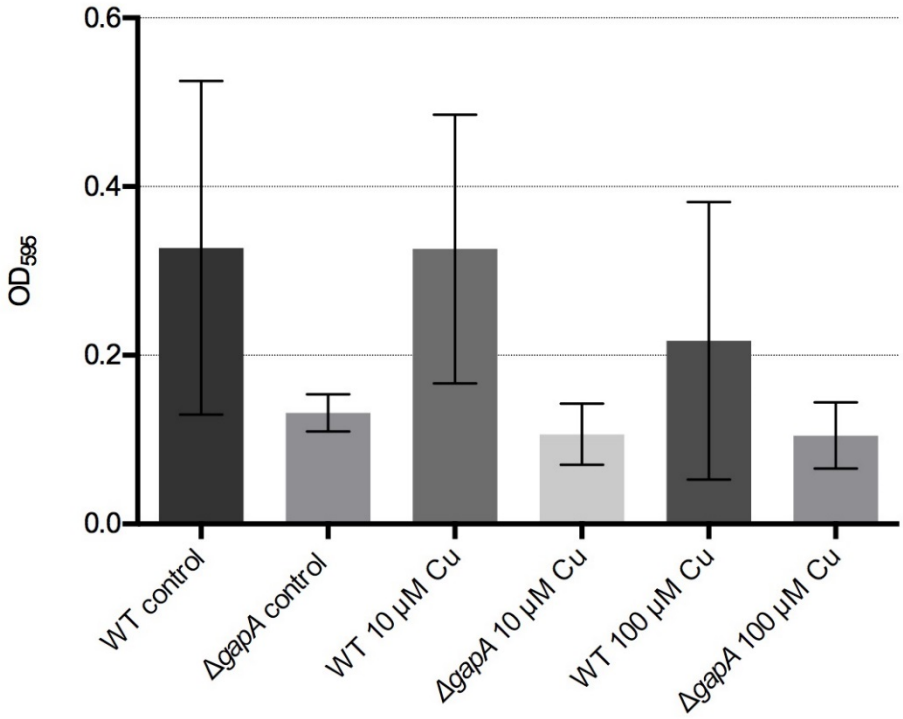

Figure 3.13. Growth analysis of SH1000 WT versus SH1000 Δ*gapA* after 16 hours in TM containing succinate. Cultures (300 µl) of SH1000 WT and SH1000 Δ*gapA* were grown from a starting OD_{595} of 0.05 in TM with the addition of succinate (1 % w/v) as a carbon source at 37 ˚C shaking in an orbital plate reader. Data shown is the OD_{595} after 16 hours of growth. Strains were grown without the addition of copper (WT control and Δ*gapA* control), with the addition of 10 µM copper (WT 10 µM CU and Δ*gapA* 10 µM Cu) and with the addition of 100 µM copper (WT 100 µM CU and Δ*gapA* 100 µM Cu)

3.9 An assay to measure the enzymatic activity of GapA in *S. aureus*

As explored in the introduction, GapA is an enzyme that catalyses the conversion of glyceraldehyde 3-phosphate into 1,3-bisphosphoglycerate, and as part of this reaction it utilises NAD^+ as a cofactor which it converts to NADH. NADH absorbs strongly at 340 nm whereas NAD^+ does not. We are therefore able to measure the activity of the enzyme *in vitro* by observing the change in absorbance of the reaction at 340 nm using an enzyme specific assay. This assay has been used successfully by others in previous studies concentrating on GapA in *S. aureus*[113].

Throughout this work, we have used an enzyme assay to observe the activity of GapA in cells and in purified *Sa*GapA preparations, and to determine the effects of adding copper and other metals and reagents on the enzyme activity.

We have taken two approaches when performing this assay *in vivo*. Firstly to grow cells within a medium containing copper, followed by cell lysis and preparation of soluble extracts to assay GapA activity; or secondly, to grow cells in a medium containing no added metal, then, after preparation of the soluble extract, to add the desired metal to the lysate prior to assaying for enzyme activity.

The former experimental approach requires uptake of the metal by cells, and/or changes to metabolism caused by the metal, and any inhibition would then be the result of intracellular metal upon GapA. The latter removes the cell wall and membrane prior to metal addition and therefore effectively increases the concentration of metal treatment to which GapA relative to the first approach. It also demonstrates the effects of a given treatment upon GapA within the complex cytoplasmic milieu of proteins and other macromolecules that are present in a lysate, but effects would not be the result of a regulatory change as cells are killed via lysis before the metal is added.

During this study this assay has been performed using two types of spectrophotometer. Firstly, using a plate-reader based spectrophotometer (Biotek) that takes a reading every 10 seconds of a number of samples simultaneously. This allows numerous samples to be analysed under precisely the same conditions. The plate reader spectrophotometer also allows for various path lengths to be used, which affects the conversion of absorbance readings into concentrations of reagents (NADH in this case)

using the Beer-Lambert law (A = εCl). Typically a reaction set up within a multi-well plate for analysis in the plate-reader spectrophotometer has a volume of 200 µl. Secondly, a cuvette based spectrophotometer (Perkin Elmer) has been used, which analyses one sample at a time, but is much more sensitive than the plate reader spectrophotometer and is able to take readings every two seconds. Reactions set up for analysis in this spectrophotometer are performed in a quartz cuvette (Hellma) that has a precise path length of 1 cm. Both of these spectrophotometers have the disadvantage of having a time lag between the initiation of the reaction and the initial reading at 340 nm, which means that the very start of the reaction cannot be measured. The nature of taking the absorbance over a time period allows the measurement of a rate of activity.

Because of the nature of the plate reader spectrophotometer having a variable path-length depending on the volume of the reaction analysed, it was necessary to compare their outputs. This allowed a correction factor to be calculated to adjust all activity assays according to a path-length of 1 cm (equivalent to the Perkin Elmer spectrophotometer). We observed that a reaction volume of 300 µl in the plate reader spectrophotometer gave very similar reading to those observed in the Perkin Elmer spectrophotometer. Results are shown in Figure 3.14.

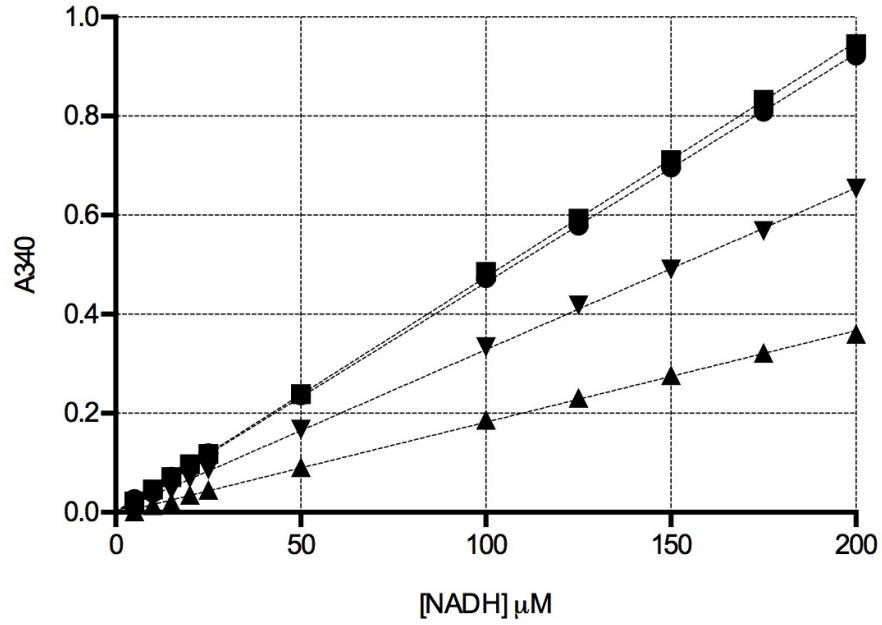

Figure 3.14. NADH absorbance at 340 nm measured in different volumes in the plate-reader spectrophotometer and in the Perkin Elmer spectrophotometer. NADH at various concentrations in buffer (150 mM NaCl, 40 mM HEPES, pH 7.5) was analysed in volumes of 100 µl (triangles), 200 µl (inverted triangles), and 300 µl (circles) and in the Perkin Elmer plate reader (squares).

3.10 *S. aureus* Δ*gapA* mutant lysates lack GAPDH activity using an enzyme-specific activity assay

Initially, using the assay described above, we assayed the activity of GapA present in a SH1000 WT lysate compared to a SH1000 Δ*gapA* mutant lysate without any added metal (Figure 3.15). This confirmed that GapA is specifically required in order to observe an increase in absorbance at 340 nm under the conditions of the reaction, and verified that the Δ*gapA* mutant constructed (Figure 3.10) was not producing an active GapA enzyme. Further to this, control reactions lacking the substrate (G3P), cofactor (NAD^+) and protein have been performed, showing that these are all required for activity to be observed in the WT lysates as would be expected from the chemistry of the reaction that GapA catalyses (Figure 3.16).

Notably, GapB, the GapA orthologue in *S. aureus* which is present in the SH1000 Δ*gapA* mutant lysate does not produce an increase in A340 as measured by this assay. This is again consistent with data shown by Purves *et al.* who demonstrated that GapB did not show NAD+ dependent activity[113].

Regarding the data shown in Figure 3.15, if the increase in absorbance at 340 nm between 10 and 20 seconds is calculated, we can present this increase in A340 as a rate of reaction over this discrete period of time. This allows for a different presentation of the data that gives a snapshot of the reaction rate and allows for the comparison of a number of samples. We can convert the change in absorbance at 340 nm into a concentration of NADH produced using the Beer-Lambert law, and the published extinction coefficient (ε) of NADH at 340 nm of 6,220 M^{-1} cm^{-1}, allowing the enzyme activity to be expressed as the amount of NADH produced per unit time, per unit concentration of protein in the sample. Thus, using the data shown in Figure 3.15 we can subsequently produce Figure 3.17.

Analysis of this data shows that the WT lysate produced 26.81 nmoles NADH $minute^{-1}$ mg $protein^{-1}$ in the given time period, much more than the Δ*gapA* lysate which shows a value that is close to zero (1.61 nmoles NADH $minute^{-1}$ mg $protein^{-1}$). The small amount of activity observed in the SH1000 Δ*gapA* lysate is within the noise generated in this assay, as defined by the rise in A340 shown in control assays that demonstrate that even when protein, cofactor or substrate are present there is still a rise in absorbance (Figure

3.16). GapA activity assays will be shown in the format shown in Figure 3.17 from herein unless otherwise stated.

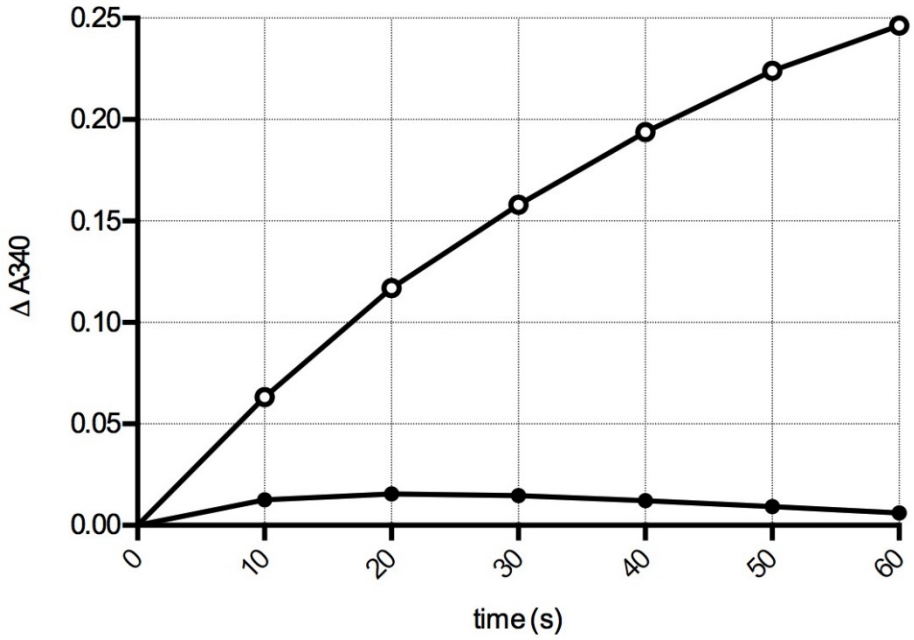

Figure 3.15. *Sa*GapA activity is detectable in a SH1000 WT lysate, but not in a SH1000 Δ*gapA* mutant lysate. A lysate from WT SH1000 cells results in an increase in absorbance at 340 nm, whilst a Δ*gapA* SH1000 lysate shows very little increase. An aliquot (15 µl) of SH1000 lysate from SH1000 WT cells (closed circles) or SH1000 Δ*gapA* cells (open circles) adjusted for equal protein concentration was added to 185 µl of reaction buffer and the absorbance of NADH (at 340 nm) was monitored over time in a plate reader. The reaction was performed at room temperature.

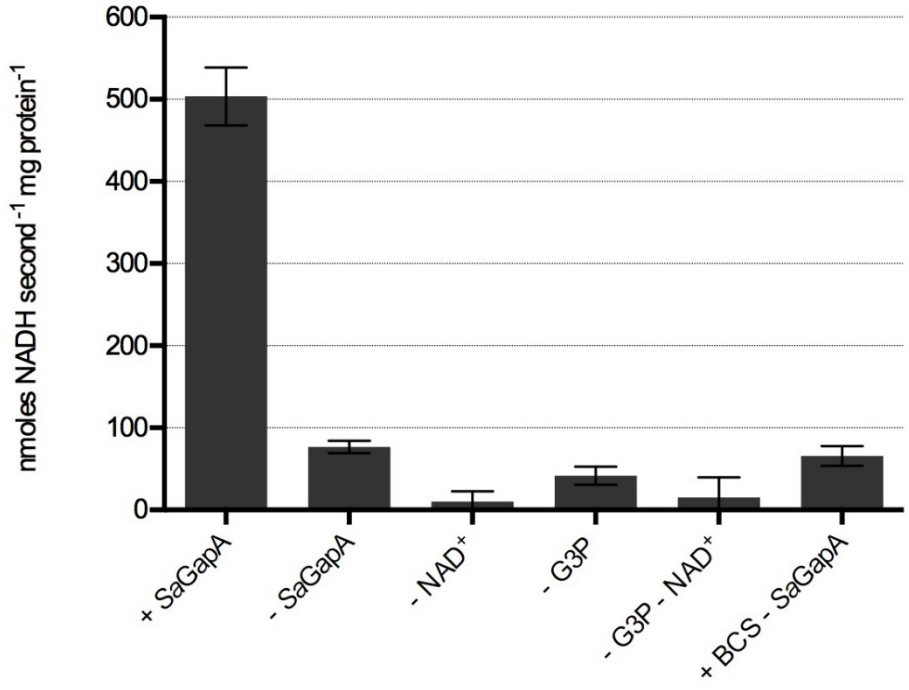

Figure 3.16. Added substrate (G3P), cofactor (NAD^+) and enzyme (GapA) are all required for a significant rise in A340 to occur. Reactions contain (see methods for concentrations): +*Sa*GapA, recombinant *Sa*GapA, NAD^+ and G3P; -*Sa*GapA, NAD^+ and G3P; -NAD^+, recombinant *Sa*GapA and G3P; -G3P, *Sa*GapA and NAD^+; -G3P – NAD^+, *Sa*GapA; +BCS -*Sa*GapA, NAD^+, G3P and BCS. Each reaction containing *Sa*GapA contained 5 µM enzyme and all reactions contained 50 mM sodium phosphate. This data was previously used in a non-publicly accessible Newcastle University-submitted dissertation written by the author (Jack Stevenson).

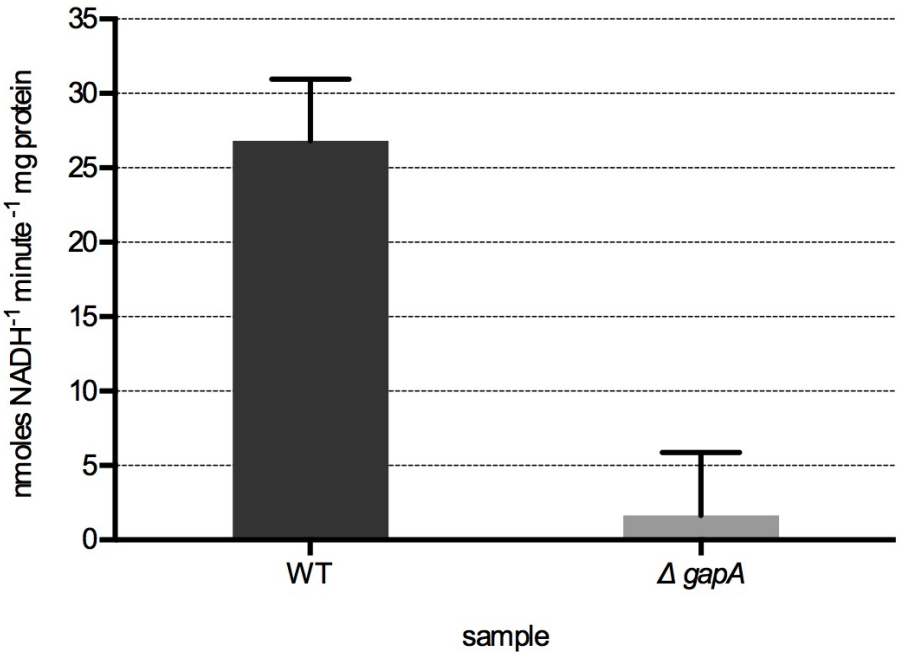

Figure 3.17. A lysate from WT SH1000 shows *Sa*GapA activity, whilst a SH1000 Δ*gapA* mutant lysate shows negligible activity. 15 µl of SH1000 lysate from SH1000 WT cells or SH1000 Δ*gapA* cells adjusted for protein concentration was added to 185 µl of reaction buffer. Data here is adapted from that shown in Figure 3.15 using data between 10 and 20 seconds..

3.11 *Sa*GapA activity is inhibited in cells grown in media containing high copper

It was of interest to examine how extracellular copper within the growth medium would affect the activity of *Sa*GapA within cytoplasmic extracts and how this correlated with growth phenotypes. The results of such an experiment can be observed in Figure 3.18.

Here, *S. aureus* was grown in TM with 0.25 % glucose (w/v) for 4 hours before lysis, extract preparation and assaying of GapA activity (Figure 3.18).

Cells were washed thoroughly in a buffer containing 5 mM EDTA (which is in excess to the highest copper concentration used in this experiment) three times before lysis was performed. This was to prevent any residual copper in the extracellular fraction from mixing with the intracellular fraction upon lysis. Such a situation could have resulted in a greater concentration of copper binding to cytoplasmic proteins and exaggerated any inhibitory effects. Thorough washing aimed to prevent this.

Growth data (though acquired from separate cultures) for some of the concentrations of copper used here can be seen, in the same medium, in Figure 3.3 (Panel A) (100 μM) and in Figure 3.4. We can see that there is inhibition of growth upon addition of 500 μM copper to the medium but that cells can cope with higher concentrations of copper than this. Ideally, a GapA assay of activity of cells in these higher concentrations would have been performed but in the interest of timely submission of this work this was not possible. The data point for the assay performed from lysates produced from cells grown in 400 μM copper shows what appears to be inhibition of activity (the difference between the control and this value is however statistically insignificant, $P = 0.1633$). One might assume that increasing concentrations would increase this effect. Presumably even at higher concentrations of copper, *Sa*GapA is not saturated with copper as within glucose, as we have observed, cells lacking *Sa*GapA activity will not grow.

Little inhibition of *Sa*GapA under elevated copper growth conditions does not rule *Sa*GapA out of involvement in copper toxicity. It may be that copper is binding to *Sa*GapA as levels of intracellular Cu(I) increase above a certain threshold, but that the cell is able to compensate for this by, for example, increasing expression of *Sa*GapA. If this was the case, the enzyme would essentially be acting as a copper sink, and would in essence

function as part of the copper homeostasis system by preventing damage to other proteins and keeping cells in a viable state.

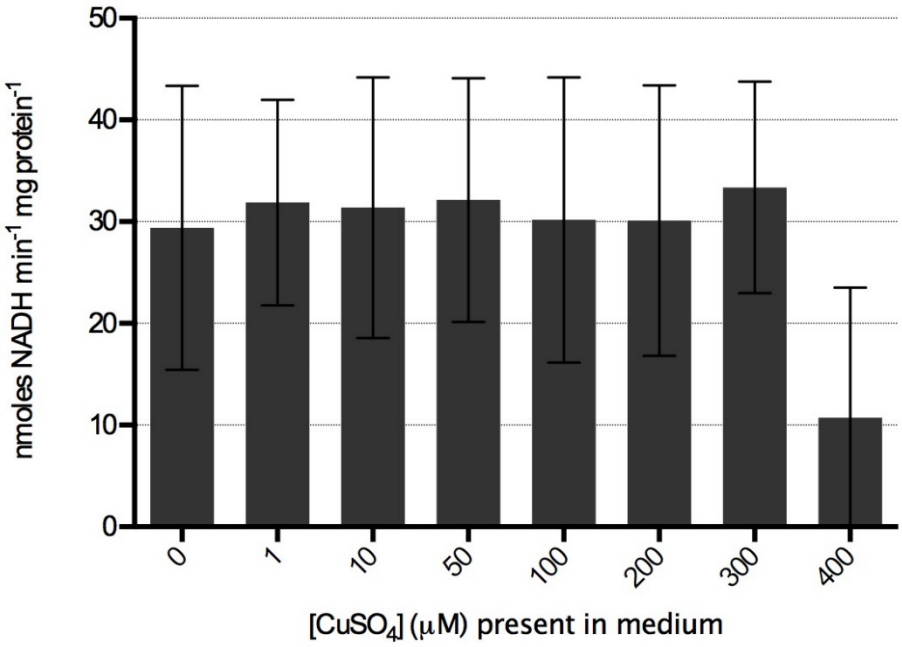

Figure 3.18. *Sa*GapA is not significantly inhibited in cell lysates produced from cells grown in concentrations of copper up to 400 μM. Cells were grown in TM with glucose (0.25% w/v) at 37 ˚C for 4 hours in an orbital shaker (180 rpm), before being thoroughly washed (3 x) in 5 mM EDTA and lysed. Lysates were assayed for *Sa*GapA activity using a plate reader spectrophotometer (Biotek) using the standard method (see materials and methods). Each lysate was adjusted to a concentration of 50 μg ml^{-1} before 15 μl was added to a 96 well plate. Reaction buffer (185 μl) was added immediately prior to observation of the reaction at A_{340}. Data shown is the production of NADH per minute per mg of added protein between 10 and 20 seconds of the reaction.

3.12 The copper peak associated with GapA in chromatographic fractions from copper-treated WT *S. aureus* cells is absent in a *S. aureus* Δ*gapA* mutant

Preliminary data that identified *Sa*GapA in SH1000 as a potential target of toxicity was performed in TSB with the addition of 50 μM copper. The fact that copper, as measured by ICP-MS, was isolated in the same fraction as *Sa*GapA implied that *Sa*GapA is binding to copper.

Having constructed a SH1000 Δ*gapA* mutant, and having verified its growth phenotype in the presence of glucose as well as showing that lysates of the mutant demonstrate no detectable *Sa*GapA activity, we repeated the metalloproteomics experiments that led to our preliminary data in this strain.

As the SH1000 Δ*gapA* mutant does not grow well in TSB or in a glucose containing media, we performed this analysis in TM medium without the addition of any carbon source. We performed the analysis in parallel with both the SH1000 WT and the SH1000 Δ*gapA* mutant, cultured and prepared simultaneously so that any changes in metal or protein profiles could not be attributed to differences in media composition or variations in growth conditions.

These metalloproteomics experiments utilise two dimensions of chromatography. Initially the soluble lysates were prepared in an anaerobic glovebox and then separated by anion exchange chromatography using a 1 ml HiTrap Q HP anion-exchange column (GE Healthcare). Here the column was loaded with the soluble lysate, washed and subsequently a set of buffers (pH 7.5) containing different concentrations of NaCl were applied to the column in a stepwise fashion, eluting a profile of different proteins with each different concentration of NaCl applied according to the affinity of the different proteins for the charged column, independent of pH. Each 1 ml fraction was analysed for its copper content by ICP-MS as well as its protein content by Bradford assay (Figure 3.19).

As observed in Figure 3.19, there was little difference in the protein or copper distribution detected in WT versus Δ*gapA* mutant fractions eluted from the initial chromatographic separation. This pattern is reflected in SDS-PAGE analysis of the same anion exchange elution samples (Figure 3.20). This presented a difficulty in identifying

which of these fractions of the WT extract contained *Sa*GapA, in order for this fraction to be further separated. Previous separations utilised in preliminary work used different chromatographic columns which means that these cannot easily be used to cross reference the location of the protein. Notably, the SDS-PAGE gels shown in Figure 3.20 show minimal differences, confirming that chromatography of the two extracts was identical, and that no major changes in protein expression was observed between strains.

To identify which fraction *Sa*GapA was in we utilised the specific GapA activity assay described previously. The results of this assay are shown in Figure 3.21

As we had treated the cells with copper, we added 50 µM BCS to aliquots of the fractions to be tested in order to check whether any inhibition of *Sa*GapA had occurred, keeping some aside for further analysis. BCS is a Cu(I) specific chelator with a very high affinity for Cu(I), as described previously, and would be expected to remove at least a proportion of copper that may be bound to *Sa*GapA and inhibiting the enzyme.

An increase in specific *Sa*GapA activity is seen when BCS is added to the reaction. This suggests strongly that the *Sa*GapA in these fractions had some copper bound and that removal of this by the addition of BCS has increased the activity of the enzyme (Figure 3.21).

We observed that fractions 300 (2), 400 (1) and 400 (2) showed activity, with 400 (1) showing the greatest value of 143.14 nmoles NADH min^{-1} mg $protein^{-1}$ in the untreated fractions and 310.93 nmoles NADH min^{-1} mg $protein^{-1}$ in the fractions treated with BCS, representing a 2-fold increase. We did not test fractions 100 (1), 100 (2), 1000 (1) or 1000 (2) as these fractions contained relatively low levels of protein (Figure 3.19). Corresponding fractions from the SH1000 Δ*gapA* separation showed no activity, confirming the absence of *Sa*GapA in the mutant.

Based on our findings from these activity assays, fraction 400 (1) was selected for further purification by size exclusion. An aliquot (500 µl) of 400 (1) was injected onto a size exclusion column (Superdex 200 Increase 10/300, GE Healthcare). Fractions (500 µl) were collected, and analysed for copper content by ICP-MS, with protein

concentration determined by UV/visible spectrophotometry at 280 nm. The resulting chromatogram is shown in Figure 3.22.

Here we can clearly see the convergence in protein concentration and copper concentration across fractions in both the SH1000 WT and the SH1000 Δ*gapA* mutant. However there are notable exceptions to this trend, with the two most obvious copper peaks in the WT elution not appearing in the Δ*gapA* mutant fractions, at 12.5 ml and 19 ml.

A number of the collected fractions were run on SDS-PAGE in order to observe which proteins were present within them which are shown in Figure 3.23. Samples on the gels shown correspond to the volume eluted between approximately 10.5 ml and 15 ml from size-exclusion chromatography (see Figure 3.22). The fractions eluted from 12 - 13.5 ml are highlighted as these areas of the SDS-PAGE gel clearly show the disappearance of a band in the SH1000 Δ*gapA* mutant fractions which corresponds to *Sa*GapA, eluting in the expected fractions, and being of the correct size on the gel itself. The fraction eluting at 13 ml demonstrates the appearance of a triplet of bands in the SH1000 WT fractions, which is observed as only a doublet of protein bands in the SH1000 Δ*gapA* mutant.

The observation of the disappearance of a copper peak as measured by ICP-MS in these fractions from the SH1000 *ΔgapA* mutant, corresponding with the disappearance of *Sa*GapA on the SDS-PAGE gel within these same fractions, when compared to the presence of a copper peak and *Sa*GapA on the SDS-PAGE gel in the equivalent SH1000 WT fractions indicates strongly that *Sa*GapA was indeed bound to copper in the WT fractions.

To further investigate the impact that copper may have had on the activity of *Sa*GapA within these fractions, fractions of the SH1000 WT, collected after size exclusion chromatography, were assayed for GapA activity. As previously, we also assayed aliquots of the fractions after treatment with 50 μM of the Cu(I) specific chelator BCS. Aliquots of the SH1000 Δ*gapA* mutant fractions were also tested for GapA activity and showed none as expected (data not shown).

As in fractions collected after the anion exchange chromatography step, it was observed that activity increases after the addition of BCS. The highest activity was found in the fraction eluting at 12.5 ml in both untreated and treated fractions with values of 86.84 and 144.74 nmoles NADH min^{-1} mg $protein^{-1}$ respectively.

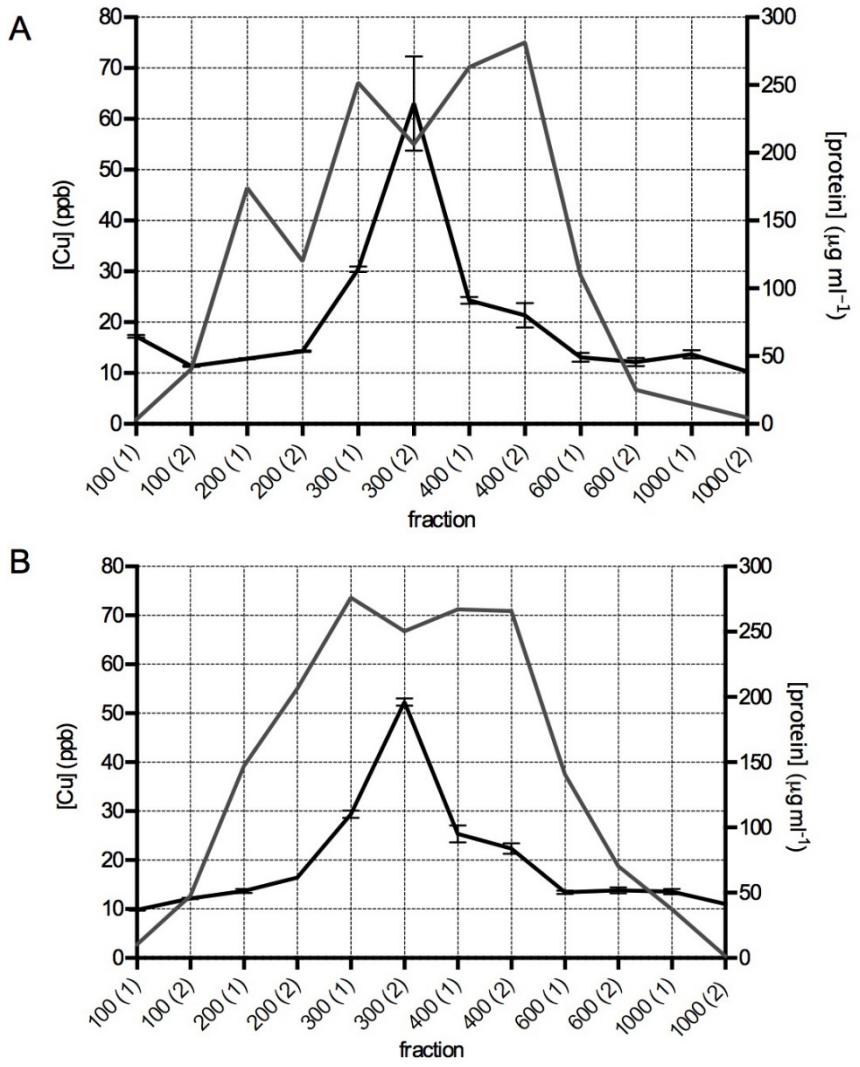

Figure 3.19. The differences between profiles of copper and protein distribution after anion exchange chromatography of WT and ΔgapA soluble extracts are minimal. Panel A: SH1000 WT lysate. Panel B: SH1000 Δ*gapA* lysate. Cells were grown in TM + 50 µM $CuSO_4$ for 6 hours shaking (180 rpm) at 37 ˚C. Cells were harvested, washed (x 3) with EDTA (5 mM) and then lysed by freeze grinding under anaerobic conditions. Soluble extract was separated by centrifugation followed by ultracentrifugation before the lysate was applied to an anion exchange column, again under anaerobic conditions (1 ml Q-HP column, GE; buffer, 40 mM Hepes, pH 7.5 with varying NaCl concentrations (100, 200, 300, 400, 600 and 1000 mM); flowrate, 0.5 ml min^{-1}). Each fraction (X axis) is labelled according to the NaCl concentration used to elute it (mM) and which millilitre of eluent volume it represents; i.e. the first (1) or second (2) millilitre. Each fraction was analysed by ICP-MS for copper content (left Y axis, black line) and protein concentration by Bradford assay (right Y axis, grey line)

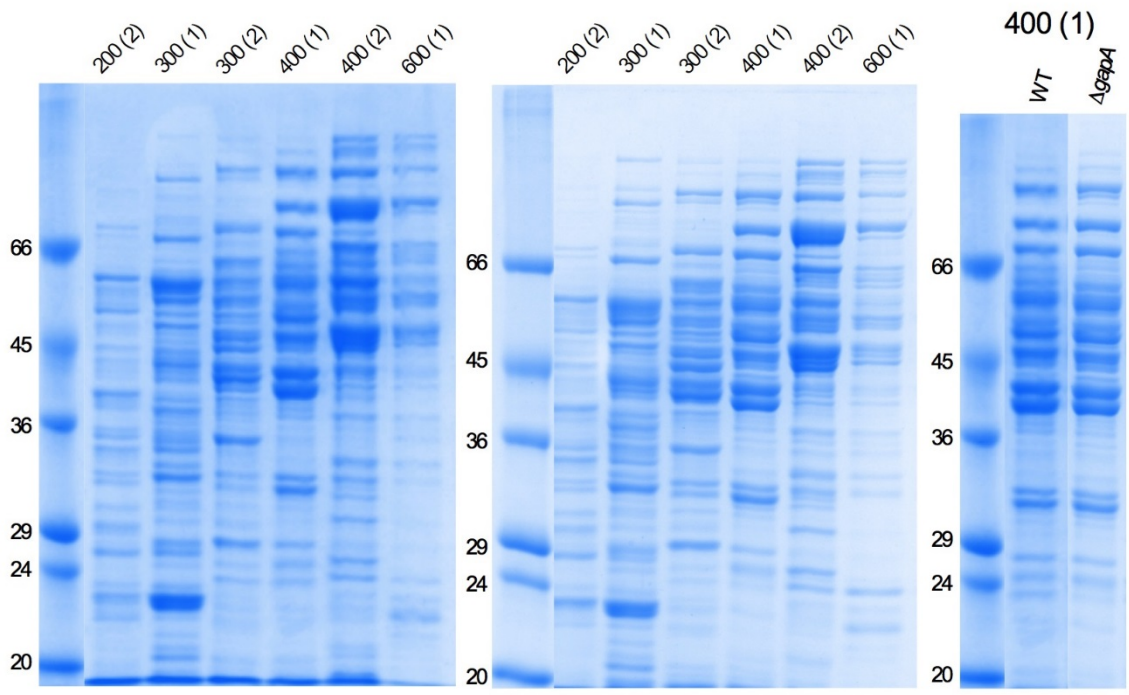

Figure 3.20. SDS-PAGE analysis of fractions from anion-exchange chromatography of copper treated SH1000 WT and SH1000 Δ*gapA* cell lysates. Aliquots (30 µl) of each anion exchange fraction from WT and Δ*gapA* extracts were loaded onto a 12 % acrylamide SDS-PAGE gel, which was stained with Coomassie blue. *Left panel*; WT fractions 200 mM (2) to 600 mM (1). *Middle panel*; Δ*gapA* fractions 200 mM (2) t0 600 mM (1). Fractions not shown contained low protein levels. Protein MW ladder (size shown in kDa) has been digitally positioned closer to the 200 mM (2) fraction in both main panels for ease of analysis. *Right panel*; aligned ladder and lanes containing 400 (1) fractions from both the WT and mutant analysis for ease of comparison.

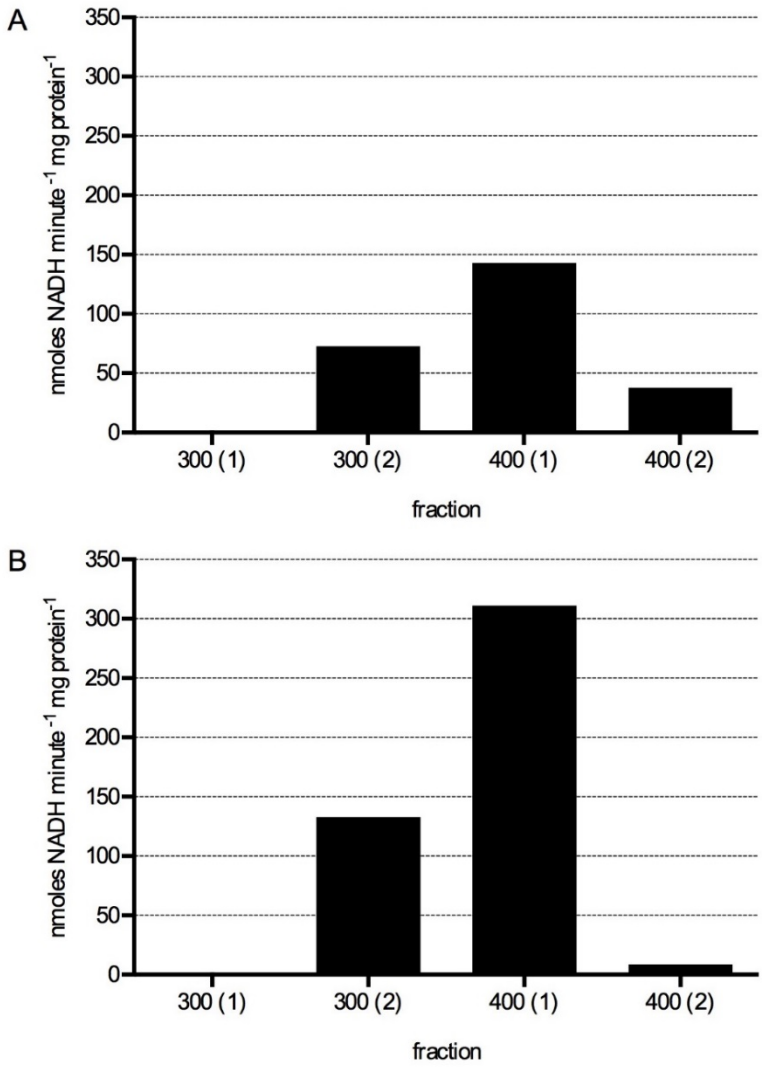

Figure 3.21. *Sa*GapA activity of WT fractions collected from anion-exchange chromatography rises after treatment with BCS. *Panel A*; The activity of WT fractions is shown. Activities are, in nmoles NADH minute^{-1} mg protein^{-1}; 300 (2), 72.70; 400 (1) 143.14; 400 (2), 37.68. *Panel B*; the activity of WT fractions is shown upon treatment with 50 µM BCS. Activities are, in nmoles NADH minute^{-1} mg protein^{-1}; 300 (2), 132.85; 400 (1) 310.93; 400 (2), 8.61. Fractions not shown gave negligible activity. Fractions from the separation of lysates from the SH1000 Δ*gapA* mutant are not shown as they showed no activity, as expected.

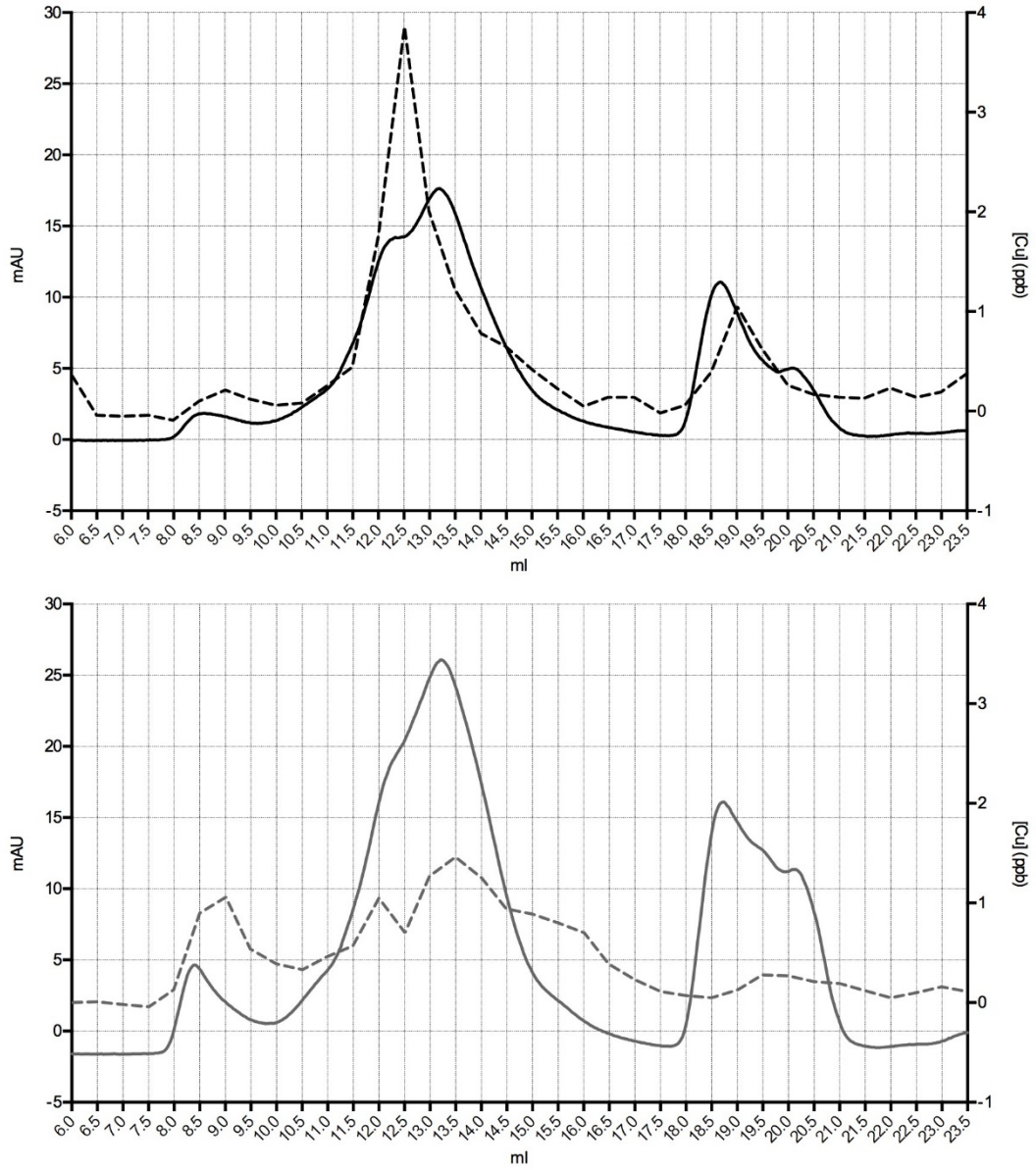

Figure 3.22. The copper peak associated with GapA in the SH1000 WT during size-exclusion chromatography is absent in the SH1000 Δ*gapA* mutant. Fraction '400 (1)', shown in Figure 3.19, was applied to a size-exclusion column (Superdex 200 10/300 GL, GE; buffer, 150 mM NaCl, 40 mM Hepes, pH 7.5; flowrate 1 ml min^{-1}) for this analysis. *Upper panel*: SH1000 WT. *Lower Panel*: SH1000 Δ*gapA*. In both panels protein concentration is displayed in mAU (left Y-axis, solid line), copper concentration in ppb (right y-axis, dashed line) and elution volume in ml (x-axis).

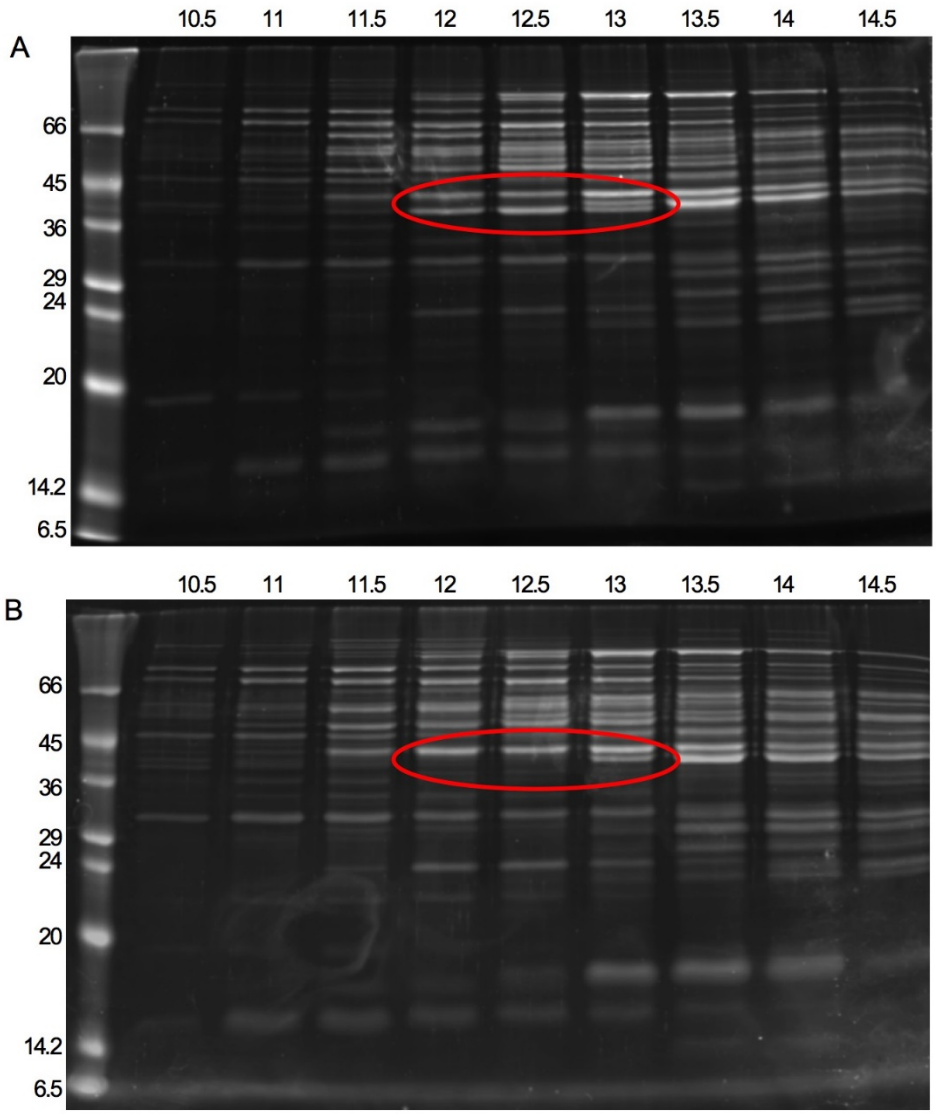

Figure 3.23. SDS-PAGE gels of fractions from SEC analysis of SH1000 lysates show that GapA is absent in the fractions from the SH1000 Δ*gapA* mutant. 40 µl of each fraction was loaded onto a 15 % (w/v) acrylamide gel (see methods). The gel was stained using Oriole staining agent for superior staining sensitivity due to the relatively low concentrations of protein within the fraction. The images were acquired under a UV light. *Top panel*: SH1000 WT. *Bottom Panel*: SH1000 Δ*gapA*. In both panels fractions eluting at 12, 12.5 and 13 ml have been highlighted (red oval) as the difference between the WT and mutant is most obvious in these.

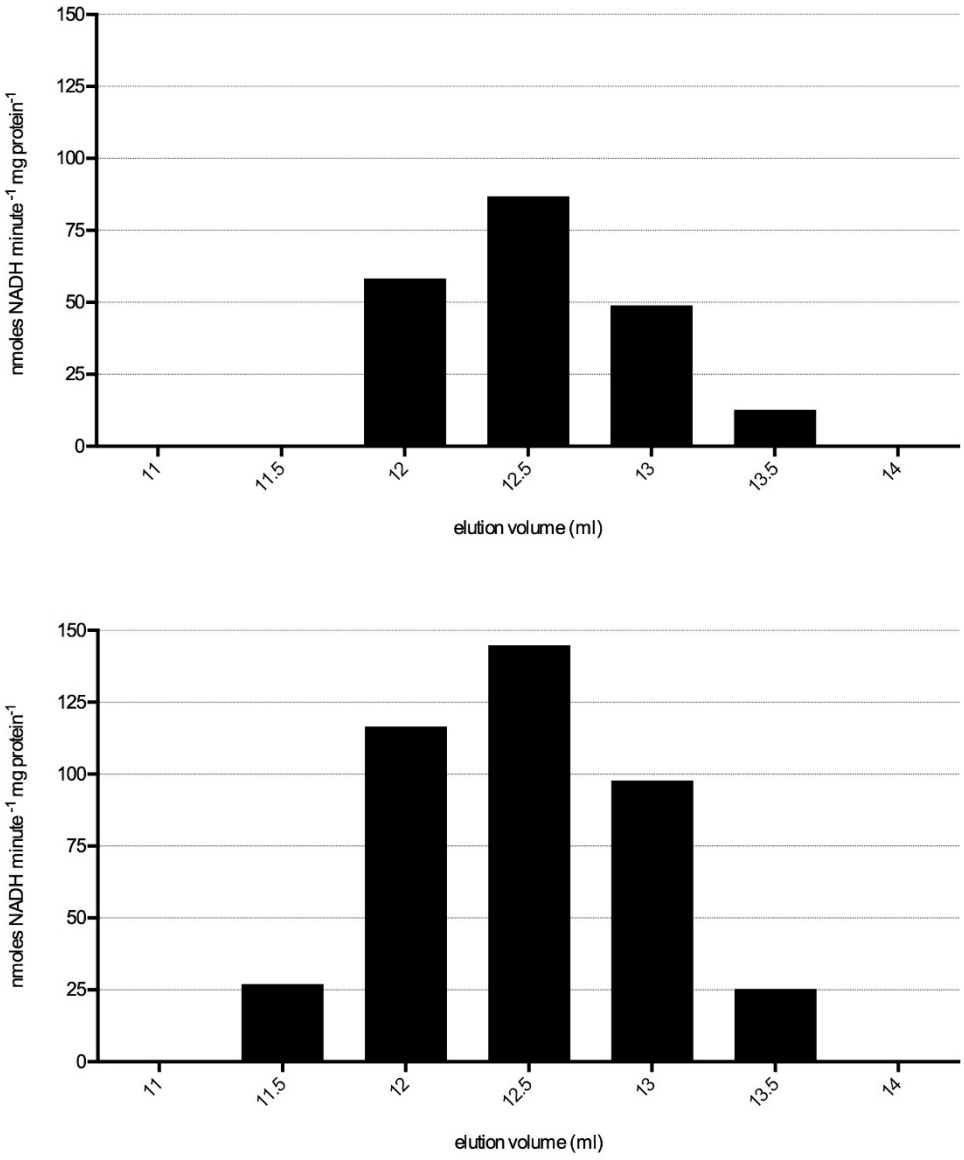

Figure 3.24. GapA activity of WT fractions collected from size-exclusion chromatography rises after treatment with BCS. Panel A; The enzyme activity present in fractions is shown without treatment with BCS. Activities are (in nmoles NADH minute^{-1} mg protein^{-1}): fraction 12, 58.29; fraction 12.5, 86.84; fraction 13, 48.93; fraction 13.5, 12.66. Panel B; the activity in the fractions is shown after treatment with 50 µM BCS. Activities are (in nmoles NADH minute^{-1} mg protein^{-1}): fraction 11.5, 27.05; fraction 12, 116.58; fraction 12.5, 114.74; fraction 13, 97.85; fraction 13.5, 25.33. Fractions not shown gave negligible activity. Fractions from the separation of lysates from the SH1000 Δ*gapA* mutant are not shown as they showed no activity, as expected.

3.13 GapA activity is inhibited in cell lysates to which copper is added

As well as observing possible inhibition of *Sa*GapA in lysates from cells grown in copper (Figure 3.18), we also observed reduced activity in lysates to which copper was added after lysis. Whilst this method does not imitate the conditions *in vivo* it is further evidence that within the complex milieu of proteins present within a lysate copper is able to inhibit the activity of *Sa*GapA.

In this case 50 μM Cu(II) was added to the lysate, we chose not to use Cu(I) as the lysate in this case was prepared in aerobic conditions. Indeed it may be the case that some Cu(II) is converted to Cu(I) by reducing agents within the lysate. The fact that activity is seen in the control lysate is indicative that the entire population of *Sa*GapA cannot be oxidised as it has been shown that oxidised *Sa*GapA is inactive[115].

3.14 Other metals also inhibit the activity of GapA within cell lysates

It was of interest to examine whether this effect was limited to copper or was also exhibited by other bio-metals. Cobalt, nickel, zinc and silver (not a bio-metal, but with similar chemistry to copper) were added to a cytoplasmic extract of *S. aureus* at a concentration of 50 μM. It was found that cobalt, nickel do not significantly inhibit *Sa*GapA activity ($p > 0.05$, unpaired t-test), whereas silver ($p = 0.0119$) and zinc ($p = 0.0274$) do. Silver had a similar effect to copper as expected, whereas zinc inhibited the enzyme significantly but not to the extent of silver or copper. Such a result would be expected on reflection upon on the Irving-Williams series of the relative stabilities of divalent metal iron complexes, which attributes stability such that copper forms the most stable complexes, followed by (of those metals used here), zinc, nickel and cobalt.

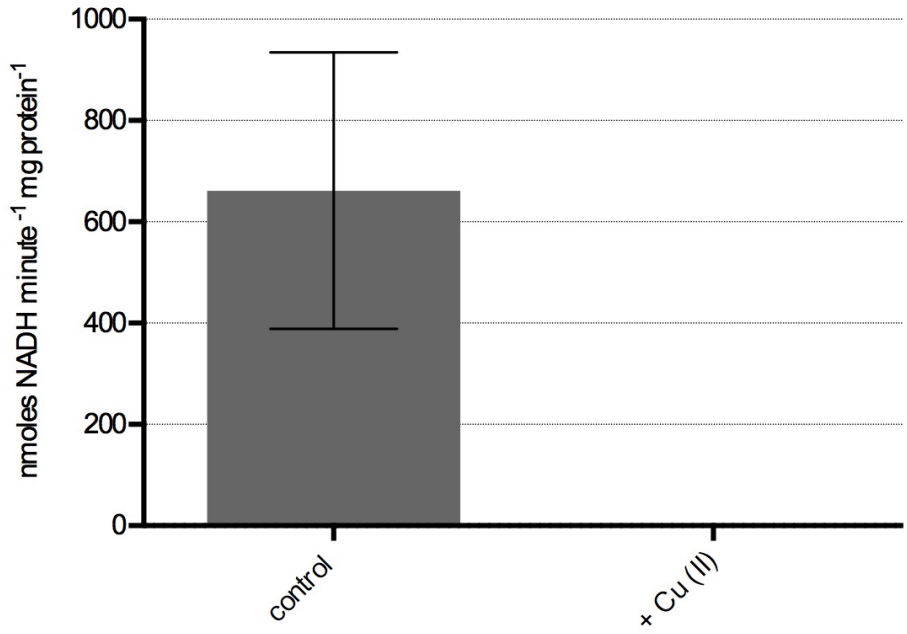

Figure 3.25. Cu(II) completely inhibits the activity of *Sa*GapA within a cytoplasmic extract of SH1000. Protein lysate extract (15 µg) of *Sa*GapA was used with 50 µM Cu(II) added and incubated with the protein for approximately 10 minutes at room temperature. The control reaction gave a mean value of 661.54 nmoles NADH minute^{-1} mg protein^{-1}, the copper treated lysate gave no activity ($p = 0.0125$). The reaction is based on the activity between 10 and 20 seconds performed in a plate reader spectrophotometer.

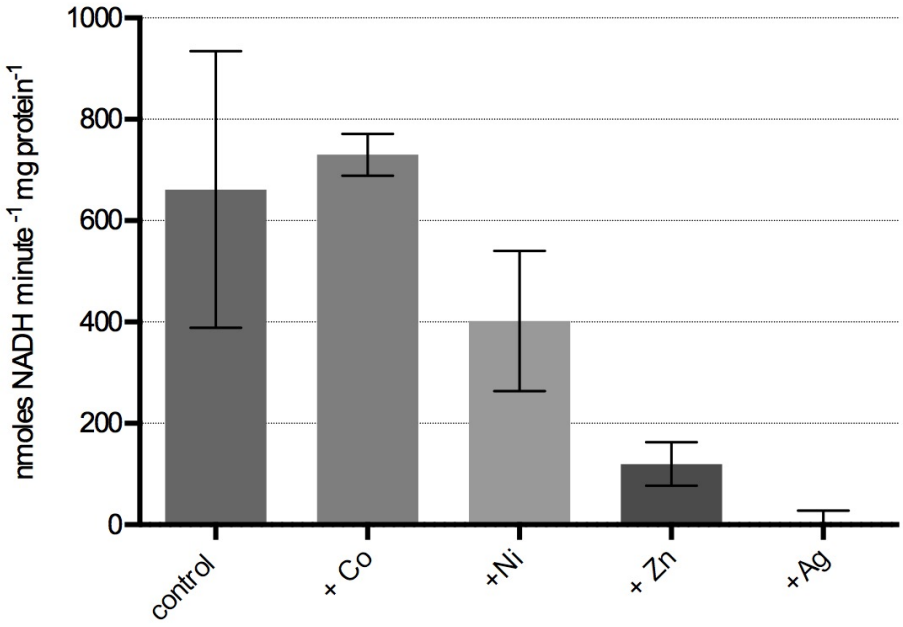

Fig 3.26. Cobalt and nickel do not inhibit the activity of *Sa*GapA within a cytoplasmic extract of SH1000, whereas zinc and silver do. Protein lysate extract (15 µg) of WT *S.* aureus was used with 50 µM of each metal added and incubated with the protein for approximately 10 minutes at room temperature. Mean reaction values were (in nmoles NADH minute^{-1} mg protein^{-1}); control, 661.54; +Co, 730.09; +Ni, 401.04; +Zn, 119.97. The silver treated sample gave no activity. The reaction is based on the activity between 10 and 20 seconds performed in a plate reader spectrophotometer.

3.15 Chapter 3 Conclusions

- The growth of *S. aureus* is inhibited in liquid media by high concentrations copper.
- Levels of copper inhibition of *S. aureus* growth are variable and dependent on the type (complexity) of media used for growth.
- *S. aureus* is particularly sensitive to copper in TM, with complete inhibition of growth occurring at 500 μM $CuSO_4$.
- The presence of a carbon source (in addition to amino acids, present in all media) increases the concentration of copper in which *S. aureus* can grow.
- *S. aureus* grows to a higher OD_{595} in glucose than in succinate.
- Different amounts of glucose above 0.25 % do not increase the growth of *S. aureus* in copper, ruling out glucose complexing effects/
- Preliminary data identified *Sa*GapA as a potential copper binding cytoplasmic protein in *S. aureus*.
- A *S. aureus* SH1000 Δ*gapA* mutant shows the same glucose growth phenotype to that of an 8325-4 Δ*gapA* mutant, previously described.
- The growth phenotype in copper of a *S. aureus* SH1000 Δ*gapA* mutant does not differ from the WT.
- A SH1000 Δ*gapA* mutant grows poorly in succinate compared to the WT, but copper does not affect growth of the Δ*gapA* mutant relative to the WT when growing with succinate as the main carbon source.
- Copper in the media does not affect the activity of *Sa*GapA detectable within those cells up to a concentration of 400 μM $CuSO_4$.
- A SH1000 Δ*gapA* mutant lysate cultured in copper is missing the copper pool present in the WT in the same fraction as *Sa*GapA, confirming that *Sa*GapA binds copper.
- Treatment of cell lysates prepared from WT *S. aureus* cells grown in copper with the copper chelator BCS results in an increase in activity.
- SH1000 lysates treated with copper *in vitro* show no *Sa*GapA activity.
- SH1000 lysates treated with nickel and cobalt show no significant reduction in *Sa*GapA activity compared to the WT, whereas zinc shows significant inhibition whilst silver shows full inhibition.

Chapter 4: Copper binding to *S. aureus* GapA *in vitro*

4.1 Introduction to Chapter 4

Having explored the effects of copper on *S. aureus in vivo* and having identified a protein that copper may bind to within the cytoplasm, *Sa*GapA, further investigation was performed involving the potential interaction of this protein with copper *in vitro*. This chapter will thus explore *in vitro* binding of copper to recombinant *S aureus* GapA (r*Sa*GapA).

As seen in Chapter 3, it is clear that fractions containing *Sa*GapA from copper treated lysates from SH1000 WT *S. aureus* cells contain copper, and that when the identically prepared cell lysates were anal ysed from the SH1000 Δ*gapA* mutant, copper is not present. We hypothesised that the result observed in the WT is due to the binding of copper to *Sa*GapA *in vivo*, hence when there is no *Sa*GapA present there is no accompanying copper pool.

There are other possibilities that could explain this result. It could be that treatment of a SH1000 Δ*gapA* mutant with copper results in a shift in copper distribution within cells to other proteins, i.e. through re-distribution of copper at the protein level. Alternatively, it may be that the background expression of genes in a SH1000 Δ*gapA* mutant varies from the SH1000 WT, again resulting in a shift in copper distribution but this time due to genetic regulation. Or indeed the result of copper treatment in the Δ*gapA* mutant may be a hybrid of these two events. The fact that protein distribution, as seen in the gels seen in Figure 3.23, between fractions from the SH1000 WT versus the SH1000 Δ*gapA* mutant remains remarkably consistent provides some evidence that expression profiles have not changed markedly, but such an observation cannot rule out more subtle changes to protein abundances which may affect copper distribution.

In this chapter, the ability of r*Sa*GapA to bind to copper *in vitro* is demonstrated, thereby strengthening the hypothesis that binding is in fact occurring *in vivo.*

Identification of *Sa*GapA in Chapter 3 as a potential copper toxicity target led to investigation of the published crystal structure of the protein in *S. aureus*[114] as well investigation of current knowledge of its function in bacteria (and more broadly in

eukaryotes) where it is widely conserved at structural and sequence levels (see introduction). In this chapter we have delved into the nature of the structural properties of *Sa*GapA that make it a potential copper binding target.

As mentioned in the introduction, *Sa*GapA contains a cysteine residue and a histidine residue within its active site that are both essential to the activity of the protein[114]. This is significant because both cysteine and histidine resides are often involved in native copper co-ordinating sites throughout nature due to their inherent abilities to co-ordinate copper with high affinity.

The structures of cysteine, histidine and methionine (another typical copper ligand) can be seen in Figures 4.2, 4.3 and 4.4 respectively. As observed, cysteine contains a thiol group as the terminal structure of its R group. This is the ligand that makes cysteine so amenable to binding copper, especially as the thiophilic ion Cu(I). Other well-known copper binding compounds such as glutathione and bacillithiol also contain functional thiol groups. The thiol group can become deprotonated, giving rise to the thiolate anion which can co-ordinate positively charged metal cations with extremely low stability constants[146].

The thiol group is thus able to undergo metallation and in the process becomes a metal-thiolate. A metal co-ordination centre usually contains a number of co-ordinating residues that may be composed of multiple cysteine residues as well as other residues that may have individually weaker bonds with the metal centre, but act to stabilise the position of the bound metal ion; however not all metal co-ordination centres contain cysteine. Of the cupric and cuprous ions, cysteine has a preference for cuprous (Cu(I)) ions, making cysteine a significant ligand in anaerobic environments, such as the cytoplasm of cells, in the binding of Cu(I).

As well as having the potential to become metallated, the thiol group of cysteine residues is also vulnerable to oxidation reactions that can damage their function in enzymes. Damage to such groups is countered by the evolved antioxidant pathways within cells which allow continued function, by protecting proteins' cysteine residues from oxidation in a buffering capacity, by detoxifying the reactive oxygen species themselves or the harmful reagents that generate the reactive species in the first place,

through repair of the proteins and other macromolecules damaged by oxidation through reduction, or through *de novo* synthesis if damage to them is irreversible.

Histidine (Figure 4.3) contains a functional imidazole group, and it is this group which is able to interact with copper ions. Specifically, the N1 nitrogen atom of the imidazole ring is able to donate electrons to a copper ion from its lone pair. In contrast with cysteine, histidine is not readily oxidised. Histidine readily binds to both the Cu(I) and the Cu(II) ion. Methionine is another common copper binding ligand within metalloproteins (see Figure 4.4). When methionine is utilised for copper binding within metalloenzymes it is often found in environments that are more likely to experience aerobic conditions, and where the lack of potential residue oxidation would be advantageous.

Examples of native copper binding proteins include those that use both histidine and cysteine in their copper co-ordination centres. Two such examples are umecyanin and plastocyanin, of which plastocyanin also incorporates a methionine residue[147]. There are few examples of enzymes which utilise just two residues to co-ordinate copper in which one is histidine. However, Cu(I) binding sites utilising dual thiol sidechains from cysteine residues are relatively common and include the copper metallochaperones CopZ and Atx1. In some instances amino acids apart from cysteine, histidine or methionine are utilised in copper binding centres; again umecyanin is an example, which also employs a glutamate residue[147].

Common to all copper complexes is the nature by which copper is bound to its ligand. Copper is held in place through multiple coordinative bonds (also known as dative covalent bonds or dipolar bonds). Such bonds are defined by their formation by a pair of electrons that are donated from one of atoms involved in the bond, as opposed to one electron originating from each atom in a standard covalent bond. This requires the donor atom of the ligand to have a lone pair of electrons that can be donated to the copper centre and it why nitrogen in histidine and sulphur in methionine and cysteine are often involved in metal chelation[148]. An example of such a co-ordination complex is shown in Figure 4.6. Another example is demonstrated in Figure 4.1, the 2:1 complex of copper and bathocuproine disulphonate (BCS), a reagent that has been used extensively throughout this work.

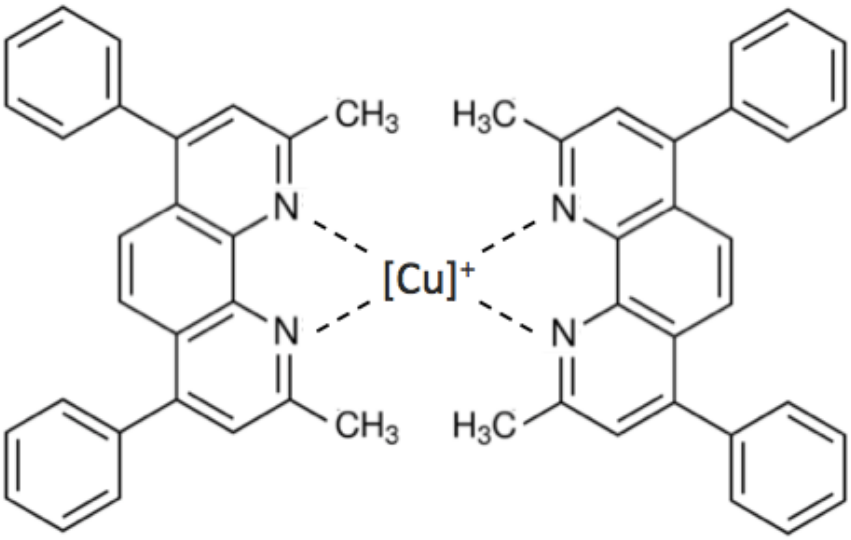

Figure 4.1. The copper (I) - BCS complex. Two molecules of BCS form co-ordinate bonds with a central Cu(I) ion. These four bonds (dashed lines) are formed from the lone pairs of electrons that exist on each of the nitrogen atoms involved; two from each BCS molecule. The sulphonate groups have been removed from this structure, as they would dissociate from the central structure of each BCS molecule in solution.

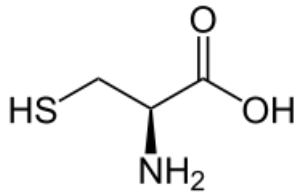

Figure 4.2. The amino acid cysteine. The thiol group of cysteine makes it an ideal ligand in the co-ordination of copper, especially Cu(I). Many native copper enzymes use cysteine residues in their active sites, whilst many non-copper enzymes also use it for catalysis, such as *Sa*GapA.

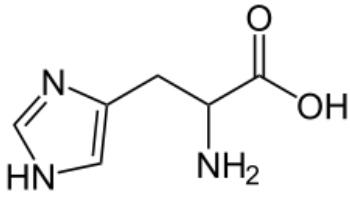

Figure 4.3. The amino acid histidine. The imidazole ring can coordinate copper. Histidine is often found in copper binding sites, of both Cu(I) and Cu(II) sites, as well as non-copper binding active sites.

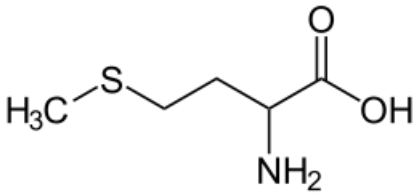

Figure 4.4. The amino acid methionine. The S-methyl thioester group of methionine is the main copper binding component of this residue. Methionine is not often found as a catalytic residue, but the sulphur centre of its sidechain can contribute to copper binding, especially in aerobic compartments.

Mukherjee *et al.* showed that Cys151 and His178 are both essential to the activity of GapA[114]. These two residues are both positioned in the active site of the protein and play a role binding the enzyme substrate, glyceraldehyde 3-phosphate. They align the substrate which in turn allows NAD^+ to interact with it. NAD^+ binds to the Rossmann fold of the protein, a conserved region amongst dinucleotide-cofactor utilising enzymes[149].

The active site within the crystal structure of *S. aureus* GapA was examined closely using published data gathered by Mukherjee *et al.*[114] in order to ascertain a more detailed view of how copper may bind to the enzyme. The N1 of the His178 imidazole ring and the sulphur of the Cys151 residues are approximately 3.5 Å apart making it feasible that these residues could together coordinate a Cu(I) ion. Other residues around these are not typical copper binding residues, but several of them may contribute to coordination alongside the cysteine and/or histidine residues. There is only one other cysteine residue (Cys96) within the structure of the monomer and the potential of this to form a disulphide bridge or copper coordination site with Cys151 was thought of as a possibility, although such a bridge has not previously been described. However, the distance between the two sulphur residues is 12.7 Å. A typical disulphide bond is approximately 2 Å, making it extremely unlikely that these would interact, unless the protein was substantially denatured. The crystal structure also shows the thiol group of Cys96 pointing towards the centre of the protein and surrounded by hydrophobic residues, making the residue even less likely to interact with Cys151 or any copper that came within proximity of the residue.

Notably, one study conducted by Matsumara *et al*. has shown copper bound to the active site of crystallised GAPDH from *Synechococcus elongatus*, *Se*GAPDH[150]. Here, copper (in the form of $CuSO_4$) was incorporated into the crystallisation conditions in which *Se*GAPDH was being co-crystallised with another protein, CP12, due to previous studies having shown that copper may be bound to CP12, which is utilised in photosynthetic organisms to regulate GAPDH activity. In the crystal structure, copper was found to interact with four residues, three from GAPDH itself (Cys155, His182 and Thr156 equivalent to Cys151, His 178 and Thr152 in *Sa*GapA) and one from CP12 (Asp76)[150]. However, it is likely that this binding through four residues is mainly attributable to the presence of copper in its oxidised, Cu(II) ionic form. In the case of Cu(I) binding to *Sa*GapA it may be that no further residues are needed, as Cu(I) can form stable two-

coordinate sites. Alternatively, another residue may take the place of the Asp76, or it may be the case that an interaction with the substrate or NAD^+ cofactor holds the copper in place, with that molecule effectively replacing the function of CP12 with regards to copper co-ordination in *Se*GAPDH. Notably, the Thr156 that is adjacent to the Cys155 in *S. elongatus* is conserved in terms of its position adjacent to the Cys151 within the *S. aureus* GapA[114]. Indeed each residue of *Se*GAPDH involved in copper binding is shifted by four residues within the primary structure of *Sa*GapA, with them being equally spaced when comparing the two sequences to each other.

Any stable interaction of copper with either of the catalytic residues of these enzyme (Cys151 or His178) would presumably inhibit the activity of the protein, either by prevent it from binding or releasing its substrate.

Interestingly Matsumara *et al*.[150] had not expected the copper ions within the structure to be located in the described position at the active site, but hypothesised that it would be more intimately bound to CP12 as this protein had already been found to interact with copper independently of *Se*GAPDH[151]. The interaction of CP12 with copper is of relatively low affinity and contrary to most copper binding proteins does not involve cysteine, histidine or methionine residues, despite the presence of the former two within its sequence. Binding of copper to CP12 has been ascribed to glutamic acid residues, which is rarely seen in copper proteins without the involvement of at least one of the conventional copper binding residues.

The fact that the crystallised GAPDH/CP12 complex from *S. elongatus* contained copper at the GAPDH active site, at least under the conditions used for crystallisation, led us to test whether copper could bind to this site in *Sa*GapA. In the case of *Synechococcus elongatus*, the question arises as to whether copper binding is artefactual. The initial binding of copper was observed when copper was present in a solution containing purified CP12[152], and has been ascribed to glutamic acid residues by further study, including crystallisation of CP12. No *in vivo* studies have gone on to attempt to demonstrate that copper binds to CP12 within living cells, and indeed the relatively low affinity glutamic acid binding site would suggest that this is not the case as the copper homeostasis systems of organisms expressing CP12, as well as native copper proteins, would almost certainly prevent such an interaction.

Furthermore, these investigations of CP12 and copper has been performed with Cu(II), whereas Cu(I) is thought to be the prevalent ion in the cytosol *in vivo* as discussed. Nonetheless, co-crystallisation of CP12 and GAPDH with copper bound to the active site of the GAPDH component overwhelmingly pointed to copper binding to this site if indeed such binding was to occur *in vivo*, for which we have presented evidence in the previous chapter.

On the basis of the above information, we hypothesised that r*Sa*GapA would bind to copper *in vitro*, and that this binding would most likely involve Cys151 and/or His178 due to their aforementioned propensity to bind copper above other amino acid residues, as well as their location in the accessible active site of *Sa*GapA. Furthermore, we hypothesised that binding of Cu(I) to these residues would lead to inhibition of enzyme activity by precluding access of the substrate to these essential catalytic residues.

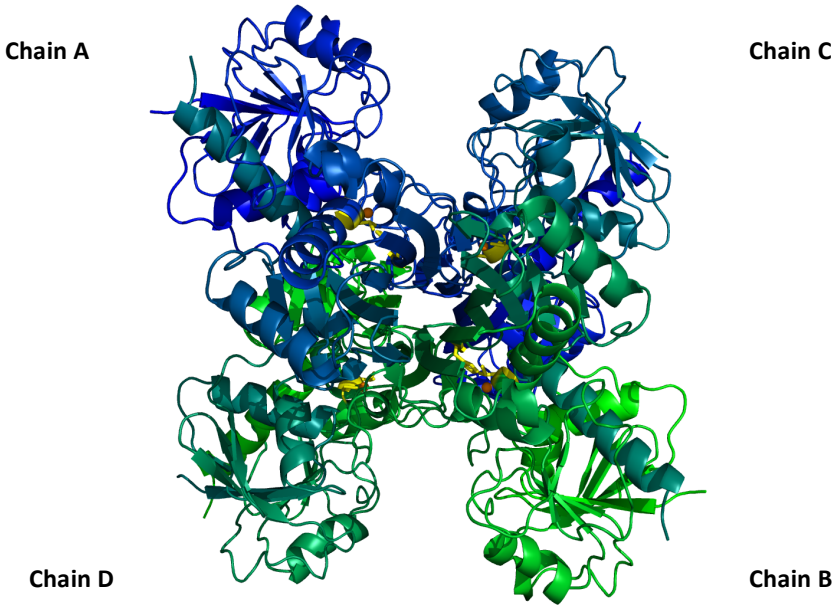

Figure 4.5. The crystal structure of the tetramer of *Se*GAPDH. Shown in cartoon representation, coloured blue to green from N to C termini, with the active site copper binding residues as sticks highlighted in yellow (C155, T156, H182) and bound copper represented as orange spheres. Data from PDB file (3b1j) collected by Matsumara *et al.*[150] and image created using PyMol software by Anna Barwinska-Sendra.

```
Query  1    MTIRVAINGFGRIGRNFLRCWFGRQNTDLEVVAINNTSDARTAAHLLEYDSVLGRFNADI  60
            M ++VAINGFGRIGR   R    ++   LEVVA+N+ +D    AHLL+YD++ GRF  ++
Sbjct  1    MAVKVAINGFGRIGRLAFRRI--QEVEGLEVVAVNDLTDDDMLAHLLKYDTMQGRFTGEV  58

Query  61   SYDENSITVNGKTMKIVCDRNPLNLPWKEWDIDLVIESTGVFVTAEGASKHIQAGAKKVP  120
               +    VNGK +K   + +   LPWK+ +ID+V+E TG +   + A  HI+AGAKKV
Sbjct  59   EVVDGGFRVNGKEVKSFSEPDASKLPWKDLNIDVVLECTGFYTDKDKAQAHIEAGAKKVL  118

Query  121  ITAPGKGEGVGTYVIGVNDSEYRHEDFAVISNASCTTNCLAPVAKVLHDNFGIIKGTMTT  180
            I+AP  G+ + T V   N  E    +  V+S ASCTTN LAPVAKVL+D+FG+++G MTT
Sbjct  119  ISAPATGD-LKTIVFNTNHQELDGSE-TVVSGASCTTNSLAPVAKVLNDDFGLVEGLMTT  176

Query  181  THSYTLDQRILDASHR--DLRRARAAAVNIVPTTTGAAKAVALVIPELKGKLNGIALRVP  238
             H+YT DQ   DA HR  D RRARAAA NI+P +TGAAKA+  VIPE+ GKL+G A RVP
Sbjct  177  IHAYTGDQNTQDAPHRKGDKRRARAAAENIIPNSTGAAKAIGKVIPEIDGKLDGGAQRVP  236

Query  239  TPNVSVVDLVVQVEKPTIT-EQVNEVLQKASQTTMKGIIKYSDLPLVSSDFRGTDESSIV  297
                S+ +L V +EK  +T EQVNE ++ AS  +      Y++  +VSSD  G    S+
Sbjct  237  VATGSLTELTVVLEKQDVTVEQVNEAMKNASNESF----GYTEDEIVSSDVVGMTYGSLF  292

Query  298  DSSLTLVM---DGDLVKVIAWYDNEWGYSQRVVD----LAELA  333
            D++ T VM   D  LVKV AWYDNE  Y+ ++V     LAEL+
Sbjct  293  DATQTRVMSVGDRQLVKVAAWYDNEMSYTAQLVRTLAYLAELS  335
```

Figure 4.6. Amino acid alignment of glyceraldehyde 3-phosphate dehydrogenase from *S. elongatus* (Query) compared with that of *S. aureus* (Sbjct). C155, T156 and H182 of *S. elongatus* GAPDH are all conserved within the sequence of *Sa*GapA (highlighted in red boxes).

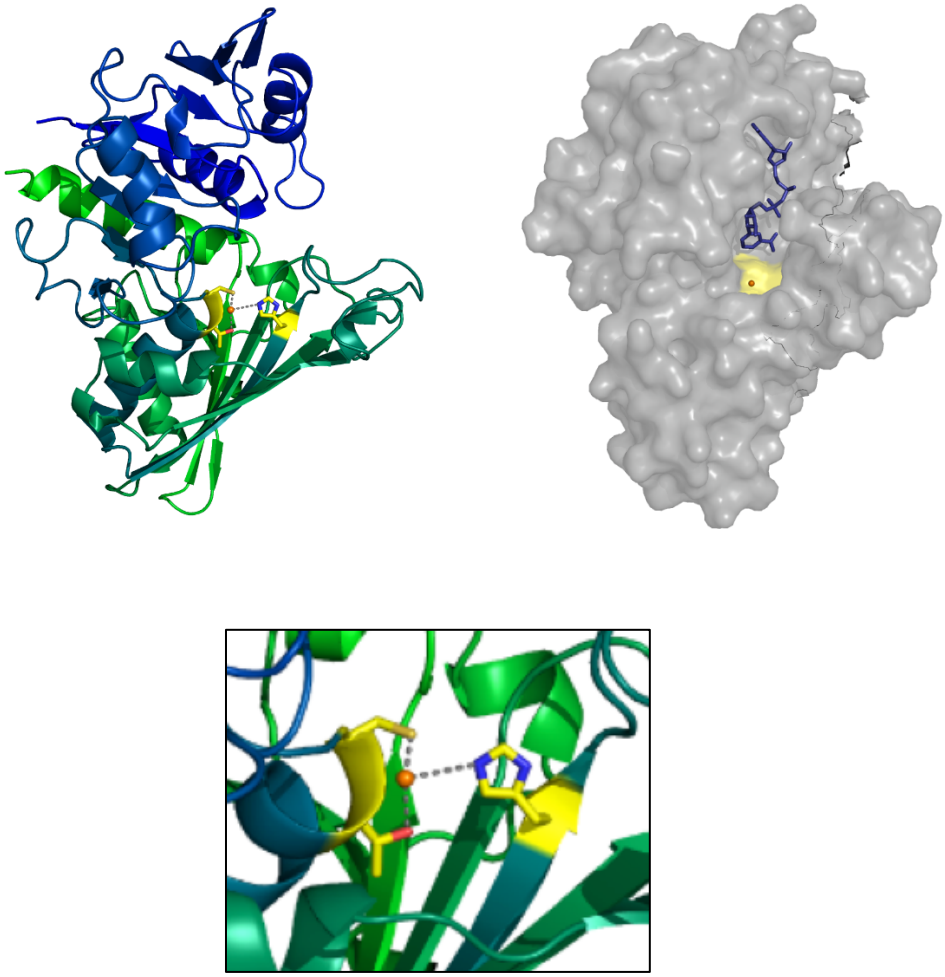

Figure 4.7. The structure of the *Se*GAPDH monomer with copper bound. *Left: Se*GAPDH cartoon representation of a single monomer (Chain A) coloured blue to green from N to C termini, with the copper binding residues highlighted in yellow (C155, T156, H182) and bound copper represented as an orange sphere. *Right: Se*GAPDH surface representation of monomer (chain A) with the copper binding residues highlighted in yellow (C155, T156, H182) and bound copper represented as an orange sphere, NAD^+ shown as blue sticks. *Below:* magnification of left image displaying copper (orange sphere) bound to residues highlighted in yellow (C155, T156, H182). Data from PDB file (3b1j) collected by Matsumara *et al.*[150] and images created using PyMol software by Anna Barwinska-Sendra.

4.2 Purification of recombinant *S. aureus* GapA

In order to study the effects of copper binding to the *Sa*GapA protein *in vitro* it was first necessary to purify recombinant *Sa*GapA. We obtained a plasmid vector, pLEICS-03 containing the *gapA* gene, from the University of Leicester (another kind gift from Dr Julie Morrissey). This plasmid was stored in *E. coli* DH5α cells prior to being isolated by use of a plasmid mini-prep kit and transformed into BL21 cells, in which the protein was expressed. Expression of the *gapA* gene was induced by addition of IPTG to BL21 cultures.

Initially, tests for optimal expression of GapA were performed. Cultures were grown to OD_{595} ~0.6 before the addition of 0.1 mM or 1 mM IPTG. Aliquots of cells were collected at 2, 4 and 6 hours after the addition of IPTG and soluble extracts were analysed by SDS-PAGE to determine which time-point and concentration of IPTG was optimal for *gapA* expression. The results are shown in Figure 4.8. It was decided to use a concentration of 1 mM IPTG for 6 hours as this was the condition which resulted in the highest level of *Sa*GapA.

The plasmid linked the *gapA* gene to a hexa-histidine tag which allowed for purification of the protein using nickel-affinity chromatography. The tag was subsequently cleaved using Tobacco Etch Virus (TEV) protease which was then removed via a second round of nickel-affinity chromatography. The tag was clearly required to be removed due to the propensity of histidine to bind metals, including copper. The TEV protease could be removed in this way as it was also tagged with a hexa-histidine motif. Further purification of *Sa*GapA was achieved using size-exclusion chromatography. A final step of anion-exchange chromatography, under anaerobic conditions, allowed for removal of reducing agents (DTT, TCEP) under conditions where *Sa*GapA would remain in a reduced state (see Materials and Methods for a comprehensive protocol). An SDS-PAGE gel of the purification can be seen in Figure 4.9. The final steps of the purification were applied in order to ensure the high purity of the protein as well as to remove reducing agents. Subsequent copper binding experiments used to examine copper binding would be easily affected by the presence of such contaminants.

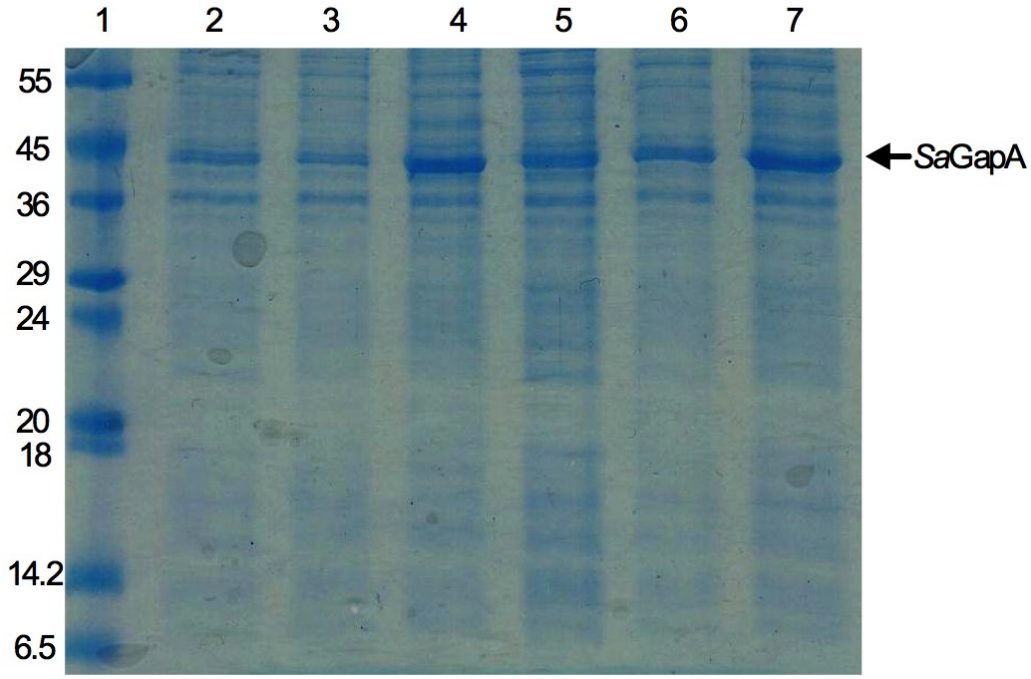

Figure 4.8. Expression test of r*Sa*GapA in BL21 cells. Expression testing of *Sa*GapA in *E. coli* BL21 cells reveals 6 hours of growth after the additon of IPTG at an OD_{595} of 0.6 provides the greatest yield of r*Sa*GapA. BL21 cell lysate (20 µl) was added to lanes 2-7. Lane 1 contains a protein marker ladder, with sizes given in kDa. Lanes 2-7 contained lysates from cultures treated with 0.1 or 1 mM IPTG and having been cultured for 2, 4 or 6 hours after its addition as follows; lane 2: 0.1 mM, 2 hours; lane 3: 1 mM, 2 hours; lane 4: 0.1 mM, 4 hours; lane 5: 1 mM, 4 hours; lane 6: 0.1 mM, 6 hours; lane 7: 1 mM, 6 hours.

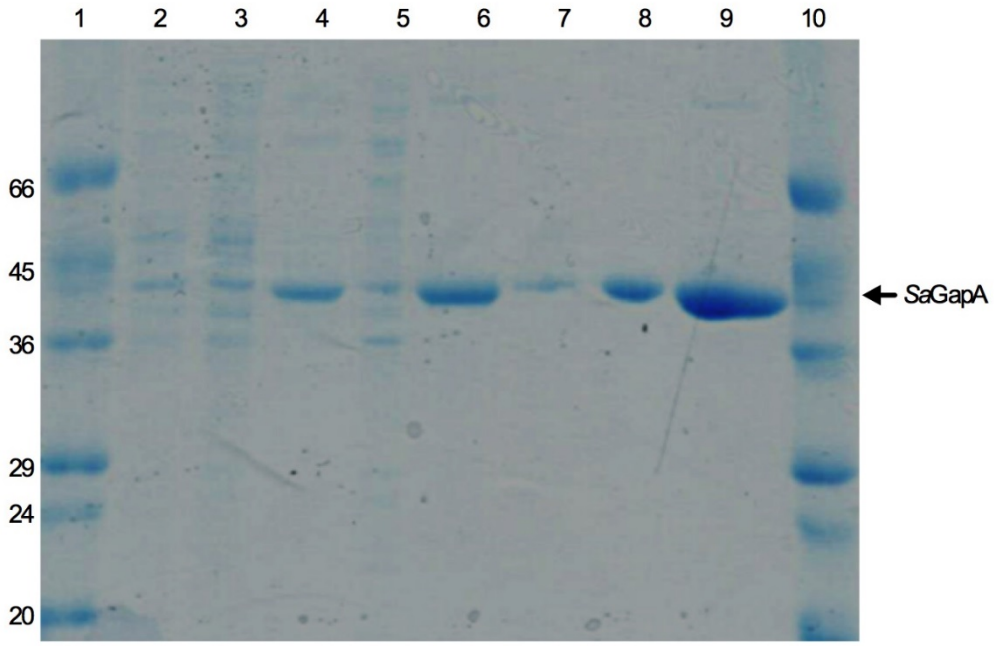

Figure 4.9. SDS-PAGE gel showing the purification steps of r*Sa*GapA through four steps of chromatography. Samples 2-8 were matched for protein concentration to 20 µg protein ml^{-1} by Bradford assay. Sample 9 was loaded at approximately 40 µg protein ml^{-1}. Lanes 1 and 10 contain protein MW marker ladders. Samples were; lane 2: insoluble lysate; lane 3: soluble lysate; lane 4: initial nickel-affinity chromatography r*Sa*GapA step product; lane 5: initial nickel-affinity chromatography flow-through; lane 6: secondary nickel-affinity chromatography r*Sa*GapA purification step product; lane 7: secondary nickel-affinity chromatography flow-through; lane 8: size-exclusion chromatography r*Sa*GapA elution; lane 9: anion-exchange chromatography r*Sa*GapA elution. The gel demonstrates the increasing purity of r*Sa*GapA throughout the purification.

4.3 Purified r*Sa*GapA contains one accessible reduced thiol

After purification of r*Sa*GapA it was necessary to test if its thiol groups were fully reduced. This was achieved using a DTNB (5,5'-dithiobis-(2-nitrobenzoic acid)) reagent based assay. DTNB contains a disulphide bridge which reacts with reduced thiols, liberating an anion which absorbs light strongly at 412 nm. The absorbance at this wavelength is thus directly proportional to the level of accessible reduced thiols within a given solution.

The difficulty of measuring the level of reduced thiols in a solution of purified r*Sa*GapA is caused by the accessibility, or lack thereof, of the reduced thiol groups to the DTNB molecules in solution. This is due to the shape of the active site and the possibility of other molecules blocking the reaction, such as G3P or NAD^+ for example, which, despite not being present in buffers during the purification, will have been present in the BL21 cells during expression prior to cell lysis, and may therefore remain within the active site of the protein upon purification, blocking access of the DTNB molecule. On the other hand, one of the cysteine residues is expected to be relatively buried within the folded protein, based on the crystal structure[114].

Our approach to solving this issue was to attempt to unfold the protein using guanidine or urea under anaerobic conditions to allow full access to all reduced thiols. Before attempting this it was necessary to evaluate the ability of these reagents to unfold r*Sa*GapA. To do this we used fluorescence spectroscopy, with an excitation wavelength of 280 nm and a detection wavelength range of 300 nm to 450 nm. If the protein under investigation is unfolded in the presence of either chaotropic agent, a shift in the emission maximum is observed as well as an increase in overall intensity of the emission (a greater maximal value); this is caused by the unfolding of the protein revealing tryptophan residues that may have been previously buried within the structure, or not as fluorescent due to a quenching of their fluorescence by the surrounding environment. Dissolution of r*Sa*GapA in 6 M guanidine resulted in a blue shift as well as an increase in intensity, whereas use of 8 M urea resulted in a blue shift but with a decrease in intensity (both denaturation using guanidine and urea were carried out at pH 7.5; data not shown). The greater increase in maximum intensity observed through use of 6 M guanidine led us to choose this as the denaturant in order to allow the DTNB reagent access to reduced thiol groups.

Figure 4.10 shows the results from an example of a DTNB assay performed on one purification of r*Sa*GapA in order to evaluate the oxidation state of its thiols. The DTNB assay, along with absorbance of the sample at 280 nm, is an additional method by which to evaluate protein concentration, assuming that all thiols are reduced and that the number of cysteine residues within the protein is known. *S. aureus* GapA monomers have two cysteine residues that do not form a disulphide bridge, Cys151 and Cys96. According to the crystal structure published by Mukherjee *et al.*[114] the thiol group of Cys96 likely points inwards towards the centre of the protein, and is therefore presumably inaccessible to DTNB under native conditions. Therefore under native conditions one would expect the absorbance from the DTNB reaction with one of these thiols to produce a 1:1 ratio with protein concentration as recorded by A_{280}. When r*Sa*GapA has been denatured, and remains under reducing conditions DTNB should have access to all reduced thiols therefore altering the ratio to 2:1, as found in the example shown in Figure 4.10.

Variability was observed in this DTNB-determined value for accessible thiol groups between protein preparations in the absence of guanidine. One factor in this variability could be discrepancies between the protein concentration as assessed by alternative methods (such as A_{280} and Bradford) and the DTNB assay itself. However, the DTNB assay gave an approximate ratio of 1 reduced thiol group to each r*Sa*GapA monomer (within an error of 15 %) without the presence of guanidine, indicating that the accessible thiol of Cys151 was reduced in the cases where subsequently used for copper binding (data not shown).

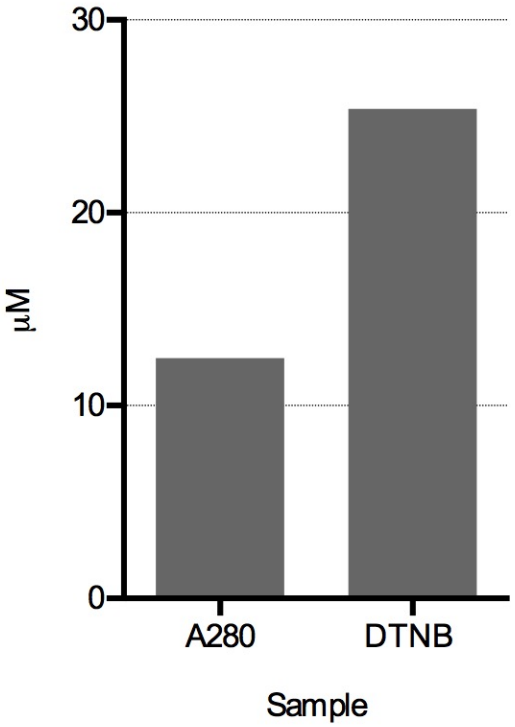

Figure 4.10. DTNB assay demonstrating reduced status of purified r*Sa*GapA. After the purification of r*Sa*GapA, a sample was dissolved in 6 M guanidine under anaerobic conditions before a UV/visible spectrum was taken using a spectrophotometer (Perkin Elmer). DTNB reagent was then added to the sample in order to quantify the number of free thiols within solution. The concentration of protein attained here by A_{280} was 12.46 µM (using an ε value of 22,920 M^{-1} cm^{-1}, acquired using ExPasy ProtParam open source software, for r*Sa*GapA at 280 nm) and the concentration of thiols observed through use of DTNB was 25.38 µM (using an ε value of 14,150 M^{-1} cm^{-1} at 412 nm). As there are two cysteine residues within r*Sa*GapA the expected value for the DTNB reaction was twice that of the value acquired via A_{280}.

4.4 r*Sa*GapA binds one equivalent of Cu(I) *in vitro*

After purification of r*Sa*GapA we wanted to assess its capability to bind copper. There are a number of methods by which to investigate this, each contributing a piece of evidence in support of the hypothesis that this protein does indeed bind to copper.

Central to potential copper binding is the hypothetical binding site, which has been predicted to involve the Cys151 residue of *Sa*GapA. When Cu(I) binds to the thiol group of a cysteine residue, the bond formed is not ionic or covalent in nature, but co-ordinate (hence the term co-ordinate metal complex), and can usually be detected spectroscopically. In the case of Cu(I) and a thiol ligand, the formation of a complex gives rise to ligand-to-metal change transfer (LMCT) absorption bands in the UV/visible spectrum. In this case, we hypothesise that such a coordination would consist of the Cu(I) and Cys151 and the co-ordination bond between them. This bond can absorb UV light energy, giving rise to the transfer of charge (electrons) from the ligand, in this case the thiol of Cys151, to the Cu(I) ion.

LMCT complexes exhibit specific absorbance characteristics that differ from the absorbance of the ligand or metal ion alone, generally increasing their absorbance across a defined range of their spectrum, relative to the spectrum of the ligand alone. The absorbance in the diagnostic region will continue to increase until the ligand is saturated. This feature can therefore be detected spectroscopically. The discrete changes in absorbance can occur at a range of different wavelengths, dependent upon the nature of the bond formed, which is inherent to the nature of the ligand, metal and the environment in which they exist. In the case of LMCT complexes of Cu(I) and thiol groups (such as cysteine residues), changes in absorbance usually occur in the region of 250 – 300 nm, but are not limited to this region[153].

In order to visualise the spectra of Cu(I) in a complex with r*Sa*GapA it was required to titrate Cu(I) into a solution of recombinant r*Sa*GapA of known concentration. Under oxidising conditions Cu(I) is not stable and rapidly oxidises to Cu(II). A solution of Cu(I) was therefore prepared under anaerobic conditions using an acetonitrile solution, forming tetrakis (acetonitrile) copper(I) hexafluorophosphate, which is a tetrahedral co-ordination complex of Cu(I) with acetonitrile. The acetonitrile ligands form a four co-ordinate complex with a Cu(I) ion that prevents its oxidation, but the weak interaction of

the ligands with the metal allows the Cu(I) to interact with other ligands present that have a stronger propensity to bond with it. Once the solution has been prepared it is subsequently kept under rigorous under anaerobic conditions to further prevent any oxidation of Cu(I). The Cu(I) within the solution must then be quantified precisely as only this would allow precise interpretation of any interaction with r*Sa*GapA spectroscopically. This experiment involves the aforementioned BCS copper chelator which forms a strong two co-ordinate complex with Cu(I) that absorbs strongly at 483 nm.

Titration of Cu(I) into BCS results in absorbance spectra with a local maximum at 483 nm that increases in absorbance value proportionally to the concentration of Cu(I) added. Subsequently the concentration of the $[Cu(I)(BCS)_2]$ complex can be calculated using the Beer-Lambert law and the published extinction coefficient of the complex at this wavelength (13,300 M^{-1} cm^{-1})[136]. An example of such a titration can be seen in Figure 4.11. Each time a new stock solution of Cu(I) was prepared, i.e. each new day that a Cu(I) titration experiment was performed, this quantification experiment was performed. Figures 4.11 and 4.12 are an example of one such quantification.

After quantification of Cu(I) within a stock with BCS, total copper (i.e. the sum of both Cu(I) and Cu(II) within solution) was quantified using atomic absorption spectroscopy (AAS), whereby a diluted sample of the copper stock is analysed spectroscopically after being atomised within an acetylene flame. This gives further verification of the total copper within the stock and theoretically allows for the calculation of the ratio of Cu(I) to Cu(II) in the stock by subtraction of the former concentration from the total as determined by AAS. After AAS quantification of copper, the stock of Cu(I) made was only used in titrations if the quantification using BCS matched that given within an error of 10% (data not shown).

We initially titrated 2 µl aliquots of a Cu(I) stock solution into 1 ml of a 25 µM GapA solution. Each 2 µl addition increased the concentration of Cu(I) within the solution by approximately 2 µM. After each addition an absorbance spectra was immediately recorded. We continued to add Cu(I) until approximately 1.25 mole equivalents of Cu(I), relative to the amount of GapA, had been added. The data are shown in Figure 4.13.

As observed in Figures 4.13, 4.14 and 4.15, each Cu(I) addition leads to an increase in absorbance at various wavelengths. Upon the addition of 1 mole equivalent of GapA, there is a sudden increase in absorbance relative to the previous additions of Cu(I). After this, there is only a slight increase in absorbance from subsequent Cu(I) additions, much smaller changes than previous to the addition of one equivalent of Cu(I). We can observe this change more clearly by plotting the change in absorbance against added Cu(I) for specific wavelengths as shown in Figure 4.16.

The increase in absorbance observed here can be explained by the binding of Cu(I) to the thiol group of a cysteine residue; most likely the Cys151 residue as this is solvent accessible in the crystal structure. As demonstrated in the previously published crystal structure of GapA, the functional group of Cys96 is buried within the centre of the protein and not solvent accessible. The change in gradient in the change in absorbance beyond 1 equivalent of Cu(I) indicates saturation of the cysteine residue with copper. Further spectral changes were nonetheless observed beyond 1 equivalent, suggesting that perhaps copper may have bound to another site with a cysteine residue (perhaps Cys96) or that addition of further copper is able to alter the initial complex and thus alter its absorbance. It should be noted that protein precipitation was observed after additions of high concentrations of Cu(I). The most likely explanation is that Cu(I) binds to a cysteine residue, most likely Cys151, at a ratio of 1:1, but that some non-specific, adventitious binding does occur on saturation of the preferred specific site. If a second cysteine site was available to Cu(I) after saturation of the first, one would expect a consistent continued increase in absorbance with further additions of Cu(I).

The relatively large increase in absorbance upon reaching one equivalent of Cu(I) compared to previous additions may be demonstrative of a change in conformation and/or oligomerisation of the protein when saturated with Cu(I). Other data (not shown) corroborates this hypothesis and suggest the formation of a higher order complex, i.e. higher molecular weight than the tetramer, which is thought to occur *in vivo* and which we purify in the absence of copper, as observed through calibration of the chromatographic columns used during purification of r*Sa*GapA.

A difficulty of these titration experiments is the predisposition of purified proteins to precipitate with the addition of sub- or super-stoichiometric concentrations of copper.

This is due to the added copper drawing the solubilised enzyme molecules together as it tries to form stable complexes; the excess of potential binding sites results in an initial weak attraction of Cu(I) to multiple potential binding sites, pulling separate enzyme units into close proximity, under which conditions the likelihood of aggregation is increased. This has made it difficult to attain consistent replication of these results. Even with the presence of increases in absorbance, if precipitation is thought to have occurred it is difficult to interpret spectra. Precipitation can be easily detected by large increases in absorbance in the wavelength range of 600 – 800 nm.

Having observed the saturation of GapA with Cu(I) when loading with super-stoichiometric concentrations, but being prevented from further characterisation spectroscopically due to protein precipitation, we decided to attempt to further confirm copper binding using chromatography. In this case we added both sub- and super-stoichiometric concentrations of copper.

This method allowed further examination of the stoichiometry of binding and eliminated some of the complexities of analysis of LMCT spectra. We applied *Sa*GapA to a size-exclusion chromatography column, using samples of *Sa*GapA before and after treatment with Cu(I). Subsequent analysis of eluted fractions by Bradford assay (for protein content) and by ICP-MS (for copper) allowed us to ascertain the ratio of protein and copper within collected fractions.

To prevent adventitious copper, bound to the column from previous analyses, from affecting the result we cleaned the column using a known high-affinity copper binding protein, recombinant *Sa*CopZ. The *Sa*CopZ was purified by Dr Gus Pelicioli-Riboldi (data not shown), with 500 µl of a 50 µM solution of the protein being applied as a wash step. Previous to *Sa*CopZ application the column was washed with EDTA to remove any residual Cu(II). Subsequent to washing the column in this manner, untreated *Sa*GapA eluted from size exclusion with no copper bound, as expected (Figure 4.17).

After this, we treated GapA with a sub-stoichiometric concentration (0.9 mole equivalents) of Cu(I) and incubated the sample at 4 ˚C for 36 hours in order to allow the mixture to reach equilibrium; we incubated at 4 ˚C to further minimise the risk of precipitation. This sample was then applied to the column, subsequent to the non-

treated sample, and fractions tested for protein and metal content. We repeated this once more with a sample that had been loaded with approximately 1.5 mole equivalents of Cu(I). The results from each of these analyses are shown in Figure 4.18.

The results seen in Figure 4.18 further confirm our hypothesis that SaGapA binds to Cu(I) *in vitro*. The enzyme has predominantly eluted at the same volume as it did in the absence of added copper, demonstrating that the tetramer is still the main form of the protein and indicating that copper does not disrupt tetramerisation. Such disruption would not be expected if copper bound to the active site of the protein, which is not located close to the interface(s) between monomers.

Most notable is the apparent stoichiometry of copper binding to the protein. In the case of adding a sub-stoichiometric amount of copper (0.9 mole equivalents) we see this reflected in our results, with sub-stoichiometric levels of copper present in fractions containing SaGapA. In terms of the elution volume from 12 to 13.5 ml the respective levels of protein and copper were (to 2 decimal places); 12 ml, 0.77 μM protein and 0.57 μM copper (0.74 mole equivalents); 12.5 ml, 1.03 μM and 0.91 μM (0.88 M equivalents); 13 ml, 0.56 μM and 0.40 μM (0.71 M equivalents). The small discrepancies between measured copper and protein are likely a reflection of the error associated with measurement of metal (by ICP-MS) and, most importantly, of protein (by Bradford assay).

In the case of the addition of super-stoichiometric addition of copper to *Sa*GapA (1.5 mole equivalents) we see a change compared to the sub-stoichiometric additions with values of protein and copper concentrations respectively in the fractions detailed above being; 12 ml, 0.84 μM and 0.82 μM (0.97 M equivalents); 12.5 ml, 1.03 μM and 1.12 μM (1.08 M equivalents); 13 ml, 0.57 μM and 0.91 μM (1.59 M equivalents). This is very close to 1 mole equivalent, with the discrepancy most likely due to error associated with the Bradford quantification of the protein. However, the presence of a second, lower affinity binding site, cannot be ruled out.

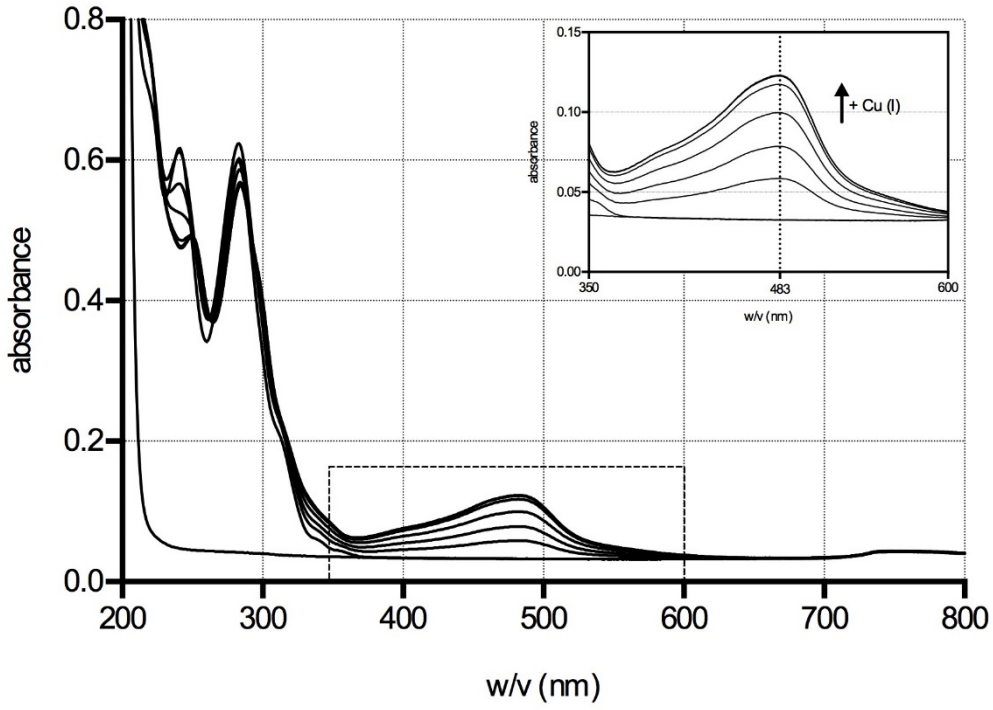

Figure 4.11. Measurement of Cu(I) stock concentration using BCS. *Main panel*; full UV/visible spectra during the titration of Cu(I) into a solution of the copper chelator BCS, and *inset:* expanded view of the region in which the $[Cu(I)(BCS)_2]$ complex absorbs. . The spectrum which shows no maximum at 483 nm is BCS with no added Cu(I). As Cu(I) is titrated into BCS, absorbance increases in the region of 360 – 600 nm with a maxima at 483 nm. When BCS has been saturated with Cu(I), the absorbance ceases to increase. The increase in absorbance at 483 nm per addition of Cu(I) can be used to calculate the concentration of Cu(I) in solution before the solution is used for titration into r*Sa*GapA. In this example, a value of 2 μM Cu(I) per addition was sought, and a BCS concentration of 15 μM was prepared. The values given by the titration itself were; Cu(I) per injection, 2.07 μM; BCS, 14.50 μM.

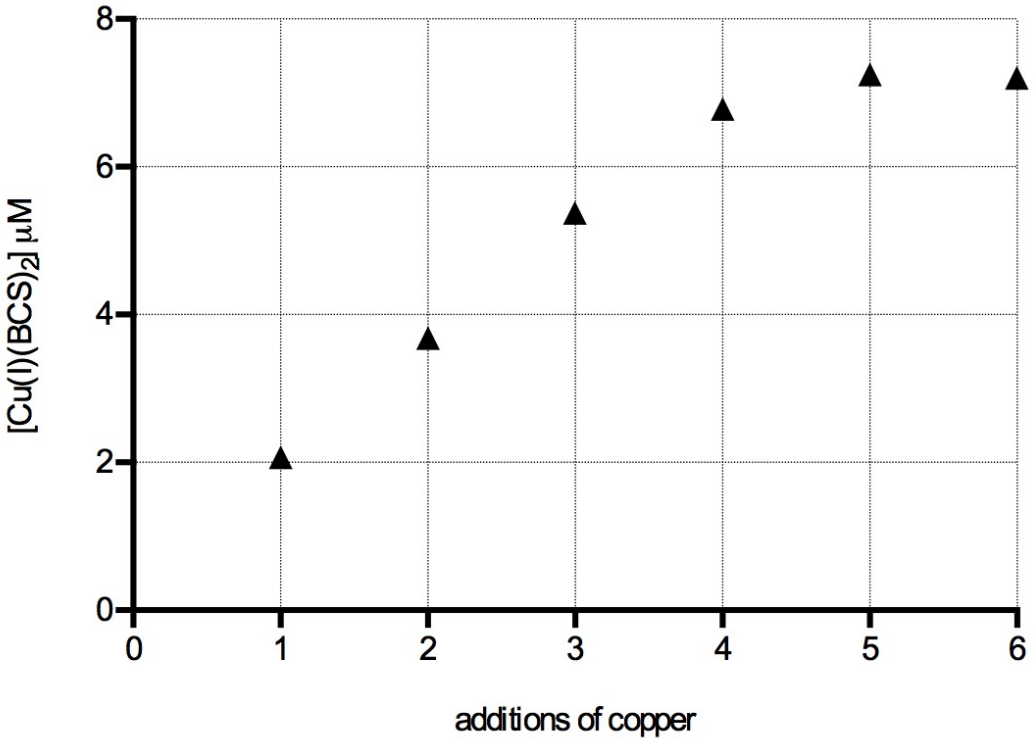

Figure 4.12. Quantitation of Cu(I) present in an anaerobic Cu(I) stock solution. The addition of Cu(I) to BCS increases the concentration of the $[Cu(I)(BCS)_2]$ complex in solution. In this example the same data is shown as in Figure 4.9, but data values only for change in absorbance at 483 nm are shown; a value of 2 µM Cu(I) per addition was sought, and a BCS concentration of 15 µM was prepared. The values given by the titration itself were; Cu(I) per injection, 2.07 µM; BCS, 14.50 µM.

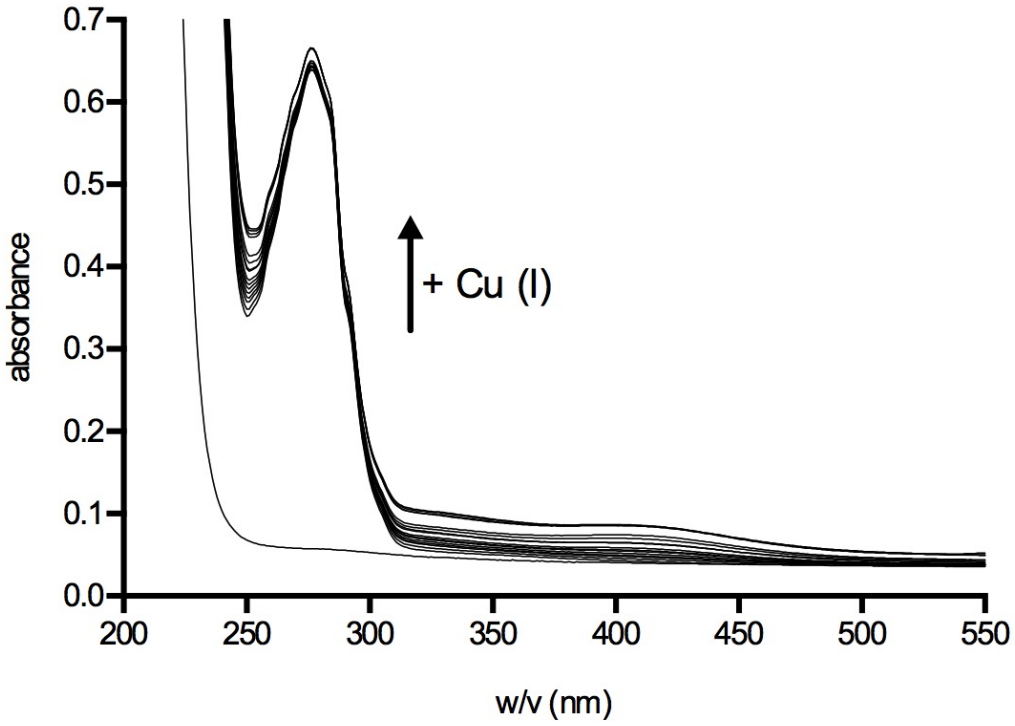

Figure 4.13. Spectroscopic titration of Cu(I) into recombinant *Sa*GapA. The concentration of *Sa*GapA was 24.39 μM as measured by absorbance at 280 nm (ε = 22,920). Each addition of Cu(I) added to the concentration of Cu(I) within the solution by approximately 1.95 μM. As more copper is added, so the absorbance of the sample generally increases (as indicated by the arrow on the figure). There are particular wavelengths where the absorbance increases more than at others (see Figure 4.14).

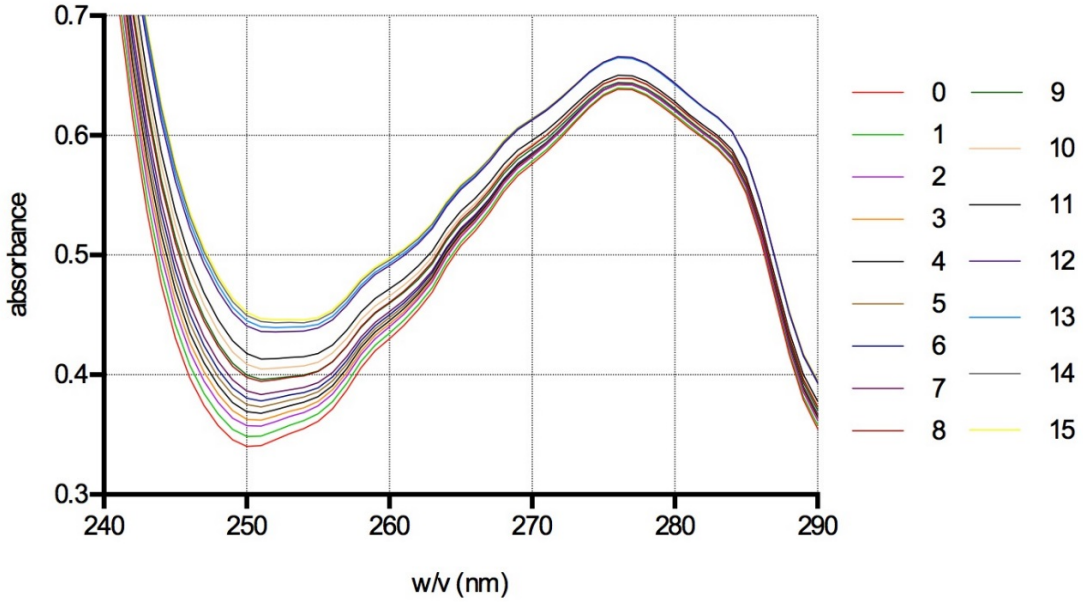

Figure 4.14. Expanded view of absorbance changes in r*Sa*GapA during titration with Cu(I). Titration of Cu(I) into recombinant *Sa*GapA (as in Figure 4.11), shown as an expanded view over a shorter range of wavelengths for clarity. The legend indicates the number of additions of copper, with each being an addition of approximately 1.95 µM Cu(I) (as described above). The wavelengths that appear to show the greatest change when copper is added are between 245 and 260 nm. The 12th addition appears to provoke a greater increase in absorbance than previous to it, and subsequent additions give relatively decreased increases in absorbance. 12 additions is equal to approximately 1 mole equivalent of the protein concentration (23.4 µM Cu(I), 24.39 µM *Sa*GapA).

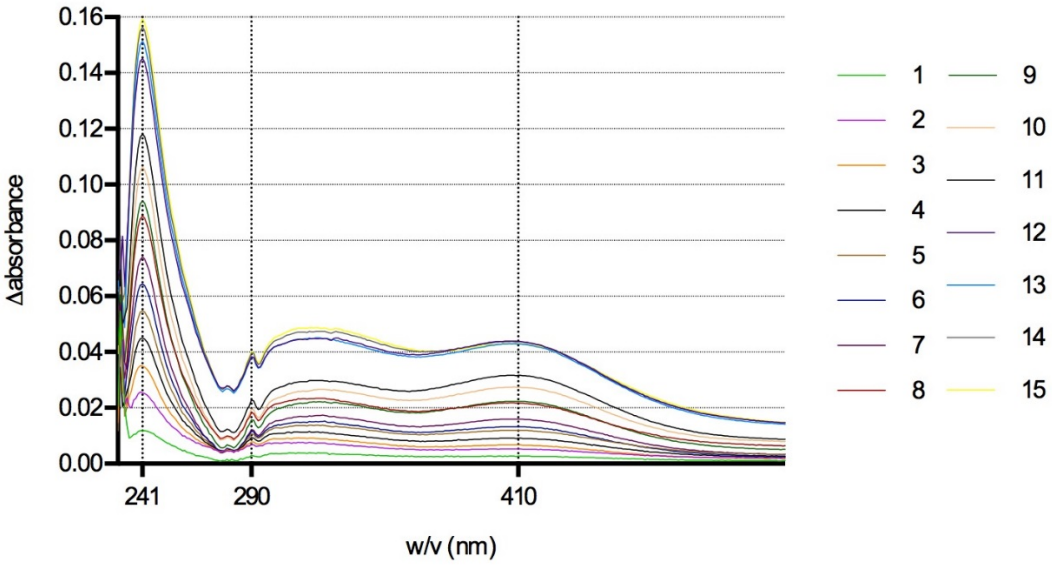

Figure 4.15. Difference spectra of r*Sa*GapA titrated with Cu(I). Note that '0' additions of Cu(I) is equivalent to the baseline, i.e. the spectrum of protein alone, so has not been included here. Again each addition as shown on the legend is equivalent of the addition of 1.95 μM Cu(I). The maximum at 241 nm shows the greatest change in absorbance, and is accompanied by local maxima at 290 and 410 nm. Those at 241 and 290 nm are in the typical region expected to show an absorbance increase when a LMCT occurs between a Cu(I) ion and a thiol group.

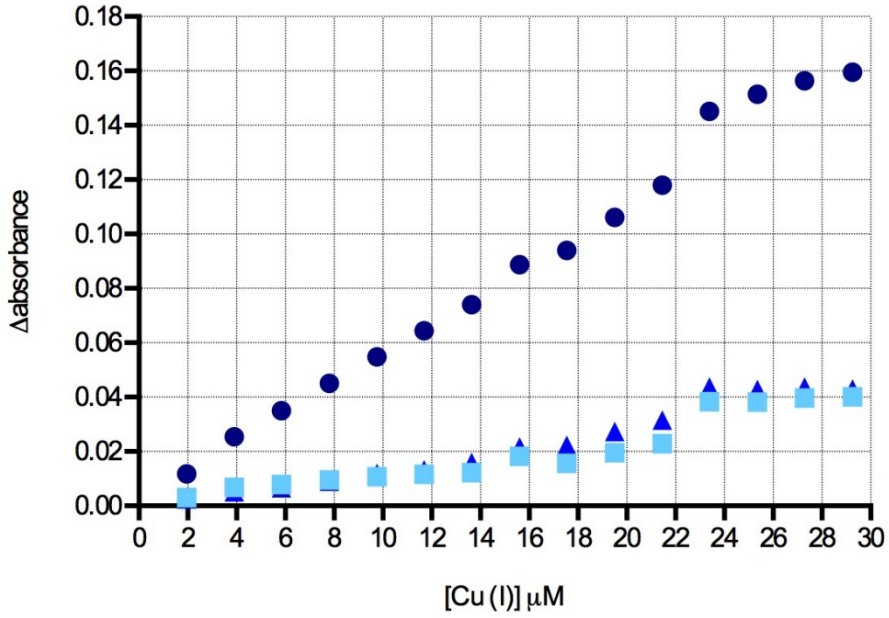

Figure 4.16. Change in the absorbance of *Sa*GapA at particular wavelengths upon the addition of Cu(I). Wavelengths correspond to those emphasised in Figure 4.13 and are represented as follows; 242 nm, navy circles; 290 nm, sky blue squares; 410 nm, blue triangles. The concentration of *Sa*GapA was 24.39 μM which corresponds approximately to the concentration of Cu(I) at which the largest change in absorbance occurs at all 3 wavelengths. After this there is a decrease in the change occurring at all three wavelengths represented here. Absorbance at 241 nm continues to increase but in a reduced manner, whereas hardly any increase at all is observed at 290 or 410 nm. The observation at 242 nm could be indicative of further interaction of Cu(I) with cysteine.

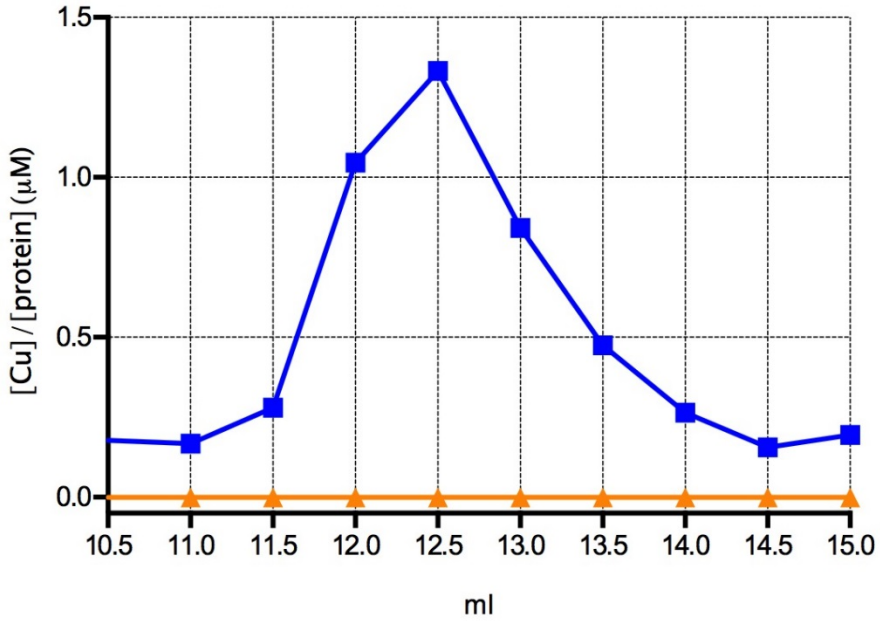

Figure 4.17. Analytical SEC of r*Sa*GapA not loaded with copper. 17.78 μM r*Sa*GapA as measured by A_{280} was loaded onto an analytical size exclusion column (Superdex 200 10/300 GL, GE; buffer, 150 mM NaCl, 40 mM Hepes, pH 7.5; flowrate, 1 ml min^{-1}) having not been treated with copper. Elution volume shown here demonstrates the fractions in which r*Sa*GapA elutes from this column, the peak value as measured by Bradford assay in the fraction eluting at 12.5 ml is 1.33 μM (blue squares). Copper as analysed by ICP-MS is shown (orange triangles). All copper values are extremely close to 0.

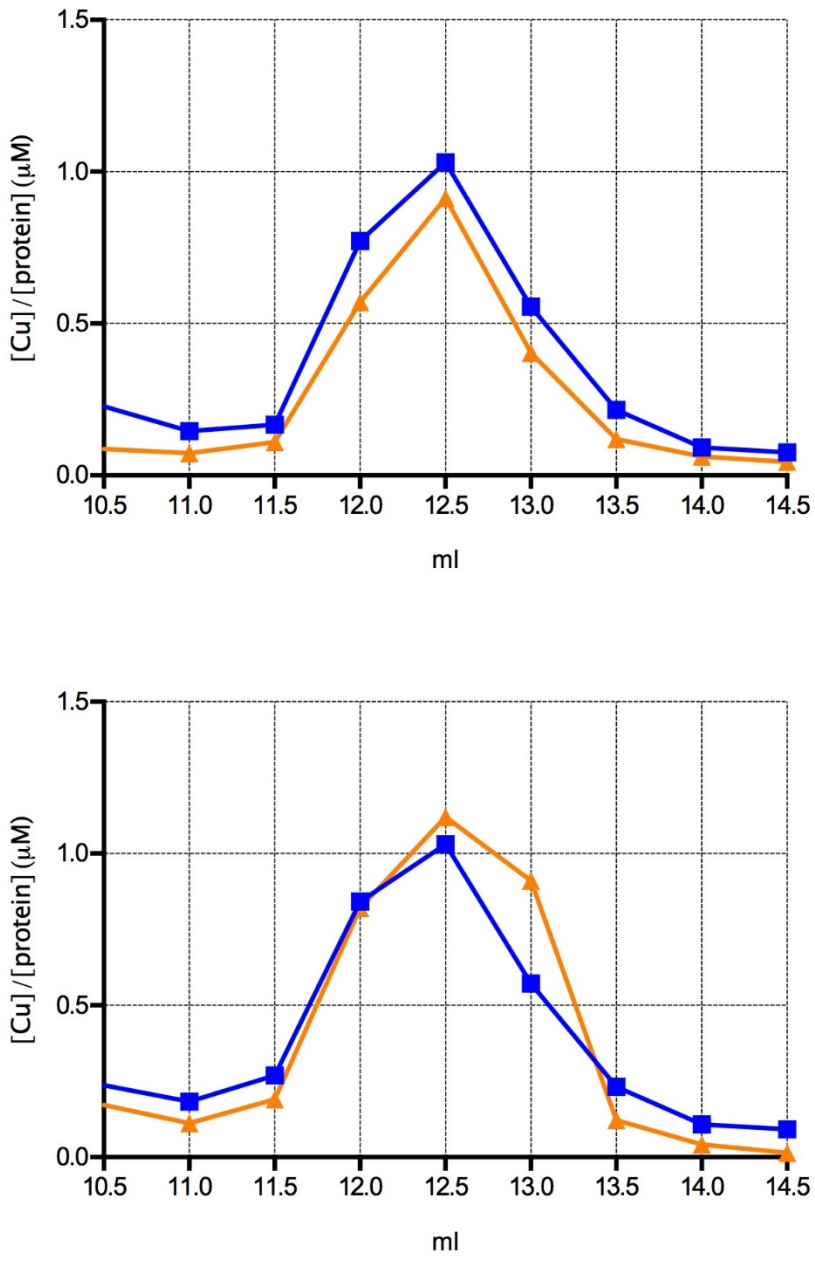

Figure 4.18. Analytical SEC of r*Sa*GapA loaded with Cu(I). *Top panel*; 17.50 μM r*Sa*GapA as measured by A_{280} was loaded onto an analytical size exclusion column (Superdex 200 10/300 GL, GE; buffer, 150 mM NaCl, 40 mM Hepes, pH 7.5; flowrate, 1 ml min^{-1}) after having been loaded with 15.47 μM Cu(I) or approximately 0.91 mole equivalents. *Bottom panel*; 17.72 μM r*Sa*GapA as measured by A_{280} was loaded onto an analytical size exclusion column (Superdex 200 10/300 GL, GE) after having been loaded with 25.13 μM Cu(I) or approximately 1.47 mole equivalents. Details of the concentrations of protein (blue squares) and copper as analysed by ICP-MS (orange triangles) in volumes containing r*Sa*GapA are given in the main text.

4.5 r*Sa*GapA binds Cu(I) with high affinity

We have established that copper binds to GapA *in vivo* and *in vitro* and we were further interested in investigating the affinity with which GapA binds this metal. The fact that binding has been observed *in vivo* suggests a relatively tight affinity, as within the cell GapA is having to compete with a range of ligands for Cu(I), not least the copper homeostasis proteins CopZ, CopA and CsoR which themselves have high affinity[45,58,154].

The Cu(I) specific chelator BCS has already been mentioned for its capacity to bind to that ion with high affinity. The calculated affinity for Cu(I) has been stated as an association constant by Xiao *et* al.[136]. and is approximately one order of magnitude lower than the same value stated for the CsoR copper sensor of *Bacillus subtilis* [155], which binds copper with one of tightest affinities observed in any protein. If GapA could demonstrate an ability to compete with BCS for Cu(I), it would be evident that the interaction between GapA and copper was biologically relevant.

Here, we titrated Cu(I) into a solution of BCS, as described above during Cu(I) quantification. We then repeated the same experiment in the presence of GapA. The absorbance maximum of the $[Cu(I)(BCS)_{2]}$ complex at 483 nm can then be observed. The increase in absorbance at 483 nm was reduced in the presence of GapA, indicating competition between GapA and BCS for Cu(I), and verifying that GapA binds copper with relatively high affinity (Figure 4.20).

Whilst GapA competes with BCS it does not compete sufficiently to prevent Cu(I) from binding to BCS until it has been saturated. This demonstrates that the affinity of GapA for Cu(I) may be at a similar order of magnitude to BCS, and is not orders of magnitude greater than that of BCS. A copper binding protein such as *Bacillus subtilis* CsoR, with an affinity greater than BCS has been shown to be completely saturated with Cu(I) before the metal binds to BCS at all[155].

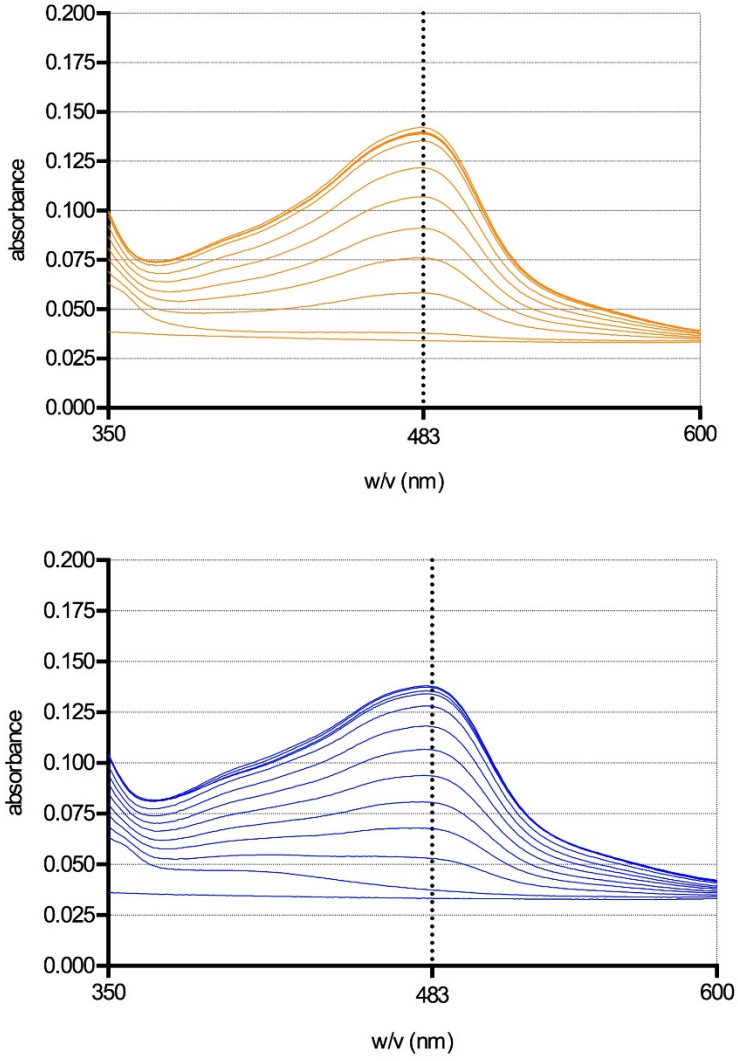

Figure 4.19. Uv/vis spectra during titration of Cu(I) into a solution of BCS and BCS with r*Sa*GapA. *Top panel:* Cu(I) was titrated into a solution of 16.66 µM BCS. Each addition of Cu(I) added 1.79 µM to the total copper concentration. *Bottom panel:* Cu(I) was titrated into a solution of 16.66 µM BCS also containing 5.9 µM *Sa*GapA. Each addition of Cu(I) added 1.79 µM to the total copper concentration. In both panels the lowest absorbance spectra is the buffer (i.e. not containing BCS or protein). Spectra were obtained after each subsequent addition of Cu(I). With each addition of Cu(I) the local maximum at 483 nm increases its absorbance proportional to the binding of Cu(I) to BCS and the formation of the $[Cu(I)(BCS)_2]$ complex which absorbs at 483 nm. When *Sa*GapA is present alongside BCS the equivalent increase in A_{483} requires a greater added concentration of Cu(I), indicating that *Sa*GapA has competed for binding of Cu(I) with BCS. In both cases spectra are displayed for 10 Cu(I) additions.

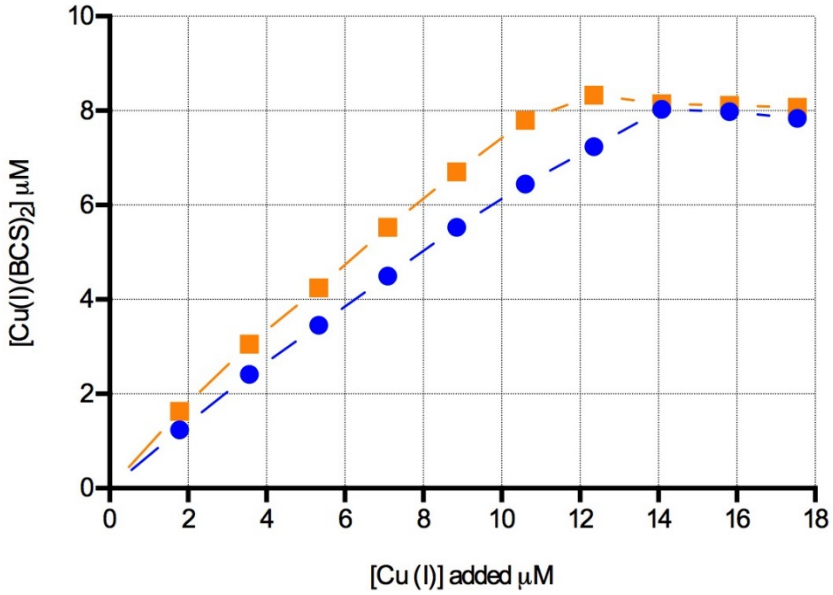

Figure 4.20. Formation of the [Cu(I)(BCS)$_2$] complex by titration of Cu(I) into a solution of BCS and BCS with r*Sa*GapA. The total formation of [Cu(I)(BCS)$_2$] complex requires the addition of a greater concentration of Cu(I) in the presence of *Sa*GapA (blue circles) than in its absence (golden squares). The data shown is the conversion of the absorbance at 483 nm shown in Figure 4.17 to the concentration of [Cu(I)(BCS)$_2$] complex using the published extinction coefficient for the complex, ε =13,300[136]. The concentration of complex increases as Cu(I) is added to the different solutions at different rates, with the presence of *Sa*GapA increasing the concentration of Cu(I) required to bind all available BCS from 12. 35 µM to 14.09 µM. This indicates that *Sa*GapA is competing with BCS, a high affinity ligand, for Cu(I).

4.6 Cu(I) binding to r*Sa*GapA reversibly inhibits enzyme activity *in vitro*

Evidence has been provided that demonstrates copper binding to r*Sa*GapA *in vitro*. It has been further shown here that copper inhibits the activity of the enzyme (Figure 4.21). The r*Sa*GapA, without treatment with copper, gave a mean value for activity of 939.61 nmoles NADH s^{-1} mg $protein^{-1}$. In the same units, r*Sa*GapA treated with one mole equivalent of Cu(I) gave 370 and with two equivalents gave 285 equivalent to a 61 % and 70 % decrease in activity respectively. When r*Sa*GapA treated with two mole equivalents of copper is then treated with BCS activity recovers to 903 which is an inhibition of only 3.8 %. Therefore, Cu(I) strongly inhibits the enzyme's activity, and this can be reversed through treatment of the inhibited enzyme with the copper chelator, demonstrating that copper-mediated enzyme inhibition is reversible.

These experiments were performed under rigorous anaerobic conditions, preventing redox cycling by Cu(I) from oxidising the enzyme. Therefore, enzyme inhibition can only have been caused by binding *in vitro* of the r*Sa*GapA to Cu(I), as opposed to oxidation via Fenton chemistry catalysed by the presence of copper.

We used silver as well as copper in this experiment for several reasons; firstly, as silver shares similar chemistry with copper and is not able to redox cycle, similar inhibition of the enzyme by silver would suggest a similar mechanism of inhibition by copper. Secondly, silver is not known to be chelated by BCS, thus using silver with BCS and not observing an alleviation of inhibition is indicative that the formation of the BCS copper complex is what is causing alleviation of inhibition in this case, and not any other property of BCS affecting absorbance or the enzyme itself.

Figure 4.21 demonstrates that r*Sa*GapA with 1 equivalent of added silver produced 199.68 nmoles NADH $second^{-1}$ mg $protein^{-1}$ and with 2 equivalents, 150.68 nmoles NADH $second^{-1}$ mg $protein^{-1-}$. When BCS is added in the presence of 2 equivalent of silver, activity is not rescued as much as in the case of copper, the reaction produced 333.98 nmoles NADH $second^{-1}$ mg $protein^{-1}$.

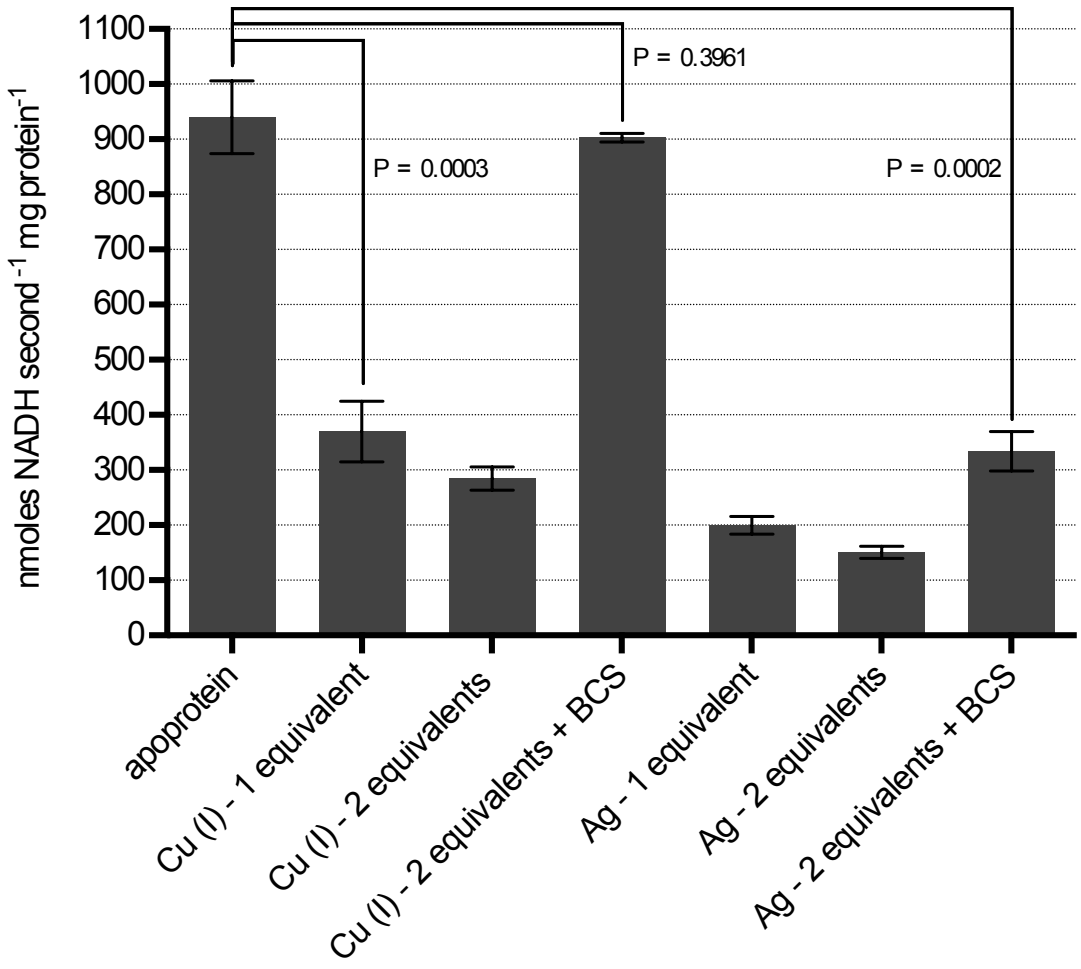

Figure 4.21. Copper and silver inhibit the activity of r*Sa*GapA. The action of copper can be reversed through the addition of BCS. Activity was assayed by spectrophotometric observation of the absorbance of the reaction at 340 nm, which increases due to the formation of NADH by r*Sa*GapA. In each reaction 5 µM r*Sa*GapA was used. Where one or two mole equivalent of copper or silver was used then 5 µM or 10 µM respectively of the respective metal was added. BCS was used at a final concentration of 50 µM. Mean values recorded in nmoles NADH second^{-1} mg protein^{-1}; apoprotein, 939.61; Cu(I) – 1 equivalent, 370.27; Cu(I) – 2 equivalents, 284.82; Cu(I) – 2 equivalents + BCS, 903.16; Ag – 1 equivalent, 199.68; Ag – 2 equivalents, 150.68; Ag – 2 equivalents + BCS, 333.98.

4.7 Mutagenesis of r*Sa*GapA residues Cys151, Cys96 and His178

Analysis of *Sa*GapA has shown clearly that GapA binds to copper. Inactivation of the enzyme's activity, alongside crystal structures of the homologous enzyme from *S. elongatus*, suggest co-ordination residues within the active site of the enzyme, namely Cys151 and His178. Furthermore, Mukherjee *et al.* showed that single point mutants of Cys151 and His178 had no activity, supporting our hypothesis that if copper binds to these residues it is likely to interfere with catalysis.

In order to analyse the involvement of these residues in copper binding we created point mutants of the essential catalytic residues of recombinant *Sa*GapA. This was achieved using a standard site-directed mutagenesis method (see Materials and Methods) to produce two site-directed mutants of the *Sa*GapA expression vector, pLEICS-03-*Sa*GapA, which was originally acquired from the Morrissey group at the University of Leicester. Both Cys151 (TGT) and His178 (CAC) codons of the ORF of *Sa*GapA within the vector were changed to alanine codons (GCT), resulting in two novel plasmids pLEICS03-*Sa*GapA(C151A) and pLEICS03-*Sa*GapA(H178A). We chose alanine because of its non-polar and non-reactive nature, and its disinclination to interact with copper.

Because of the nature of cysteine residues' tendency to interact with Cu(I), we also decided to construct the vector pLEICS03-*Sa*GapA(C96A), despite Cys96 of *Sa*GapA not being involved in the active site of the enzyme. This was done using the same method as used in construction of the construction of pLEICS03-SaGapA(C151A)/pLEICS03-SaGapA(H178A).

Once the mutated vectors had been constructed we were able to use a restriction digest to confirm the presence of the correct mutation in the case of pLEICS03-*Sa*GapA(C151A) and pLEICS03-*Sa*GapA(C96A). In these cases the codon changes resulted in the removal of a restriction site of the restriction enzyme *Rsa*I. We amplified the *gapA* ORF on the vector and then digested this with *Rsa*I. For pLEICS03-*Sa*GapA(H178A) no restriction site was removed, thus we relied only on sequencing for the verification of the correct point mutation; sequencing was also carried out for the two cysteine point mutant vectors, which alongside the restriction digest demonstrated that the mutation protocol had been successful.

Figure 4.22 shows the restriction digest of the amplified *gapA* ORF from pLEICS03-*Sa*GapA, pLEICS03-*Sa*GapA(C151A), pLEICS03-*Sa*GapA(C96A) and pLEICS03-*Sa*GapA(H178A). The digest of the non-mutated amplicon gives three fragments, whilst the digest of both cysteine mutated amplicons give two fragments. The digest of the histidine mutated amplicon gives the same digest pattern as the non-mutated amplicon.

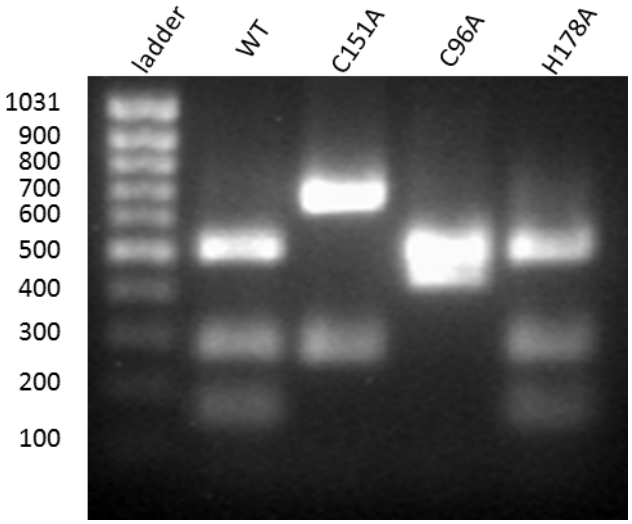

Figure 4.22. Diagnostic DNA agarose electrophoresis gel of the point mutant vectors of pLEICS-03-SaGapA. Stained agarose gel showing the sizes of DNA fragments after treatment of amplicons from pLEICS03-*Sa*GapA and its site-directed mutant derivatives with the restriction enzyme *Rsa*I. Number labels represent fragment sizes in base pairs. Lanes (from left to right) contain: Lane 1: DNA mass-ruler ladder (ladder), fragment sizes shown in bps; Lane 2: *Rsa*I treated amplicon from pLEICS03-*Sa*GapA (WT), expected size 557, 289 and 165 bp; Lane 3: *Rsa*I treated amplicon from pLEICS03-*Sa*GapA(C151A), expected sizes 722 and 289 bp; Lane 4: *Rsa*I treated amplicon from pLEICS03-*Sa*GapA(C96A), expected sizes 557 and 454 bp; Lane 5: *Rsa*I treated amplicon from pLEICS03-*Sa*GapA(H178A), expected sizes 557, 289 and 165 bps.

4.8 Purification of *Sa*GapA(C151A), *Sa*GapA(C96A) and *Sa*GapA(H178A)

The three point mutants of r*Sa*GapA were purified using the same method used for the WT r*Sa*GapA (see above). SDS-PAGE gels shown in Figure 4.23 demonstrate that the three proteins were expressed well in BL21 cells and that in each case the monomer was of the expected size.

The gels shown in Figure 4.23 are from the second round of nickel affinity chromatography, after cleavage of the his-tag from the protein. These fractions contain a number of contaminating proteins, although the abundance of these compared to r*Sa*GapA is minor. After this stage of chromatography, further size exclusion and anion-exchange rounds of chromatography were performed (as with WT r*Sa*GapA) which ensured the removal of contaminants and reductants (data not shown).

Fractions shown below are all equivalent from this step of purification. There is clearly less r*Sa*GapA C96A and r*Sa*GapA H178A than r*Sa*GapA C151A. It is not quite clear why this would be the case, as all the mutants were expressed in the same way. One possibility is that the former two mutant proteins are slightly less stable than the latter which leads to a lower amount of expression.

Further to this, it was found that upon flash freezing of the r*Sa*GapA C96A after the second round of nickel affinity chromatography and subsequent thawing in preparation for size exclusion chromatography, the sample was prone to high levels of precipitation. The purification was repeated and the protein diluted in an attempt to prevent this, but precipitation continued to occur, which made potential experiments upon this protein impossible to undertake in the interests of timely submission of this work.

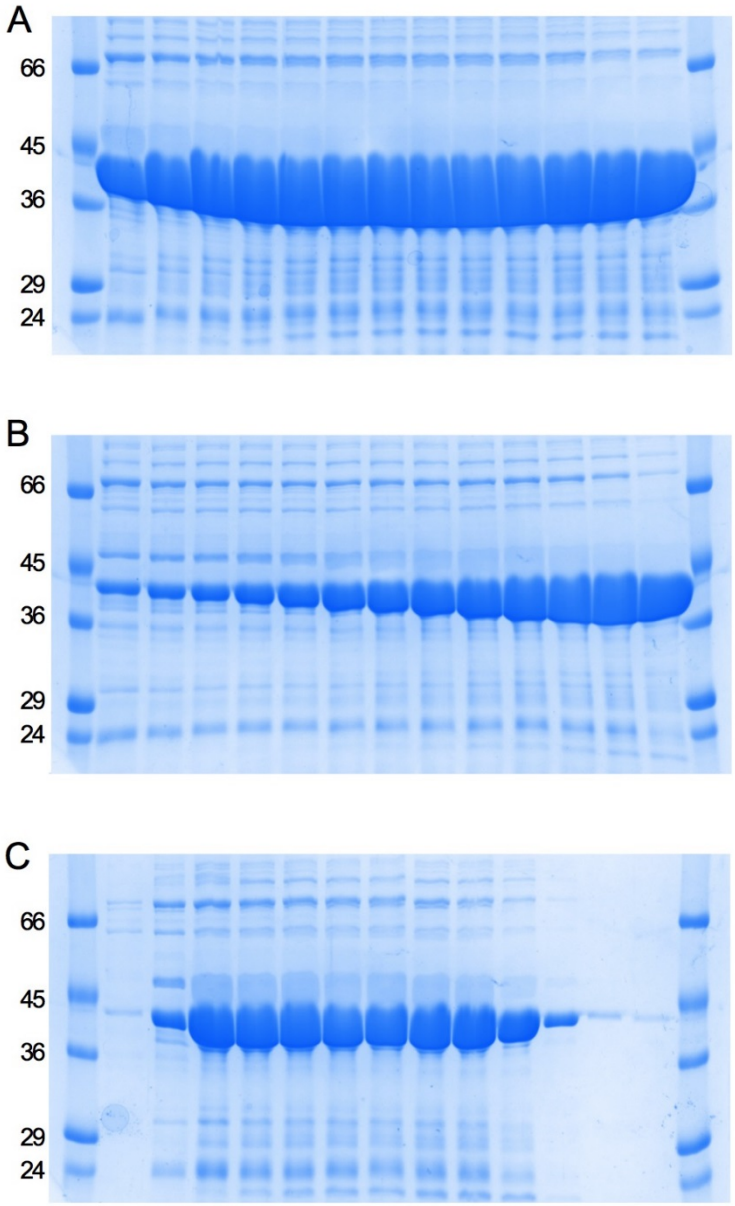

Figure 4.23. SDS-PAGE gels of partially purified r*Sa*GapA(C151A), r*Sa*GapA(H178A) and r*Sa*GapA(C96A). *Panel A*; r*Sa*GapA(C151A); *Panel B*; r*Sa*GapA(H178A) and *Panel C*; r*Sa*GapA(C96A). In each case 20 µl of fractions collected after the initial stage of Ni-NTA chromatography containing recombinant protein (as assessed by the UV-Vis trace data produced by AKTA FPLC equipment, not shown) was loaded onto a 12 % acrylamide SDS-PAGE gel before electrophoresis (180 V, 60 mins).

4.9 Cu(I) binds r*SaGapA* through co-ordination by Cys151

As observed previously recombinant *Sa*GapA loaded with copper binds 1 mole equivalent of copper. Examination the involvement of Cys151 and His182 in copper binding through utilisation of the point mutants of the recombinant enzyme was then undertaken. To this end both mutants were applied, after copper loading, to the same size-exclusion column as used for analysis of WT r*Sa*GapA.

As previously, spectra of the recombinant mutated enzymes were taken as they were loaded with copper. In this case sub-stoichiometric amounts of copper were added to the recombinant protein and spectra taken upon each injection of Cu(I) taken to observe the change in absorbance as levels of Cu(I) were increased incrementally.

Here, the raw spectra have not been shown upon the addition of copper as clear interpretation requires the observation of changes at particular wavelengths, as seen in Figure 4.16. In this figure the increase in absorbance at 242 nm is observed upon the addition of copper. The wavelength 242 was chosen due to this being the wavelength at which the greatest increase in absorbance was seen in WT r*Sa*GapA (Figure 4.16).

In Figure 4.24 the concentrations of protein used were different between WT and the two mutants. The data recorded for Δ242 has therefore been normalised, using protein concentration value of 10 μM, to take account of this. The concentration of r*Sa*GapA(C151) was 10.33 μM, of r*Sa*GapA(H178A) was 12.55 μM and of the r*Sa*GapA WT was 24.39 μM (the data shown here for the r*Sa*GapA WT is the same as that shown in Figure 4.14 but normalised as stated). Absorbance at 242 nm increases as copper is added in the case of r*Sa*GapA WT and r*Sa*GapA(H178A), but not in the case of r*Sa*GapA(C151). This result shows what was expected; a rise in absorbance at 242 nm, caused by an LMCT that occurs between Cu(I) and the Cys151 residue which is present in the r*Sa*GapA WT and the r*Sa*GapA(H178A). When this residue is not present (as in r*Sa*GapA(C151)) the LMCT does not occur, and an increase in absorbance is not observed. This supports the hypothesis that Cu(I) binds to r*Sa*GapA via its Cys151 residue. Inset within Figure 4.24 is the non-normalised data for r*Sa*GapA(C151) and r*Sa*GapA(H178A) enzymes, showing the same result as observed for the normalised data.

Subsequent to loading with copper, samples of r*Sa*GapA(C151) and r*Sa*GapA(H178) were investigated further by analytical size exclusion chromatography. The two mutated recombinant enzymes, r*Sa*GapA(C151) and r*Sa*GapA(H178A) were loaded onto the analytical column with and without the addition of copper. The data for the absorbance of the protein at 242 nm for the same samples analysed by SEC is shown in Figure 4.24. Fractions collected from analytical SEC were analysed for metal content by ICP-MS and for protein concentration by Bradford assay.

Figure 4.25 demonstrates data gathered from fractions produced from analytical SEC of r*Sa*GapA(H178A). The top panel shows the data from the sample analysed after copper loading, copper is present in the same volume in which the protein elutes. The bottom panel shows data from the sample analysed without being loaded with copper, in this case, no copper is present in the volume in which r*Sa*GapA(H178) elutes. These data demonstrate that the r*Sa*GapA(H178) enzyme is binding to Cu(I), as also demonstrated by increased absorbance at 242 nm due to a LMCT observed in Figure 4.24.

Figure 4.26 demonstrates data gathered from fractions produced from analytical SEC of r*Sa*GapA(C151A). The top panel shows the data from the sample analysed after copper loading, and the bottom panel the data from the sample analysed without coper loading. In both cases no copper is observed in volumes where r*Sa*GapA(C151) elutes

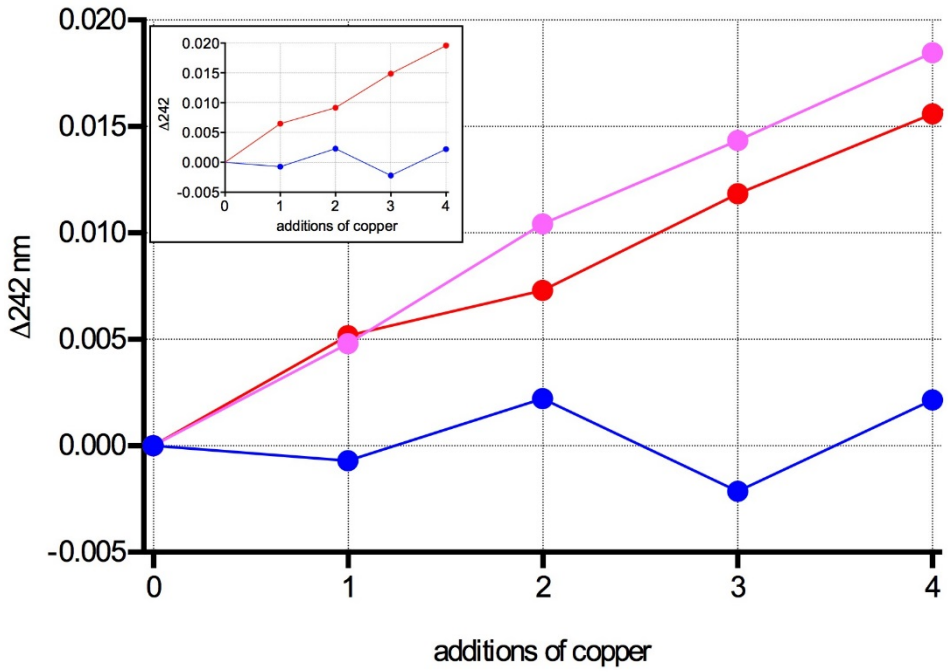

Figure 4.24. Titration of Cu(I) into r*Sa*GapA(C151A) and r*Sa*GapA(H178A). *Main panel*: Data showing the change in absorbance at 242 nm from the titration of Cu(I) into the r*Sa*GapA (WT) (pink), r*Sa*GapA(C151A) (blue) and r*Sa*GapA(H178A) (red) normalised to a protein concentration of 10 μM r*Sa*GapA. Data for r*Sa*GapA (WT) is as shown in Figure 4.14 at 242 (normalised as stated). In the case of r*Sa*GapA(C151A), 10.33 μM r*Sa*GapA(C151A) was titrated with Cu(I) with each addition adding approximately 1.75 μM Cu(I). In the case of r*Sa*GapA(H178A), 12.56 μM r*Sa*GapA(H178A) was titrated with Cu(I) with each addition adding approximately 1.91 μM Cu(I). *Inset*; the non-normalised data as in the main panel for r*Sa*GapA(C151A) (blue) and r*Sa*GapA(H178A) (red).

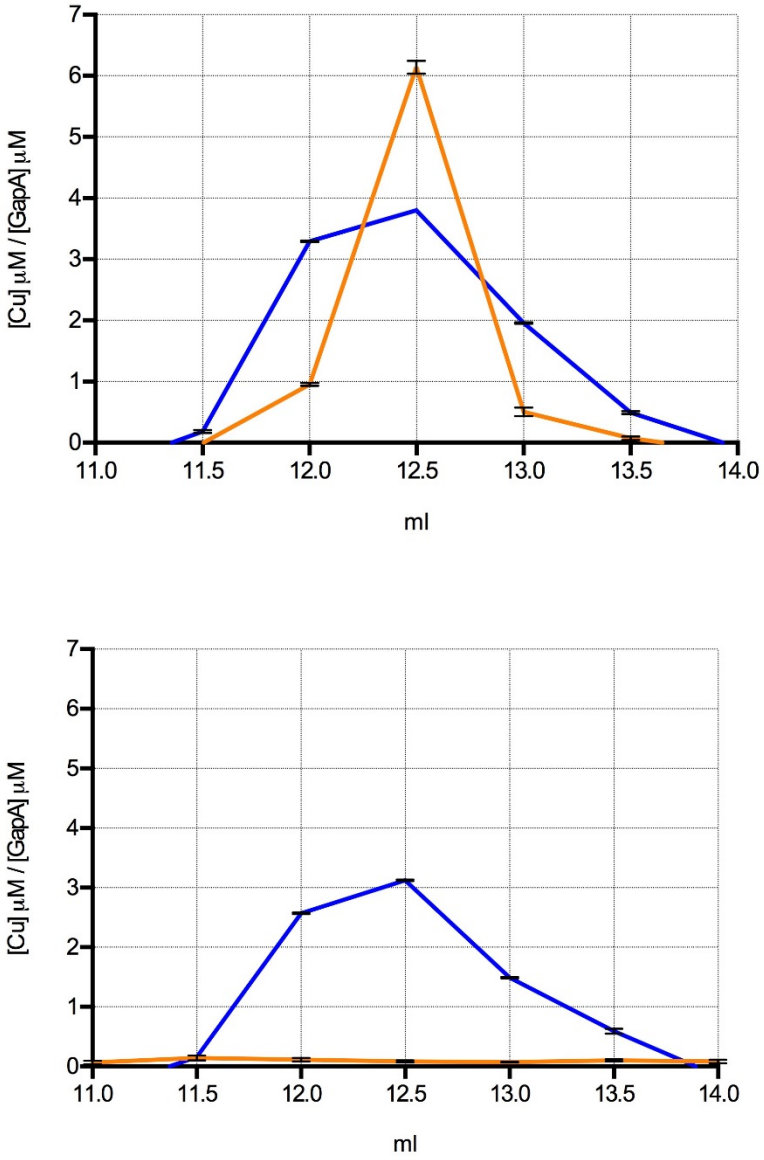

Figure 4.25. Analytical SEC of Cu(I) loaded and non-loaded r*Sa*GapA(H178A). [Cu] shown by orange line, [GapA] shown in blue. *Top panel*; r*Sa*GapA(H178A) was titrated with copper as described in Figure 4.22, 12.56 µM r*Sa*GapA(H178A) was titrated with approximately 9.55 µM Cu(I) (0.76 mole equivalents). An aliquot (0.5 ml) of this was loaded on a size exclusion column (Superdex 200 10/300 GL, GE; buffer, 150 mM NaCl, 40 mM Hepes, pH 7.5; flowrate, 1 ml min^{-1}). *Sa*GapA(H178A) binds copper at a similar stoichiometry to the WT. *Bottom panel*; 0.5 ml r*Sa*GapA(H178A) not titrated with Cu(I) was loaded onto the same column using the same buffer and flowrate. When Cu(I) was not titrated onto r*Sa*GapA(H178A), the eluent fractions containing that protein did not contain copper. Copper concentrations were measured using ICP-MS and protein concentrations using the Bradford assay.

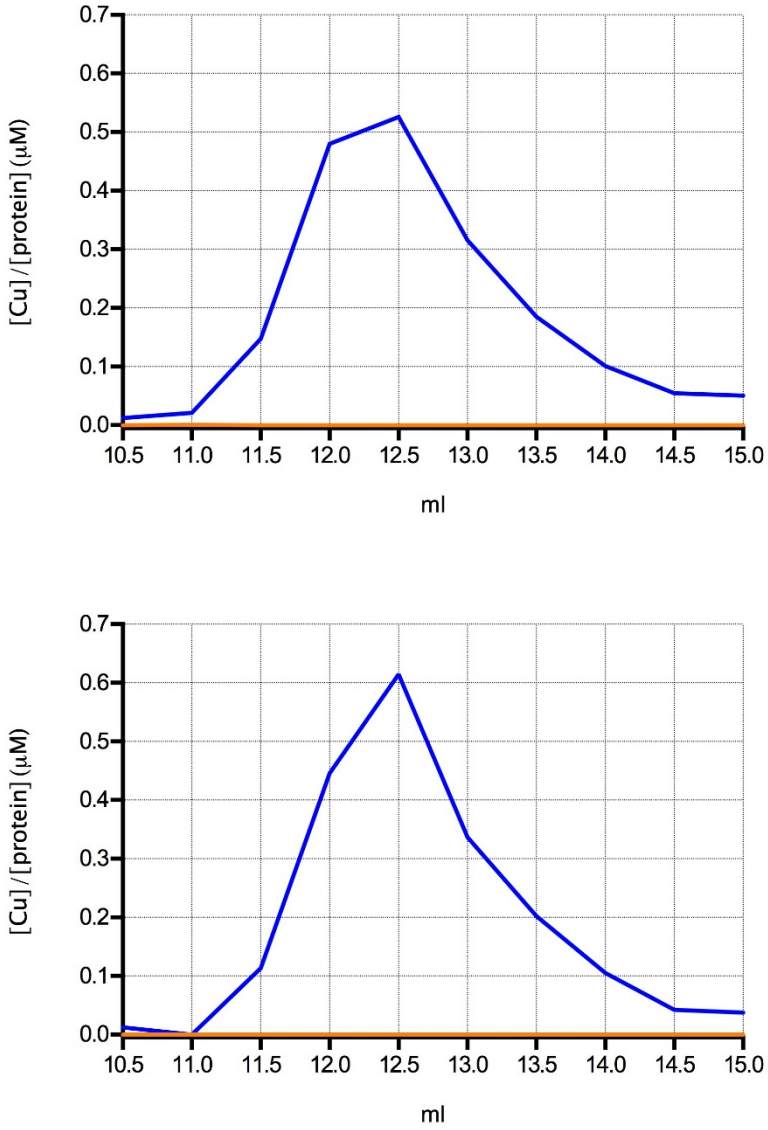

Figure 4.26. Analytical SEC of Cu(I) loaded and non-loaded *Sa*GapA(C151A). [Cu] shown by orange line, [protein] shown in blue. *Top panel*; *Sa*GapA(C151A)was titrated with copper as described in Figure 4.22, 10.33 μM *Sa*GapA(C151A) was titrated with approximately 7 μM Cu(I) (0.68 mole equivalents). 0.5 ml of this was loaded on a size exclusion column (Superdex 200 10/300 GL, GE; buffer, 150 mM NaCl, 40 mM Hepes, pH 7.5; flowrate, 1 ml min^{-1}). *Sa*GapA(C151A) loaded with Cu(I) has bound none of that Cu(I). *Bottom panel*; 0.5 ml *Sa*GapA(C151A) not titrated with Cu(I) was loaded onto the same column using the same buffer and flowrate. When Cu(I) was not titrated onto *Sa*GapA(C151A) the eluent volume containing that protein did not contain copper either. Copper concentrations were measured using ICP-MS and protein concentrations using the Bradford assay.

4.10 *Sa*GapA(C151A) shows no activity as expected

Mukherjee *et al.*[114] have previously shown that a Cys151 mutant of recombinant r*Sa*GapA has no activity. Here, it was desired that the r*Sa*GapA mutant created in our lab be tested for its activity. We did not test the activity of the recombinant protein directly, but of a lysate of BL21 cells that had been expressing the protein, and compared this with the activity of a lysate that had been producing the WT recombinant protein and a lysate that had not been induced for expression from pLEICS03-*Sa*GapA,

The results are shown in Figure 4.27. The lysate expressing the WT enzyme gives the highest activity (105 nmoles NADH min^{-1} mg $protein^{-1}$) the lysate of cells expressing the mutant enzyme (rSaGapA(C151A) showed a similar activity (22.50 nmoles NADH min^{-1} mg $protein^{-1}$) to the lysate from the non-induced cells (16.814 nmoles NADH min^{-1} mg $protein^{-1}$). The activities demonstrated by the lysates from these latter samples can be accounted for by the activity of the endogenous GAPDH of the BL21 cells. It was concluded that rSaGapA(C151A) showed no activity.

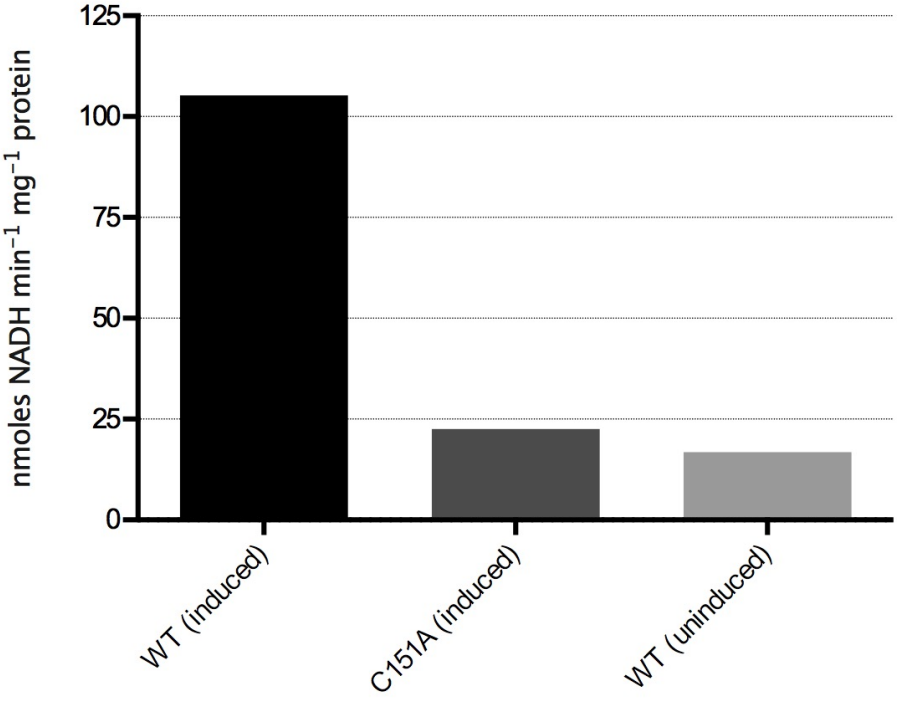

Figure 4.27. BL21 cell lysate activity assay of cells expressing *Sa*GapA (WT) and *Sa*GapA(C151A). Activity was assayed by spectrophotometric observation of the absorbance of the reaction at 340 nm, which increases due to the formation of NADH by r*Sa*GapA. The assay was performed in the plate reader spectrophotometer (Biotek) in this case. Lysates from BL21 cells (15 µl) induced to express; *Sa*GapA (WT) (WT induced), *Sa*GapA(C151A), and non-induced cells were pipetted into a 96 well plate. All samples were at a protein concentration of 50 µg ml^{-1}. Reaction buffer (185 µl) was added (see methods) immediately before initiation of observation at 340 nm. The lysate expressing the WT enzyme shows the highest activity (105 nmoles NADH min^{-1} mg protein^{-1}) the lysate expressing the mutant showed similar activity to the non-induced lysate. The activities of both of these can be accounted for by the activity of the endogenous GAPDH of the BL21 cells. Error bars could not be added as only one iteration of this experiment was performed.

4.11 Nickel, cobalt, and zinc do not inhibit *Sa*GapA to the same extent as copper or silver

We have been investigating the nature of the interaction of copper with *SaG*apA and have provided evidence for the proposed mechanism of copper binding and inhibition of the enzyme. Data has also shown that silver inhibits the protein to a similar extent and we hypothesise that silver achieves this in a similar way to copper due to its related chemistry.

It was of interest whether other metals also inhibited *Sa*GapA *in vitro* and if so, did they do this at similar levels of stoichiometry as copper and silver. We decided to test the activity of recombinant *Sa*GapA after treatment with nickel, cobalt and zinc. These metals are all biologically essential metals that cells require and may encounter on a regular basis in their environment.

Inhibition of the enzyme by iron was also of interest, but due to the experimental complexities of preparing, quantifying and maintaining solutions of the different oxidation states of iron, as well as the potential involvement of oxidation via the Fenton reaction (see introduction), it was decided to omit the investigation of iron.

Results, shown in Figure 4.28, demonstrate the much lower levels of inhibition caused by these metals than by either silver or copper. The concentration of recombinant *Sa*GapA used was 100 nM, and 4 mole equivalents of metal were added to protein. In the cases of nickel, this resulted in an insignificant change in enzyme activity ($p > 0.05$) Cobalt significantly inhibited activity ($P = 0.0035$). In the case of zinc, 4 mole equivalents did result in a significant decrease in activity ($P < 0.0001$). We decided to use 1 mole equivalent of zinc alongside silver to compare the inhibitions of these metals directly. As shown, 1 equivalent of zinc also significantly inhibits the activity of the enzyme ($P = 0.0035$) but not as significantly as with 4 equivalents or compared to silver and copper, which inhibit to the greatest extent (as shown above also). The Irving-Williams series of the relative stability of divalent metal ion complexes places zinc lower than copper, which may explain the requirement of a higher concentration of zinc relative to protein than copper (or silver). It is probable that zinc binds to a similar site within the structure as proposed for copper due to the thiophilic properties of zinc being similar to those of copper, hence the observed inhibition of activity, but less so than copper..

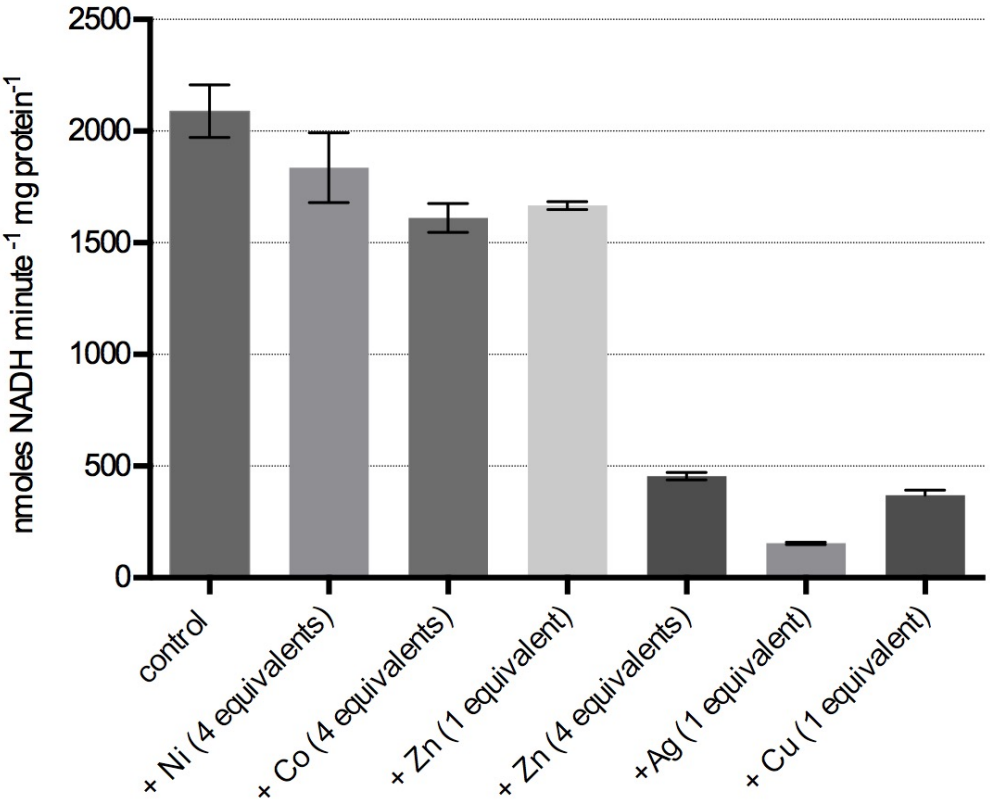

Figure 4.28. GapA activity assay of r*Sa*GapA treated with various metals. Treatment of r*Sa*GapA with nickel, cobalt, zinc and silver. Values of enzyme activity and standard deviations obtained were (nmoles NADH min^{-1} mg $protein^{-1}$); control (no added metal), 2089, 117.6; +Ni (4 equivalents), 1836, 155.7; +Co (4 equivalents), 1611, 65.43; +Zn (1 equivalent), 1667, 17.52; +Zn (4 equivalents), 454.9, 16.01; +Ag (1 equivalent), 154.3, 4.381; +Cu (1 equivalent), 370.1, 22. In each case the concentration of *Sa*GapA was 100 nM.

4.12. Chapter 4 conclusions

- r*Sa*GapA contains one accessible reduced thiol under anaerobic conditions
- r*Sa*GapA does not have copper bound without copper treatment
- Binding of r*Sa*GapA to Cu(I) inhibits its activity
- Cu(I) binds to r*Sa*GapA via its Cys151 residue
- The loss of the His178 residue from r*Sa*GapA does not abolish Cu(I) binding.
- r*Sa*GapA(C151A) shows no enzymatic activity as shown previously[114].
- Nickel, cobalt, and zinc do not inhibit SaGapA to the same extent as copper or silver, but do shown partial inhibit, in line with the Irving Williams series[80].

Chapter 5. Discussion and unifying concepts

Historically, copper has been known since ancient times to inhibit the spoilage of food and drink, and has been used in hospital settings more recently to reduce the spread of infection[156]. These uses are known to be effective. Various hypotheses have been proposed to explain these phenomena, yet a firm mechanistic conclusion has yet to be drawn from data gathered. As discussed in the introduction, copper has been proposed to exhibit its antimicrobial activity through the production of ROS *in vivo*, via the depolarisation and rupture of the cell membrane, and via aberrant binding to non-metalloproteins *in vivo*. None of these mechanisms has been ruled out in all organisms, and none have been demonstrated as the overwhelming cause of toxicity in any organism.

Within *E. coli* Macomber and Imlay have described how copper is not causative of oxidative damage to DNA[70], and have gone on to show that it damages the iron sulphur clusters of that same organism[66]. This effect of copper toxicity on iron sulphur clusters has also been confirmed in *Bacillus subtilis*[90] and in *Neisseria gonorrhoeae*[91]. Despite many assumptions within the literature that ROS production by copper was the main cause of intracellular damage it is clear that the role of aberrant copper binding and the identification of such copper targets has been under-investigated. One reason for this may be the difficulty inherent to such investigations. Chemically the cuprous ion, Cu(I), is quite unstable under aqueous, aerobic environments, creating a requirement for anaerobic conditions and procedures which are technically complex.

As part of an on-going effort in the Waldron laboratory to understand the mechanisms of copper toxicity, and to identify cellular targets of copper toxicity, a metalloproteomic study of cellular copper distribution in *Staphylococcus aureus* under conditions of copper stress is being undertaken. Preliminary data, obtained prior to the commencement of this project, had identified several possible candidate proteins as potential copper toxicity targets. One of these potential targets was the glyceraldehyde-3-phosphate dehydrogenase family protein, GapA.

Interest in *S. aureus* specifically stemmed from its presence in the community and hospitals, in which settings it is becoming increasingly virulent and resistant to standard

treatments using antibiotics, alongside the fact that to our knowledge, no such investigation has been undertaken in *S. aureus* before.

5.1. Effects of copper on the growth of *S. aureus*.

Initial investigation of the growth of *S. aureus* in copper demonstrated that copper is toxic to this organism. It was shown that the concentrations of copper required to inhibit growth varied largely depending on the media used. Richer media, such as LB and TSB, led to the highest growth of *S. aureus*, with growth not strongly affected until concentrations of above 1 mM $CuSO_4$ were used, whereas in TM we found that a concentration of 500 µM $CuSO_4$ was enough to completely inhibit growth. Investigation of the effect of glucose concentration on the ability to resist copper toxicity was tested and it was found that increasing glucose did not alter the effects of copper on growth, demonstrating that glucose was not preventing copper uptake through chelation. Glucose however did lead to increased growth of *S. aureus* relative to the addition of succinate or no carbon source, consistent with its status as a source of greater energy. The fact that these richer media are able to allow *S. aureus* to grow in such high levels of copper is probably due to a combination of being richer sources of energy and their copper chelating capacity (although the latter of these is not caused by the presence of glucose). It was also shown that cells grown in copper had a higher concentration of copper within their cytoplasmic extract, confirming that copper ions enter *S. aureus* cells, despite the absence of any known copper import mechanism, and accumulate in the cytosol.

5.2. Identification and confirmation of *Sa*GapA as associated with copper *in vivo*

*Sa*GapA was identified initially through preliminary studies as a potential copper binding protein using a metalloproteomics approach (see Chapter 3). In this study, the metalloproteomics technique used previously was altered and now included one step of anion exchange chromatography followed by SEC. As well as analysing the SH1000 WT, here we repeated the analysis on a SH1000 Δ*gapA* mutant. The mutant was created by Anna Barwinska-Sendra of the Waldron group. The mutant was confirmed its genotype, by its growth phenotype in glucose (showing no growth), by PCR amplification of the mutated ORF of *gapA* and by restriction digest of the *rsbU* gene (the predominant difference between SH1000 Δ*gapA* and 8325-4 Δ*gapA*, the parent strain, being an 11 bp deletion in the *rsbU* gene of the latter), and the absence of detectable GapA activity.

Metalloproteomic analysis revealed that the SH1000 Δ*gapA* mutant lost the copper pool present in WT cells in fractions where *Sa*GapA was present; demonstrating that *Sa*GapA was definitely associated with copper within these cells when grown in copper.

5.3. Copper-dependent inhibition of *Sa*GapA activity in *S. aureus* cells.

Activity assays of the WT fractions collected after metalloproteomic SEC revealed that despite being bound to some copper, the enzyme showed some activity. This increased upon treatment of the samples with the Cu(I) specific chelator BCS, reflecting that only part of the *Sa*GapA population was bound to copper, and the unbound part remained functional. This also demonstrates the unbound copper had not been oxidised, confirming the effectiveness of our anaerobic conditions and implying that copper catalysed Fenton chemistry had not resulted in the oxidation of the unbound pool of *Sa*GapA *in vivo*.

*Sa*GapA inhibition was also demonstrated by the addition of copper and other metals to SH1000 WT lysates. Cu(II) consistent with its strong binding properties according to the Irving Williams series of divalent metals[80], resulted in complete inhibition of *Sa*GapA within these lysates, a result replicated by silver. Zinc also showed some inhibition, although not complete inhibition. Nickel no significant inhibition, and cobalt the least significant, again these results reflect the expected binding affinities of these divalent metal ions, implying that binding of the metals (in the case of Cu(II) and Zn(II)) is the causative factor of inhibition.

The lack of inhibition observed in cell lysates prepared from cells grown in copper could be due to the complexity of these assay which contain not just *Sa*GapA but all of the other cytoplasmic proteins. It may be the case that higher concentrations within the medium would show inhibition but these were not examined in the interest of time.

5.4. Copper-binding properties of r*Sa*GapA *in vitro*.

The mechanism of catalysis of G3P to 1,3-BPG by *Sa*GapA has been investigated via crystal structures by Mukherjee *et al*.[114]. The initial step as reported by them involves the nucleophilic attack of the C1 carbon of the substrate (G3P) by the Cys151 thiolate form (Figure 5.1). The previously highlighted propensity of such a thiolate ligand to bind Cu(I), along with data published by Matsumara *et al*. (Figures 4.4 and 4.5)[150] showing copper bound to the homologous residue in *Se*GAPDH, led to the hypothesis that copper was most likely binding to *Sa*GapA at this site within the active site of the protein.

Copper binding to such a site would almost certainly lead to the inhibition of the protein, as the catalytic Cys151 residue would be unable to initiate nucleophilic attack of the substrate; indeed, we have shown that inhibition of the protein does occur *in vitro*. His178 forms a hydrogen bond with the substrate at the step shown in Figure 5.1 and at no point is thought to from a covalent bind with the substrate; the significance of His178 in copper binding is therefore likely to be less so than that of Cys151 but may certainly act to stabilise the interaction.

Other metals have also been shown to inhibit the enzyme *in vitro* and the pattern of inhibition is very similar to that seen in lysates as reported, following the pattern expected from the Irving Williams series[80].

Notably this work has also provided evidence that *Sa*GapA binds to copper with a stoichiometry of one Cu(I) ion to each GapA monomer. Such a conclusion can be drawn from SEC analysis of the WT recombinant protein, which, even when loaded with super-stoichiometric copper levels did not appear to bind more copper than protein present, although such experiments require repetition. LMCT data also showed a clear change in gradient in the change in absorbance at 3 different wavelengths indicating that one main high-affinity site is likely, a second, lower affinity site, has not yet been ruled out though. Competition with BCS for Cu(I) by *Sa*GapA also points toward a potentially biochemically relevant affinity of the enzyme for copper, (that is; within less than five orders of magnitude of native copper binding proteins in *S. aureus*, such as CsoR), demonstrating that the interaction is likely to occur *in vivo*.

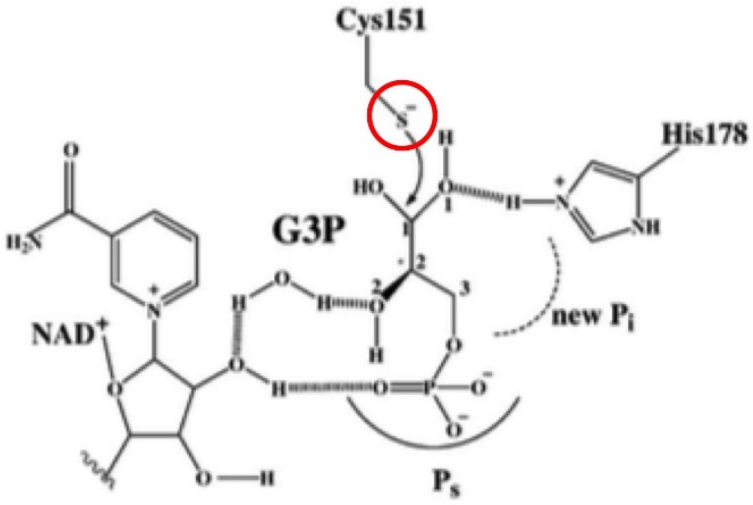

Figure 5.1. The initial step of the catalysis of G3P to 1,3-BPG by *Sa*GapA. Adapted from Mukherjee *et al*.[114]. Circled in red is the catalytic thiolate nucleophile which attacks the C1 of G3P. It is this thiolate ligand that is proposed binds to copper, hence inactivating the enzyme.

5.5. Identification of *Sa*GapA residue Cys151 as a Cu(I) ligand.

Changes in absorbance of the enzyme *Sa*GapA caused by LMCT interaction between the thiol sidechain of cysteine residues and Cu(I) have been used in this study to investigate binding of Cys151 to Cu(I). Mutation of the pLEICS-03-*Sa*GapA vector in order to produce recombinant *Sa*GapA(C151A) and *Sa*GapA(H178A) have enabled comparison of the result of Cu(I) titration into these three protein variants. Figure 4.14 highlights the occurrence of an LMCT when titrating Cu(I) into WT r*Sa*GapA. Figure 4.22 reveals that this feature disappears in the case of the C151A mutant and is retained in the H178A mutant.

Further investigation of these r*Sa*GapA recombinant proteins by analytical SEC reveal that Cu(I) binds to the WT and H178A mutant, but not to the C151A mutant. Such results point firmly to the involvement of Cys151 in the mechanism of copper binding. Further repetition is required however to completely confirm this observation. The observation that the His178 residue is not required for copper binding implies that other residues may stabilise the co-ordination of Cu(I) by Cys151. Matsumara *et al.* demonstrated that copper was bound to *Se*GAPDH through the active site histidine and cysteine residues, which were accompanied by a threonine residue (Thr156), this threonine residue is conserved in *Sa*GapA (Thr152) and maybe hypothesised to stabilise copper co-ordination in this case as well.

5.6. Conclusions and future directions.

In this study it has been demonstrated that *Sa*GapA does indeed bind copper both *in vivo* and *in vitro* and that this inhibits the activity of the protein, evidence for a hypothesised binding site has also been provided. What has proven more difficult is to define the consequences of such an inhibition. When *Sa*GapA is inhibited by copper in the cell how does the cell react?

5.6.1. The effects of copper binding to *Sa*GapA upon *S. aureus* cells

It is clear that relatively high concentration of copper within the medium (400 μM $CuSO_4$) do not significantly inhibit *Sa*GapA when it is grown in glucose. Yet in these conditions cells uptake of copper is significant compared to cells grown in a non-copper environment (Figure 3.7). We have also observed that at much lower concentrations of copper (50 μM $CuSO_4$) in TSB and in TM media, copper is bound to *Sa*GapA (metalloproteomics data, Chapter 3) at least to some extent.

The difference in carbon source between such experiments is of importance. In TSB the presence of glucose means that cells are relying overwhelmingly on glucose metabolism, meaning that *Sa*GapA is being expressed and used for this purpose. In TM (as used for metalloproteomics work conducted in this study as a Δ*gapA* mutant will not grow in glucose) glucose is not present; cells are using amino acids as their primary carbon source, yet *Sa*GapA is still present as it can be detected in such conditions, both through detection of its activity, and on SDS-PAGE gels. Under these conditions *Sa*GapA would not be being used for glycolysis and presumably is expressed for its alternative functions or perhaps is present within the cell constitutively in order to be able to metabolise any glucose that does appear in the environment efficiently. The effects upon the cell of copper binding to SaGapA may therefore vary depending on the conditions.

Thus, the SH1000 WT and SH1000 Δ*gapA* mutant were grown in succinate to try to remove such a complication (Figure 3.13). It was assumed that the WT and mutant would grow in the same manner in such a medium, as they do in a medium containing only amino acids as a carbon source, but this was not the case; the SH1000 Δ*gapA* mutant was significantly inhibited in its growth in succinate compared to SH1000 WT. This is surprising since succinate enters carbon metabolism at a later point in carbon metabolism than should involve *Sa*GapA. This further implies that *Sa*GapA has more far-reaching effects than its supposed primary role within the glycolytic pathway, but the nature of such a phenotype hindered our investigation of *Sa*GapA copper dependent phenotypes under such conditions. It has therefore been very difficult to interpret the consequences of copper binding to *Sa*GapA *in vivo* through growth assays. Nonetheless, *Sa*GapA is binding to copper under both glycolytic (as demonstrated by preliminary data shown in Chapter 3 gather by Emma Tarrant of the Waldron Group, which was conducted with glucose present in the growth media) and non-glycolytic conditions (Figure 3.22), for which there surely are metabolic consequences.

The sensitivity of non-copper proteins such as *Sa*GapA to copper *in vivo* must be viewed from the same perspective as has been suggested by Waldron *et al*[157]; that is taking into account the affinity, allostery and access of proteins with regards to copper binding. We are not aware of the affinity or allosteric based differences between such proteins in terms of their interaction with copper as these values have not been published, but we do know that the active site of *Sa*GapA is accessible by its very nature. Another factor that plays a role in metallation of proteins *in vivo* is abundance of the protein, as this will

affect the amount of any protein binding to copper, and determine if the collective activity of that particular protein pool is completely or partially inhibited.

It is thought that *Sa*GapA could make up as much as 2 % of the cytoplasmic protein under some conditions[115], or one fiftieth, a vast amount considering the vast number of proteins being expressed at any one time within a cell, making it one of the most abundant cytoplasmic proteins. It is not quite clear why cells express so much *Sa*GapA, especially as other glycolytic proteins are not expressed to anywhere near this level (Waldron and Saito, unpublished data). However, it is known that *Sa*GapA is the rate limiting step of glycolysis, therefore higher levels of the protein may be needed to keep glycolysis functioning efficiently relative to other enzymes in the pathway. Suspected moonlighting functions of the protein may also mean that it is being expressed more than other glycolytic proteins which perhaps have more restricted purposes. Interestingly, studies have suggested that in yeast and muscle tissue the concentrations of the GAPDH tetramer may be as high as 210 μM and 75 μM respectively[110] (with each tetramer containing four copper binding sites). This is a huge number of potential binding sites compared to the number of copper ions per cell, which has been estimated for *E. coli* cells to be in the region of 10,000 atoms per cell, or approximately 10 μM[72].

It may be the case that such vast amounts of protein make a population of it susceptible to copper binding in high-copper conditions, despite having a lower affinity than other potential targets of copper binding toxicity (such as Fe-S cluster enzymes for example). Our data leads us to hypothesise that a *Sa*GapA monomer binds one equivalent of copper with a physiologically relevant affinity, and with such a high total number of SaGapA tetramers present, such a pool would provide a large number of potential binding sites.

The complexities of metal binding have been discussed in the introduction to this work and elsewhere. It is tempting to envisage copper binding as being extremely defined but we know that affinity, allostery, access and abundance of proteins change with the conditions that cells are grown in, thus the distribution of metals, governed in part by these factors, must also be dynamic. It is also worth pointing out that the parameters set by such guiding factors are very unlikely to be sharply defined. That is, unlike the shells of a nucleus for example, which must be filled systematically, copper may 'fill', for example, the CsoR protein pool to 75 % whilst also 'filling' the CopZ protein pool by 50 % (such musings are completely theoretical in nature). Phrased differently; at which concentration of intracellular copper various proteins bind to that copper will overlap.

Teasing apart the details of global copper binding would not be easy to attempt but is a long-term research goal of the Waldron lab, among others..

Such overlapping of binding events may also influence our ability to detect the effects of copper binding using techniques such as growth assays, RT-PCR or using microarrays. This is because the pool of protein bound may not be proportional to the change of the impact of that particular protein pools interaction with copper within the cell. Such a situation is analogous to certain organs in the body, for instance the liver can lose much of its capacity before major overt effects of such damage can be observed.

Thus it may be the case that the effect of *Sa*GapA binding to copper is not seen until the concentration of copper within the cell reaches a concentration at which it saturates a high percentage of SaGapA, or until it begins to bind to other proteins which are far less abundant, but the effects of copper binding on which are much more damaging to the cell.

5.6.2. A potential model for the physiological role of copper binding to *Sa*GapA

Life has evolved over billions of years to be prepared in numerous ways for the adverse conditions encountered throughout the natural world. The case could be that in binding to copper, *Sa*GapA is providing the cell with a protective barrier against copper induced damage; acting potential both as a copper buffering agent and potentially as a metabolic switch.

When an *S. aureus* cell enters a high copper environment, copper accumulates within the cytoplasm and enhances expression of enzymes responsible for copper homeostasis. Upon the cytoplasm reaching a certain concentration of copper, such systems will be overwhelmed and other intracellular components may begin to be effected by the presence of the copper, indeed this has been demonstrated by Macomber and Imlay[66] as well as being the focus of this work. *Sa*GapA is likely to be one such component as it has been, in this work, shown to bind to copper *in vivo*. Inactivation of of *Sa*GapA could lead to the shut down of glycolysis within the cell inducing the aforementioned metabolic switch, leading the cell to use alternative methods of energy production.

Under such conditions the main pathways for energy generation likely to be used are the pentose phosphate pathway and gluconeogenesis. Notably these pathways predominantly produce as their reducing equivalents NADPH. NADPH is an important cofactor for many anabolic pathways within the cell and is involved in the reduction of oxidised reducing agents also.

Thus, a shutdown of glucose metabolism caused by the inactivation of *Sa*GapA by copper may well lead to activation of the pathways that most enable the cell to maintain itself for the longest possible time in the presence of this stress, therefore increasing its likelihood of survival. Indeed, such a metabolic switch may be the same mechanism utilised in other cases where glycolysis is inhibited, such as inhibition of different enzymes or via the presence of different metals.

5.6.3. Alternative strategies for identifying the role of *Sa*GapA in copper toxicity

The main strategy used in this work for trying to elucidate the wider effects of copper toxicity have been to use growth assays in different conditions when growing SH1000 versus the SH1000 Δ*gapA* mutant. This has failed to give an insight into how *Sa*GapA might be affecting the cell metabolically.

There are several further options that could have been explored given more time. Firstly, a strain non-functional in CCR would be useful as this would allow a Δ*gapA* mutant in such a genetic background to grow in glucose. Such a growth phenotype would allow for direct comparison of the WT to the Δ*gapA* mutant in replete glucose conditions, which may make a Δ*gapA* growth phenotype in copper identifiable. The disadvantages of this would relate to the regulation that is inherent to the CCR system, which may make any result completely artefactual.

Other genetic backgrounds that would have been favourable for looking for a remarkable phenotype when growing in copper would have been mutants of the copper homeostasis system; that is, mutants of *copA*, *copZ*, or *csoR*. Such mutants would have increased the sensitivity of *S. aureus* to copper and removed one (or more in the case of a double or triple mutant) of the most important copper chelating protein pools, which would allow any phenotype caused by the absence of *Sa*GapA t become more prominent in growth assays.

Whilst using such strains, and also in the SH1000 WT and Δ*gapA* mutant already in existence it would be of interest to use other methods, concurrent to growth assay.

These include RT-PCR and microarrays as well as proteomic techniques involving MS. Towards the end of this study, samples of SH1000 WT that had been grown in TSB and TM containing glucose at various concentrations of copper (1 mM, 2 mM and 5 mM) (samples prepared by Emma Tarrant of the Waldron group) were analysed for protein content by MS by collaborators (data not shown; Dr M. Saito, Woods Hole Oceanographic Institute). Such results were in broad agreement with data published by Baker *et al*.[59]. Some of these MS data also show a change in proteins involved in other pathways of metabolism, including the PPP (glucose-phosphate dehydrogenase) and the TCA cycle (succinate dehydrogenase), indicating that these pathways may be upregulated when cells are cultured in copper, consistent with a copper-dependent decrease in metabolic flux through glycolysis.

5.6.4. Where does *Sa*GapA sit in the context of whole cell copper binding?

As stated, copper distribution *in vivo* is governed by affinity, allostery, access and abundance of metal binding species within a cell, as well as the concentration of the metal present. In terms of the affinities of proteins, we have an idea of copper binding for very few proteins relative to the number produced by *S. aureus*, and those that we are aware of are mainly those that have been studied for their native metal binding properties. The concept of copper (and metal) toxicity involves aberrant binding, which requires that sites that under standard conditions should not bind copper are examined.

As we have seen, the identification of *Sa*GapA involved the matching of metal peaks within separated cytoplasmic extracts to corresponding protein peaks. *Sa*GapA represents just one of the proteins that were identified with a peak, and that has been subsequently investigated further to confirm its copper binding property. Preliminary work to this also identified other potential binding targets. Such targets included the amino acid synthesis protein, RocA, which is involved in the synthesis of glutamate from proline, as well as one of the subunits of the pyruvate dehydrogenase complex, LpdA.

Such targets are yet to be fully investigated but may also play a part in copper toxicity if confirmed to be *bona fide* copper binding targets in raised copper conditions. Similar experiments could be performed as have been in this work to ascertain their involvement in toxicity. Having identified these proteins amongst others, as targets, it may be possible to conduct a wider screen of toxicity targets using growth screens of copper homeostasis mutants in various conditions in different concentrations of copper to try to identify which proteins play major roles in copper toxicity, extending this to

double or even triple mutants to attempt to elicit a cumulative effect. Such studies represent possible future research directions for the Waldron lab.

5.6.5. Overall conclusions

This study has confirmed the binding of *Sa*GapA to copper *in vivo* and *in vitro*. It has also been demonstrated that copper inhibits the activity of the protein *in vitro* and *in vivo*. Moreover, evidence for the binding site has been produced, indicating that binding likely requires the presence of the catalytic Cys151 residue within the active site of the protein, which is the probable reason for inhibition of the protein.

Whilst identification of potential targets may be relatively straight forward, investigating the potential regulatory and allosteric changes that copper may have on proteins is more complex and we have been unable to confirm the precise consequences of copper binding to *Sa*GapA, although unpublished data would point to changes in carbon metabolism in order to redirect the cell from glycolysis when the intracellular pool of *Sa*GapA is not functioning to its full capacity. Further studies of the cellular consequences of copper inhibition of *Sa*GapA *in vivo* are ongoing.

References

1 Marshall, J. H. & Wilmoth, G. J. Pigments of Staphylococcus aureus, a series of triterpenoid carotenoids. *Journal of bacteriology* 147, 900-913 (1981).

2 den Heijer, C. D. J. *et al.* Prevalence and resistance of commensal Staphylococcus aureus, including meticillin-resistant S aureus, in nine European countries: a cross-sectional study. *The Lancet Infectious Diseases* 13, 409-415, doi:http://dx.doi.org/10.1016/S1473-3099(13)70036-7 (2013).

3 Barber, M. & Rozwadowska-Dowzenko, M. INFECTION BY PENICILLIN-RESISTANT STAPHYLOCOCCI. *The Lancet* 252, 641-644, doi:http://dx.doi.org/10.1016/S0140-6736(48)92166-7 (1948).

4 Rolinson, G. N. "Celbenin" - resistant Staphylococci. *British Medical Journal* 1, 125-126 (1961).

5 Enright, M. C. *et al.* The evolutionary history of methicillin-resistant Staphylococcus aureus (MRSA). *Proceedings of the National Academy of Sciences* 99, 7687-7692 (2002).

6 Gardete, S. & Tomasz, A. Mechanisms of vancomycin resistance in Staphylococcus aureus. *The Journal of clinical investigation* 124, 2836-2840 (2014).

7 Chambers, H. F. & DeLeo, F. R. Waves of resistance: Staphylococcus aureus in the antibiotic era. *Nat Rev Micro* 7, 629-641, doi:http://www.nature.com/nrmicro/journal/v7/n9/suppinfo/nrmicro2200_S1.html (2009).

8 Skinner, D. & Keefer, C. S. Significance of bacteremia caused by Staphylococcus aureus: a study of one hundred and twenty-two cases and a review of the literature concerned with experimental infection in animals. *Archives of Internal Medicine* 68, 851-875 (1941).

9 Mikolay, A. *et al.* Survival of bacteria on metallic copper surfaces in a hospital trial. *Appl Microbiol Biotechnol* 87, 1875-1879, doi:10.1007/s00253-010-2640-1 (2010).

10 Casey, A. L. *et al.* Role of copper in reducing hospital environment contamination. *Journal of Hospital Infection* 74, 72-77, doi:http://dx.doi.org/10.1016/j.jhin.2009.08.018 (2010).

11 Otto, M. Staphylococcus epidermidis [mdash] the 'accidental' pathogen. *Nat Rev Micro* 7, 555-567 (2009).

12 Foster, T. J. & Höök, M. Surface protein adhesins of Staphylococcus aureus. *Trends in Microbiology* 6, 484-488, doi:http://dx.doi.org/10.1016/S0966-842X(98)01400-0 (1998).

13 Otto, M. Basis of virulence in community-associated methicillin-resistant Staphylococcus aureus*. *Annual review of microbiology* 64, 143-162 (2010).

14 Boakes, E. *et al.* Distinct Bacteriophages Encoding Panton-Valentine Leukocidin (PVL) among International Methicillin-Resistant Staphylococcus aureus Clones Harboring PVL. *Journal of Clinical Microbiology* 49, 684-692, doi:10.1128/jcm.01917-10 (2011).

15 Hidron, A. I., Low, C. E., Honig, E. G. & Blumberg, H. M. Emergence of community-acquired meticillin-resistant Staphylococcus aureus strain USA300 as a cause of necrotising community-onset pneumonia. *The Lancet Infectious Diseases* 9, 384-392, doi:http://dx.doi.org/10.1016/S1473-3099(09)70133-1 (2009).

16 de Kraker, M. E. A., Wolkewitz, M., Davey, P. G., Grundmann, H. & on behalf of the, B. S. G. Clinical Impact of Antimicrobial Resistance in European Hospitals: Excess Mortality and Length of Hospital Stay Related to Methicillin-Resistant

Staphylococcus aureus Bloodstream Infections. *Antimicrobial Agents and Chemotherapy* 55, 1598-1605, doi:10.1128/aac.01157-10 (2011).
17 Sheldon Paul, S. *et al.* Evaluation of the national Cleanyourhands campaign to reduce Staphylococcus aureus bacteraemia and Clostridium difficile infection in hospitals in England and Wales by improved hand hygiene: four year, prospective, ecological, interrupted time series stu…. *BMJ* 344, doi:10.1136/bmj.e3005 (2012).
18 Gagné, D., Bédard, G. & Maziade, P. J. Systematic patients' hand disinfection: impact on meticillin-resistant Staphylococcus aureus infection rates in a community hospital. *Journal of Hospital Infection* 75, 269-272, doi:http://dx.doi.org/10.1016/j.jhin.2010.02.028 (2010).
19 Saïd-Salim, B. P., Mathema, B. M. P. H. & Kreiswirth, B. N. P. Community-Acquired Methicillin-Resistant Staphylococcus aureus: An Emerging Pathogen • *Infection Control and Hospital Epidemiology* 24, 451-455, doi:10.1086/502231 (2003).
20 Lindsay, J. A. Evolution of Staphylococcus aureus and MRSA during outbreaks. *Infection, Genetics and Evolution*, doi:http://dx.doi.org/10.1016/j.meegid.2013.04.017.
21 Popovich, K. J., Weinstein, R. A. & Hota, B. Are Community-Associated Methicillin-Resistant Staphylococcus aureus (MRSA) Strains Replacing Traditional Nosocomial MRSA Strains? *Clinical Infectious Diseases* 46, 787-794, doi:10.1086/528716 (2008).
22 Harper, A. L. *et al.* An Overview of Livestock-Associated MRSA in Agriculture. *Journal of Agromedicine* 15, 101-104, doi:10.1080/10599241003627110 (2010).
23 Herbert, S. *et al.* Repair of Global Regulators in Staphylococcus aureus 8325 and Comparative Analysis with Other Clinical Isolates. *Infection and Immunity* 78, 2877-2889, doi:10.1128/iai.00088-10 (2010).
24 Horsburgh, M. J. *et al.* σB Modulates Virulence Determinant Expression and Stress Resistance: Characterization of a Functional rsbU Strain Derived from Staphylococcus aureus 8325-4. *Journal of Bacteriology* 184, 5457-5467, doi:10.1128/jb.184.19.5457-5467.2002 (2002).
25 Kullik, I. & Giachino, P. The alternative sigma factor σB in Staphylococcus aureus: regulation of the sigB operon in response to growth phase and heat shock. *Arch Microbiol* 167, 151-159, doi:10.1007/s002030050428 (1997).
26 Bischoff, M., Entenza, J. M. & Giachino, P. Influence of a Functional sigB Operon on the Global Regulators sar and agr inStaphylococcus aureus. *Journal of Bacteriology* 183, 5171-5179, doi:10.1128/jb.183.17.5171-5179.2001 (2001).
27 Wu, S., de Lencastre, H. & Tomasz, A. Sigma-B, a putative operon encoding alternate sigma factor of Staphylococcus aureus RNA polymerase: molecular cloning and DNA sequencing. *Journal of Bacteriology* 178, 6036-6042 (1996).
28 Rasigade, J. P., Dumitrescu, O. & Lina, G. New epidemiology of Staphylococcus aureus infections. *Clinical Microbiology and Infection* 20, 587-588, doi:10.1111/1469-0691.12718 (2014).
29 Parker, D., Soong, G., Planet, P. & Prince, A. 195: Type I interferon signaling distinguishes commensal from virulent Staphylococcus aureus. *Cytokine* 63, 289, doi:http://dx.doi.org/10.1016/j.cyto.2013.06.198 (2013).
30 Gould, I. M. Costs of hospital-acquired methicillin-resistant Staphylococcus aureus (MRSA) and its control. *International Journal of Antimicrobial Agents* 28, 379-384, doi:http://dx.doi.org/10.1016/j.ijantimicag.2006.09.001 (2006).
31 de Niederhäusern, S. *et al.* Vancomycin-resistance Transferability from VanA Enterococci to Staphylococcus aureus. *Curr Microbiol* 62, 1363-1367, doi:10.1007/s00284-011-9868-6 (2011).

32 Djoko, K. Y., Ong, C.-l. Y., Walker, M. J. & McEwan, A. G. The Role of Copper and Zinc Toxicity in Innate Immune Defense against Bacterial Pathogens. *Journal of Biological Chemistry* 290, 18954-18961, doi:10.1074/jbc.R115.647099 (2015).
33 Hodgkinson, V. & Petris, M. J. Copper Homeostasis at the Host-Pathogen Interface. *Journal of Biological Chemistry* 287, 13549-13555, doi:10.1074/jbc.R111.316406 (2012).
34 White, C., Lee, J., Kambe, T., Fritsche, K. & Petris, M. J. A role for the ATP7A copper-transporting ATPase in macrophage bactericidal activity. *Journal of Biological Chemistry* 284, 33949-33956 (2009).
35 Wertheim, H. F. L. *et al.* The role of nasal carriage in Staphylococcus aureus infections. *The Lancet Infectious Diseases* 5, 751-762, doi:http://dx.doi.org/10.1016/S1473-3099(05)70295-4 (2005).
36 Lyon, B. R., Iuorio, J. L., May, J. W. & Skurray, R. A. Molecular epidemiology of multiresistant Staphylococcus aureus in Australian hospitals. *Journal of Medical Microbiology* 17, 79-89, doi:10.1099/00222615-17-1-79 (1984).
37 Stapleton, P. D. & Taylor, P. W. Methicillin resistance in Staphylococcus aureus: mechanisms and modulation. *Science progress* 85, 57-72 (2002).
38 Chambers, H. F. The changing epidemiology of Staphylococcus aureus? *Emerging Infectious Diseases* 7, 178-182 (2001).
39 Baba, T. *et al.* Genome and virulence determinants of high virulence community-acquired MRSA. *The Lancet* 359, 1819-1827, doi:http://dx.doi.org/10.1016/S0140-6736(02)08713-5 (2002).
40 Fey, P. D. *et al.* Comparative Molecular Analysis of Community- or Hospital-Acquired Methicillin-Resistant Staphylococcus aureus. *Antimicrobial Agents and Chemotherapy* 47, 196-203, doi:10.1128/aac.47.1.196-203.2003 (2003).
41 Deurenberg, R. H. *et al.* The molecular evolution of methicillin-resistant Staphylococcus aureus. *Clinical Microbiology and Infection* 13, 222-235, doi:10.1111/j.1469-0691.2006.01573.x (2007).
42 Tang, S. S., Apisarnthanarak, A. & Hsu, L. Y. Mechanisms of β-lactam antimicrobial resistance and epidemiology of major community- and healthcare-associated multidrug-resistant bacteria. *Advanced Drug Delivery Reviews* 78, 3-13, doi:http://dx.doi.org/10.1016/j.addr.2014.08.003 (2014).
43 Sitthisak, S., Knutsson, L., Webb, J. W. & Jayaswal, R. K. Molecular characterization of the copper transport system in Staphylococcus aureus. *Microbiology* 153, 4274-4283, doi:10.1099/mic.0.2007/009860-0 (2007).
44 Baker, J., Sengupta, M., Jayaswal, R. K. & Morrissey, J. A. The Staphylococcus aureus CsoR regulates both chromosomal and plasmid-encoded copper resistance mechanisms. *Environmental Microbiology* 13, 2495-2507, doi:10.1111/j.1462-2920.2011.02522.x (2011).
45 Liu, T. *et al.* CsoR is a novel Mycobacterium tuberculosis copper-sensing transcriptional regulator. *Nat Chem Biol* 3, 60-68, doi:http://www.nature.com/nchembio/journal/v3/n1/suppinfo/nchembio844_S1.html (2007).
46 Sitthisak, S., Howieson, K., Amezola, C. & Jayaswal, R. K. Characterization of a Multicopper Oxidase Gene from Staphylococcus aureus. *Applied and environmental microbiology* 71, 5650-5653, doi:10.1128/aem.71.9.5650-5653.2005 (2005).
47 Banci, L. *et al.* Structural Basis for Metal Binding Specificity: the N-terminal Cadmium Binding Domain of the P1-type ATPase CadA. *Journal of Molecular Biology* 356, 638-650, doi:http://dx.doi.org/10.1016/j.jmb.2005.11.055 (2006).

48 Banci, L., Bertini, I., Ciofi-Baffoni, S., Gonnelli, L. & Su, X.-C. Structural Basis for the Function of the N-terminal Domain of the ATPase CopA from Bacillus subtilis. *Journal of Biological Chemistry* 278, 50506-50513, doi:10.1074/jbc.M307389200 (2003).

49 Lübben, M. *et al.* Structural model of the CopA copper ATPase of Enterococcus hirae based on chemical cross-linking. *BioMetals* 22, 363-375, doi:10.1007/s10534-008-9173-4 (2009).

50 Gourdon, P. *et al.* Crystal structure of a copper-transporting PIB-type ATPase. *Nature* 475, 59-64, doi:http://www.nature.com/nature/journal/v475/n7354/abs/nature10191-f1.2.html - supplementary-information (2011).

51 Mandal, A. K. & Argüello, J. M. Functional Roles of Metal Binding Domains of the Archaeoglobus fulgidus Cu+-ATPase CopA†. *Biochemistry* 42, 11040-11047, doi:10.1021/bi034806y (2003).

52 Arnesano, F. *et al.* Metallochaperones and metal-transporting ATPases: a comparative analysis of sequences and structures. *Genome research* 12, 255-271, doi:10.1101/gr.196802 (2002).

53 Wimmer, R., Herrmann, T., Solioz, M. & Wüthrich, K. NMR Structure and Metal Interactions of the CopZ Copper Chaperone. *Journal of Biological Chemistry* 274, 22597-22603, doi:10.1074/jbc.274.32.22597 (1999).

54 Banci, L., Bertini, I., Ciofi-Baffoni, S., Del Conte, R. & Gonnelli, L. Understanding Copper Trafficking in Bacteria: Interaction between the Copper Transport Protein CopZ and the N-Terminal Domain of the Copper ATPase CopA from Bacillus subtilis†. *Biochemistry* 42, 1939-1949, doi:10.1021/bi027096p (2003).

55 González-Guerrero, M. & Argüello, J. M. Mechanism of Cu+-transporting ATPases: Soluble Cu+ chaperones directly transfer Cu+ to transmembrane transport sites. *Proceedings of the National Academy of Sciences* 105, 5992-5997, doi:10.1073/pnas.0711446105 (2008).

56 Fu, Y. *et al.* A new structural paradigm in copper resistance in Streptococcus pneumoniae. *Nat Chem Biol* 9, 177-183, doi:http://www.nature.com/nchembio/journal/v9/n3/abs/nchembio.1168.html - supplementary-information (2013).

57 Rosenzweig, A. C. Copper delivery by metallochaperone proteins. *Acc Chem Res* 34, 119 - 128 (2001).

58 Rensing, C., Fan, B., Sharma, R., Mitra, B. & Rosen, B. P. CopA: an Escherichia coli Cu (I)-translocating P-type ATPase. *Proc Natl Acad Sci USA* 97, 652 - 656 (2000).

59 Baker, J. *et al.* Copper Stress Induces a Global Stress Response in Staphylococcus aureus and Represses sae and agr Expression and Biofilm Formation. *Applied and environmental microbiology* 76, 150-160, doi:10.1128/aem.02268-09 (2010).

60 Ma, Z., Cowart, D. M., Scott, R. A. & Giedroc, D. P. Molecular Insights into the Metal Selectivity of the Copper(I)-Sensing Repressor CsoR from Bacillus subtilis†. *Biochemistry* 48, 3325-3334, doi:10.1021/bi900115w (2009).

61 Strausak, D. & Solioz, M. CopY Is a Copper-inducible Repressor of the Enterococcus hirae Copper ATPases. *Journal of Biological Chemistry* 272, 8932-8936, doi:10.1074/jbc.272.14.8932 (1997).

62 Grossoehme, N. *et al.* Control of Copper Resistance and Inorganic Sulfur Metabolism by Paralogous Regulators in Staphylococcus aureus. *Journal of Biological Chemistry* 286, 13522-13531, doi:10.1074/jbc.M111.220012 (2011).

63 Urvoas, A. *et al.* Metal-binding stoichiometry and selectivity of the copper chaperone CopZ from Enterococcus hirae. *European Journal of Biochemistry* 271, 993-1003, doi:10.1111/j.1432-1033.2004.04001.x (2004).

64 Aruoma, O. I., Halliwell, B., Gajewski, E. & Dizdaroglu, M. Copper-ion-dependent damage to the bases in DNA in the presence of hydrogen peroxide. *Biochem. J* 273, 601-604 (1991).
65 Yesilkaya, H., Andisi, V. F., Andrew, P. W. & Bijlsma, J. J. E. Streptococcus pneumoniae and reactive oxygen species: an unusual approach to living with radicals. *Trends in Microbiology* 21, 187-195, doi:http://dx.doi.org/10.1016/j.tim.2013.01.004 (2013).
66 Macomber, L. & Imlay, J. A. The iron-sulfur clusters of dehydratases are primary intracellular targets of copper toxicity. *Proceedings of the National Academy of Sciences* 106, 8344-8349, doi:10.1073/pnas.0812808106 (2009).
67 Grass, G., Rensing, C. & Solioz, M. Metallic Copper as an Antimicrobial Surface. *Applied and Environmental Microbiology* 77, 1541-1547, doi:10.1128/aem.02766-10 (2011).
68 Weaver, L., Noyce, J. O., Michels, H. T. & Keevil, C. W. Potential action of copper surfaces on meticillin-resistant Staphylococcus aureus. *Journal of applied microbiology* 109, 2200-2205, doi:10.1111/j.1365-2672.2010.04852.x (2010).
69 Cooke, M. S., Evans, M. D., Dizdaroglu, M. & Lunec, J. Oxidative DNA damage: mechanisms, mutation, and disease. *The FASEB Journal* 17, 1195-1214, doi:10.1096/fj.02-0752rev (2003).
70 Macomber, L., Rensing, C. & Imlay, J. A. Intracellular copper does not catalyze the formation of oxidative DNA damage in Escherichia coli. *J Bact* 189, 1616 - 1626 (2007).
71 Cabiscol, E., Tamarit, J. & Ros, J. Oxidative stress in bacteria and protein damage by reactive oxygen species. *International microbiology : the official journal of the Spanish Society for Microbiology* 3, 3-8 (2000).
72 Changela, A. *et al.* Molecular basis of metal-ion selectivity and zeptomolar sensitivity by CueR. *Science* 301, 1383-1387 (2003).
73 Outten, C. E., O'Halloran & Thomas, V. Femtomolar Sensitivity of Metalloregulatory Proteins Controlling Zinc Homeostasis. *Science* 292, 2488-2492, doi:10.1126/science.1060331 (2001).
74 Finney, L. A. & O'Halloran, T. V. Transition Metal Speciation in the Cell: Insights from the Chemistry of Metal Ion Receptors. *Science* 300, 931-936, doi:10.1126/science.1085049 (2003).
75 Corbett, D. *et al.* The combined actions of the copper-responsive repressor CsoR and copper-metallochaperone CopZ modulate CopA-mediated copper efflux in the intracellular pathogen Listeria monocytogenes. *Molecular Microbiology* 81, 457-472, doi:10.1111/j.1365-2958.2011.07705.x (2011).
76 Dupont, C. L., Grass, G. & Rensing, C. Copper toxicity and the origin of bacterial resistance—new insights and applications. *Metallomics* 3, 1109-1118 (2011).
77 Valko, M., Morris, H. & Cronin, M. T. D. Metals, toxicity and oxidative stress. *Current medicinal chemistry* 12, 1161-1208 (2005).
78 Letelier, M. E. *et al.* Possible mechanisms underlying copper-induced damage in biological membranes leading to cellular toxicity. *Chemico-Biological Interactions* 151, 71-82, doi:http://dx.doi.org/10.1016/j.cbi.2004.12.004 (2005).
79 Weaver, L., Noyce, J. O., Michels, H. T. & Keevil, C. W. Potential action of copper surfaces on meticillin-resistant Staphylococcus aureus. *Journal of applied microbiology* 109, 2200-2205 (2010).
80 Irving, H. & Williams, R. J. P. 637. The stability of transition-metal complexes. *Journal of the Chemical Society (Resumed)* 0, 3192-3210, doi:10.1039/JR9530003192 (1953).

81 Waldron, K. J. & Robinson, N. J. How do bacterial cells ensure that metalloproteins get the correct metal? *Nat Rev Micro* 7, 25-35 (2009).
82 Solioz, M., Abicht, H. K., Mermod, M. & Mancini, S. Response of Gram-positive bacteria to copper stress. *J Biol Inorg Chem* 15, 3 - 14 (2010).
83 Harris, E. D. CELLULAR COPPER TRANSPORT AND METABOLISM. *Annual Review of Nutrition* 20, 291-310, doi:doi:10.1146/annurev.nutr.20.1.291 (2000).
84 Newton, G. L. *et al.* Bacillithiol is an antioxidant thiol produced in Bacilli. *Nat Chem Biol* 5, 625-627, doi:http://www.nature.com/nchembio/journal/v5/n9/suppinfo/nchembio.189_S1.html (2009).
85 Robinson, N. J. A bacterial copper metallothionein. *Nat Chem Biol* 4, 582-583 (2008).
86 Blindauer, C. A. *et al.* Multiple bacteria encode metallothioneins and SmtA-like zinc fingers. *Molecular Microbiology* 45, 1421-1432, doi:10.1046/j.1365-2958.2002.03109.x (2002).
87 Tottey, S. *et al.* Cyanobacterial metallochaperone inhibits deleterious side reactions of copper. *Proceedings of the National Academy of Sciences* 109, 95-100, doi:10.1073/pnas.1117515109 (2012).
88 Tsai, Y.-P. & Chen, H.-T. Influence of sludge retention time on tolerance of copper toxicity for polyphosphate accumulating organisms linked to polyhydroxyalkanoates metabolism and phosphate removal. *Bioresource Technology* 102, 11043-11047, doi:http://dx.doi.org/10.1016/j.biortech.2011.09.050 (2011).
89 Dupont, C. L., Grass, G. & Rensing, C. Copper toxicity and the origin of bacterial resistance-new insights and applications. *Metallomics* 3, 1109-1118, doi:10.1039/C1MT00107H (2011).
90 Chillappagari, S. *et al.* Copper Stress Affects Iron Homeostasis by Destabilizing Iron-Sulfur Cluster Formation in Bacillus subtilis. *Journal of bacteriology* 192, 2512-2524, doi:10.1128/jb.00058-10 (2010).
91 Djoko, K. Y. & McEwan, A. G. Antimicrobial action of copper is amplified via inhibition of heme biosynthesis. *ACS chemical biology* 8, 2217-2223 (2013).
92 Faundez, G., Troncoso, M., Navarrete, P. & Figueroa, G. Antimicrobial activity of copper surfaces against suspensions of Salmonella enterica and Campylobacter jejuni. *BMC Microbiology* 4, 19 (2004).
93 Noyce, J. O., Michels, H. & Keevil, C. W. Use of Copper Cast Alloys To Control Escherichia coli O157 Cross-Contamination during Food Processing. *Applied and environmental microbiology* 72, 4239-4244, doi:10.1128/aem.02532-05 (2006).
94 Wilks, S. A., Michels, H. & Keevil, C. W. The survival of Escherichia coli O157 on a range of metal surfaces. *International Journal of Food Microbiology* 105, 445-454, doi:http://dx.doi.org/10.1016/j.ijfoodmicro.2005.04.021 (2005).
95 Wilks, S. A., Michels, H. T. & Keevil, C. W. Survival of Listeria monocytogenes Scott A on metal surfaces: Implications for cross-contamination. *International Journal of Food Microbiology* 111, 93-98, doi:http://dx.doi.org/10.1016/j.ijfoodmicro.2006.04.037 (2006).
96 Mehtar, S., Wiid, I. & Todorov, S. D. The antimicrobial activity of copper and copper alloys against nosocomial pathogens and Mycobacterium tuberculosis isolated from healthcare facilities in the Western Cape: an in-vitro study. *Journal of Hospital Infection* 68, 45-51, doi:http://dx.doi.org/10.1016/j.jhin.2007.10.009 (2008).

97 Weaver, L., Michels, H. T. & Keevil, C. W. Survival of Clostridium difficile on copper and steel: futuristic options for hospital hygiene. *Journal of Hospital Infection* 68, 145-151, doi:http://dx.doi.org/10.1016/j.jhin.2007.11.011 (2008).
98 Wheeldon, L. J. *et al.* Antimicrobial efficacy of copper surfaces against spores and vegetative cells of Clostridium difficile: the germination theory. *Journal of Antimicrobial Chemotherapy* 62, 522-525, doi:10.1093/jac/dkn219 (2008).
99 Noyce, J. O., Michels, H. & Keevil, C. W. Potential use of copper surfaces to reduce survival of epidemic meticillin-resistant Staphylococcus aureus in the healthcare environment. *Journal of Hospital Infection* 63, 289-297, doi:http://dx.doi.org/10.1016/j.jhin.2005.12.008 (2006).
100 Michels, H. T., Noyce, J. O. & Keevil, C. W. Effects of temperature and humidity on the efficacy of methicillin-resistant Staphylococcus aureus challenged antimicrobial materials containing silver and copper. *Letters in Applied Microbiology* 49, 191-195, doi:10.1111/j.1472-765X.2009.02637.x (2009).
101 Weaver, L., Michels, H. T. & Keevil, C. W. Potential for preventing spread of fungi in air-conditioning systems constructed using copper instead of aluminium. *Letters in Applied Microbiology* 50, 18-23, doi:10.1111/j.1472-765X.2009.02753.x (2010).
102 Santo, C. E., Taudte, N., Nies, D. H. & Grass, G. Contribution of Copper Ion Resistance to Survival of Escherichia coli on Metallic Copper Surfaces. *Applied and environmental microbiology* 74, 977-986, doi:10.1128/aem.01938-07 (2008).
103 Molteni, C., Abicht, H. K. & Solioz, M. Killing of Bacteria by Copper Surfaces Involves Dissolved Copper. *Applied and environmental microbiology* 76, 4099-4101, doi:10.1128/aem.00424-10 (2010).
104 McPhail, D. B. & Goodman, B. A. Tris buffer--a case for caution in its use in copper-containing systems. *The Biochemical journal* 221, 559-560 (1984).
105 Mathews, S., Hans, M., Mücklich, F. & Solioz, M. Contact Killing of Bacteria on Copper is Suppressed if Bacteria-Metal Contact is Prevented and Is Induced on Iron by Copper Ions. *Applied and environmental microbiology*, doi:10.1128/aem.03608-12 (2013).
106 Avery, S. V. Molecular targets of oxidative stress. *Biochemical Journal* 434, 201-210, doi:10.1042/bj20101695 (2011).
107 Jomova, K., Baros, S. & Valko, M. Redox active metal-induced oxidative stress in biological systems. *Transition Met Chem* 37, 127-134, doi:10.1007/s11243-012-9583-6 (2012).
108 Figge, R. M., Schubert, M., Brinkmann, H. & Cerff, R. Glyceraldehyde-3-phosphate dehydrogenase gene diversity in eubacteria and eukaryotes: evidence for intra- and inter-kingdom gene transfer. *Molecular Biology and Evolution* 16, 429-440 (1999).
109 Nicholls, C., Li, H. & Liu, J.-P. GAPDH: A common enzyme with uncommon functions. *Clinical and Experimental Pharmacology and Physiology* 39, 674-679, doi:10.1111/j.1440-1681.2011.05599.x (2012).
110 Seidler, N. in *GAPDH: Biological Properties and Diversity* Vol. 985 *Advances in Experimental Medicine and Biology* Ch. 1, 1-36 (Springer Netherlands, 2013).
111 Dreisbach, A., van Dijl, J. M. & Buist, G. The cell surface proteome of Staphylococcus aureus. *PROTEOMICS* 11, 3154-3168, doi:10.1002/pmic.201000823 (2011).
112 Dumke, R., Hausner, M. & Jacobs, E. Role of Mycoplasma pneumoniae glyceraldehyde-3-phosphate dehydrogenase (GAPDH) in mediating interactions with the human extracellular matrix. *Microbiology* 157, 2328-2338, doi:10.1099/mic.0.048298-0 (2011).

113 Purves, J., Cockayne, A., Moody, P. C. E. & Morrissey, J. A. Comparison of the Regulation, Metabolic Functions, and Roles in Virulence of the Glyceraldehyde-3-Phosphate Dehydrogenase Homologues gapA and gapB in Staphylococcus aureus. *Infection and Immunity* 78, 5223-5232, doi:10.1128/iai.00762-10 (2010).
114 Mukherjee, S., Dutta, D., Saha, B. & Das, A. K. Crystal Structure of Glyceraldehyde-3-Phosphate Dehydrogenase 1 from Methicillin-Resistant Staphylococcus aureus MRSA252 Provides Novel Insights into Substrate Binding and Catalytic Mechanism. *Journal of Molecular Biology* 401, 949-968, doi:http://dx.doi.org/10.1016/j.jmb.2010.07.002 (2010).
115 Weber, H., Engelmann, S., Becher, D. & Hecker, M. Oxidative stress triggers thiol oxidation in the glyceraldehyde-3-phosphate dehydrogenase of Staphylococcus aureus. *Molecular Microbiology* 52, 133-140, doi:10.1111/j.1365-2958.2004.03971.x (2004).
116 Deng, X. *et al.* Steady-State Hydrogen Peroxide Induces Glycolysis in Staphylococcus aureus and Pseudomonas aeruginosa. *Journal of bacteriology* 196, 2499-2513, doi:10.1128/jb.01538-14 (2014).
117 Winterbourn, C. C., Hampton, M. B., Livesey, J. H. & Kettle, A. J. Modeling the reactions of superoxide and myeloperoxidase in the neutrophil phagosome implications for microbial killing. *Journal of Biological Chemistry* 281, 39860-39869 (2006).
118 Danshina, P. V., Schmalhausen, E. V., Avetisyan, A. V. & Muronetz, V. I. Mildly Oxidized Glyceraldehyde-3-Phosphate Dehydrogenase as a Possible Regulator of Glycolysis. *IUBMB Life* 51, 309-314, doi:10.1080/152165401317190824 (2001).
119 Grant, C. M., Quinn, K. A. & Dawes, I. W. Differential Protein S-Thiolation of Glyceraldehyde-3-Phosphate Dehydrogenase Isoenzymes Influences Sensitivity to Oxidative Stress. *Molecular and Cellular Biology* 19, 2650-2656 (1999).
120 Jung, C. H. & Thomas, J. A. S-glutathiolated hepatocyte proteins and insulin disulfides as substrates for reduction by glutaredoxin, thioredoxin, protein disulfide isomerase, and glutathione. *Archives of biochemistry and biophysics* 335, 61-72 (1996).
121 Ludwig, H. *et al.* Transcription of glycolytic genes and operons in Bacillus subtilis: evidence for the presence of multiple levels of control of the gapA operon. *Molecular Microbiology* 41, 409-422, doi:10.1046/j.1365-2958.2001.02523.x (2001).
122 Naterstad, K., Rud, I., Kvam, I. & Axelsson, L. Characterisation of the gap Operon from Lactobacillus plantarum and Lactobacillus sakei. *Curr Microbiol* 54, 180-185, doi:10.1007/s00284-006-0013-x (2007).
123 Gorke, B. & Stulke, J. Carbon catabolite repression in bacteria: many ways to make the most out of nutrients. *Nat Rev Micro* 6, 613-624 (2008).
124 Strasters, K. C. & Winkler, K. C. Carbohydrate metabolism of Staphylococcus aureus. *Journal of general microbiology* 33, 213-229 (1963).
125 Becker, S. & Palsson, B. Genome-scale reconstruction of the metabolic network in Staphylococcus aureus N315: an initial draft to the two-dimensional annotation. *BMC Microbiology* 5, 8 (2005).
126 Newton, G. L., Fahey, R. C. & Rawat, M. Detoxification of toxins by bacillithiol in Staphylococcus aureus. *Microbiology* 158, 1117-1126, doi:10.1099/mic.0.055715-0 (2012).
127 Hartmann, T. *et al.* Catabolite Control Protein E (CcpE) Is a LysR-type Transcriptional Regulator of Tricarboxylic Acid Cycle Activity in Staphylococcus aureus. *Journal of Biological Chemistry* 288, 36116-36128, doi:10.1074/jbc.M113.516302 (2013).

128 Postma, P. W. & Roseman, S. The bacterial phosphoenolpyruvate: sugar phosphotransferase system. *Biochimica et Biophysica Acta (BBA)-Reviews on Biomembranes* 457, 213-257 (1976).
129 Cooper, R. A. Metabolism of methylglyoxal in microorganisms. *Annual Reviews in Microbiology* 38, 49-68 (1984).
130 Stülke, J. & Hillen, W. Carbon catabolite repression in bacteria. *Current Opinion in Microbiology* 2, 195-201, doi:http://dx.doi.org/10.1016/S1369-5274(99)80034-4 (1999).
131 Chakraborty, S., Karmakar, K. & Chakravortty, D. Cells producing their own nemesis: Understanding methylglyoxal metabolism. *IUBMB Life* 66, 667-678, doi:10.1002/iub.1324 (2014).
132 Ferguson, G. P., Tötemeyer, S., MacLean, M. J. & Booth, I. R. Methylglyoxal production in bacteria: suicide or survival? *Archives of microbiology* 170, 209-218 (1998).
133 Sukdeo, N. & Honek John, F. in *Drug Metabolism and Drug Interactions* Vol. 23 29 (2008).
134 Chandrangsu, P., Dusi, R., Hamilton, C. J. & Helmann, J. D. Methylglyoxal resistance in Bacillus subtilis: contributions of bacillithiol-dependent and independent pathways. *Molecular microbiology* 91, 706-715 (2014).
135 Bradford, M. M. A rapid and sensitive method for the quantitation of microgram quantities of protein utilizing the principle of protein-dye binding. *Analytical biochemistry* 72, 248-254 (1976).
136 Xiao, Z., Loughlin, F., George, G. N., Howlett, G. J. & Wedd, A. G. C-Terminal Domain of the Membrane Copper Transporter Ctr1 from Saccharomyces cerevisiae Binds Four Cu(I) Ions as a Cuprous-Thiolate Polynuclear Cluster: Sub-femtomolar Cu(I) Affinity of Three Proteins Involved in Copper Trafficking. *Journal of the American Chemical Society* 126, 3081-3090, doi:10.1021/ja0390350 (2004).
137 Dawson, R. M. C., Elliott, D. C., Elliott, W. H. & Jones, K. M. in *Data for Biochemical Research* 131-134 (Oxford Science Publications Oxford, 1986).
138 Krausz, K. & Bose, J. *Methods in Molecular Biology* Ch. 185, 1-6 (Humana Press, 2015).
139 Li, Z.-y., Xu, K.-l. & Pan, X.-y. Rubidium chloride method for the preparation of competent E. coli cells [J]. *Acta Academiae Medicinae Xuzhou* 4, 010 (2004).
140 Shafeeq, S. *et al.* The cop operon is required for copper homeostasis and contributes to virulence in Streptococcus pneumoniae. *Molecular Microbiology* 81, 1255-1270, doi:10.1111/j.1365-2958.2011.07758.x (2011).
141 Gaetke, L. M. & Chow, C. K. Copper toxicity, oxidative stress, and antioxidant nutrients. *Toxicology* 189, 147-163, doi:http://dx.doi.org/10.1016/S0300-483X(03)00159-8 (2003).
142 Tu, W. Y. *et al.* Cellular Iron Distribution in Bacillus anthracis. *Journal of bacteriology* 194, 932-940, doi:10.1128/jb.06195-11 (2012).
143 Taylor, J. M. & Heinrichs, D. E. Transferrin binding in Staphylococcus aureus: involvement of a cell wall-anchored protein. *Molecular Microbiology* 43, 1603-1614, doi:10.1046/j.1365-2958.2002.02850.x (2002).
144 Saier Jr, M. H. *et al.* Catabolite repression and inducer control in Gram-positive bacteria. *Microbiology* 142, 217-230 (1996).
145 Seidl, K. *et al.* Effect of a glucose impulse on the CcpA regulon in Staphylococcus aureus. *BMC Microbiology* 9, 95 (2009).
146 Badarau, A., Firbank, S. J., McCarthy, A. A., Banfield, M. J. & Dennison, C. Visualizing the metal-binding versatility of copper trafficking sites. *Biochemistry* 49, 7798-7810 (2010).

147 Rubino, J. T. & Franz, K. J. Coordination chemistry of copper proteins: How nature handles a toxic cargo for essential function. *Journal of Inorganic Biochemistry* 107, 129-143, doi:http://dx.doi.org/10.1016/j.jinorgbio.2011.11.024 (2012).
148 Karlin, K. D. & Zubieta, J. *Copper coordination chemistry: biochemical & inorganic perspectives*. (Adenine press, 1983).
149 Nagy, E. & Rigby, W. F. C. Glyceraldehyde-3-phosphate Dehydrogenase Selectively Binds AU-rich RNA in the NAD+-binding Region (Rossmann Fold). *Journal of Biological Chemistry* 270, 2755-2763, doi:10.1074/jbc.270.6.2755 (1995).
150 Matsumura, H. *et al.* Structure Basis for the Regulation of Glyceraldehyde-3-Phosphate Dehydrogenase Activity via the Intrinsically Disordered Protein CP12. *Structure* 19, 1846-1854, doi:http://dx.doi.org/10.1016/j.str.2011.08.016 (2011).
151 Erales, J., Gontero, B., Whitelegge, J. & Halgand, F. *Mapping of a copper-binding site on the small CP12 chloroplastic protein of Chlamydomonas reinhardtii using top-down mass spectrometry and site-directed mutagenesis*. Vol. 419 (2009).
152 Delobel, A. *et al.* Mass spectrometric analysis of the interactions between CP12, a chloroplast protein, and metal ions: a possible regulatory role within a PRK/GAPDH/CP12 complex. *Rapid Communications in Mass Spectrometry* 19, 3379-3388, doi:10.1002/rcm.2192 (2005).
153 Nagasawa, Y. *et al.* Coherent dynamics and ultrafast excited state relaxation of blue copper protein; plastocyanin. *Physical Chemistry Chemical Physics* 12, 6067-6075 (2010).
154 Banci, L., Bertini, I., Del Conte, R., Markey, J. & Ruiz-Dueñas, F. J. Copper Trafficking: the Solution Structure of Bacillus subtilis CopZ†. *Biochemistry* 40, 15660-15668, doi:10.1021/bi0112715 (2001).
155 Ma, Z., Cowart, D. M., Scott, R. A. & Giedroc, D. P. Molecular Insights into the Metal Selectivity of the Copper (I)-Sensing Repressor CsoR from Bacillus subtilis†. *Biochemistry* 48, 3325-3334 (2009).
156 Borkow, G. & Gabbay, J. Copper as a biocidal tool. *Current medicinal chemistry* 12, 2163-2175 (2005).
157 Waldron, K. J., Rutherford, J. C., Ford, D. & Robinson, N. J. Metalloproteins and metal sensing. *Nature* 460, 823-830 (2009).